Risks and Rewards of Multiphase Flow Simulations

Stéphane Zaleski

∂'Alembert, *Sorbonne Université, IUF & CNRS*

web site http://www.ida.upmc.fr/~zaleski

Collaborators in the past ten years on atomisation.

Ruben Scardovelli, Stephane Popinet, Tomas Arrufat, Peng Cheng, Gretar Tryggvason, Leon Malan, Yue Stanley Ling, Alexandre Guion, Subin Tomas, Taraneh Sayadi, Florence Marcotte, Wojciech Aniszewski, Sagar Pal, Nelson Joubert, Marco Crialesi, Youssef Saadeh, Alexandre Limare, Raphael Villiers.

Current Students and postdocs

Tomas Fullana, Mandeep Saini, Saeed Bidi, Ahmed Basil K., Cesar Pairetti, Jacob Maarek, Leonardo Chirco, Yash Kulkarni, Xiangbin Chen, Désir-André Koffi-Bi, Damien Thomas, Tobias Bauer, Elena Batzella, Jieyun Pan, Tian Long.

This title was given to me at a thermal and fluid engineering conference panel.

This title was given to me at a thermal and fluid engineering conference panel. Or rather the title was "Risks, rewards and remorse". So the plan of the talk should be:

1. Rewards
   - for mankind
   - for scientists

2. Risks

3. Remorse

420

Ten times the number 42 ?

420 ppm is the current CO_2 level in earth's atmosphere

If you measure more than 420 ppm in a room, it is a sign that aeration is not sufficient and you are at risk of contamination by a respiratory disease such as SARS, MERS, Covid-19, the flu or a common cold.

The 420 CO2 level is also the result of 150 years of fossil fuel burning

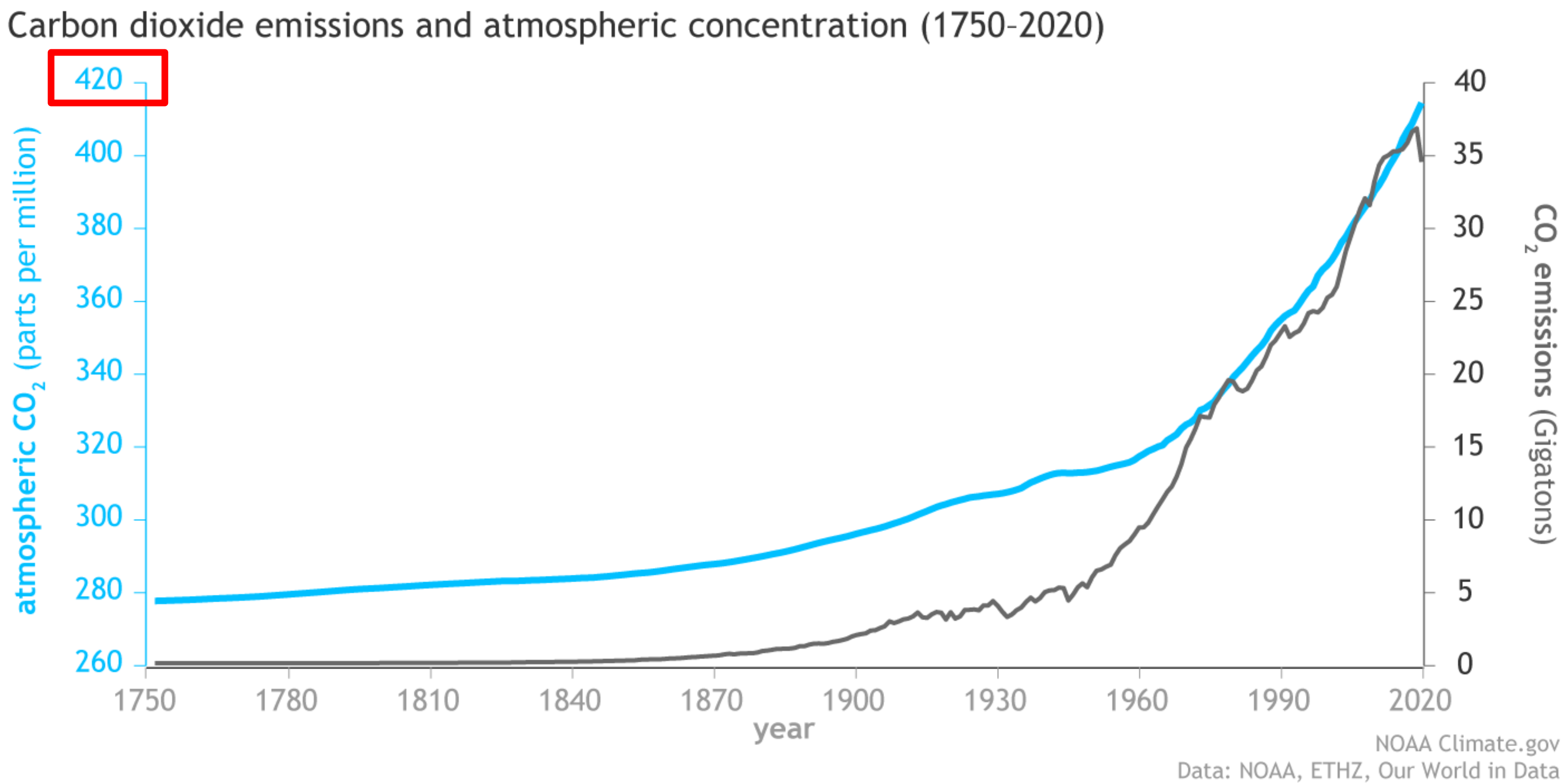

ipcc

INTERGOVERNMENTAL PANEL ON climate change

Climate Change 2022

Mitigation of Climate Change

Summary for Policymakers

ORBONNE
NIVERSITÉ
ÉATEURS DE FUTURS
PUIS 1257

pathways

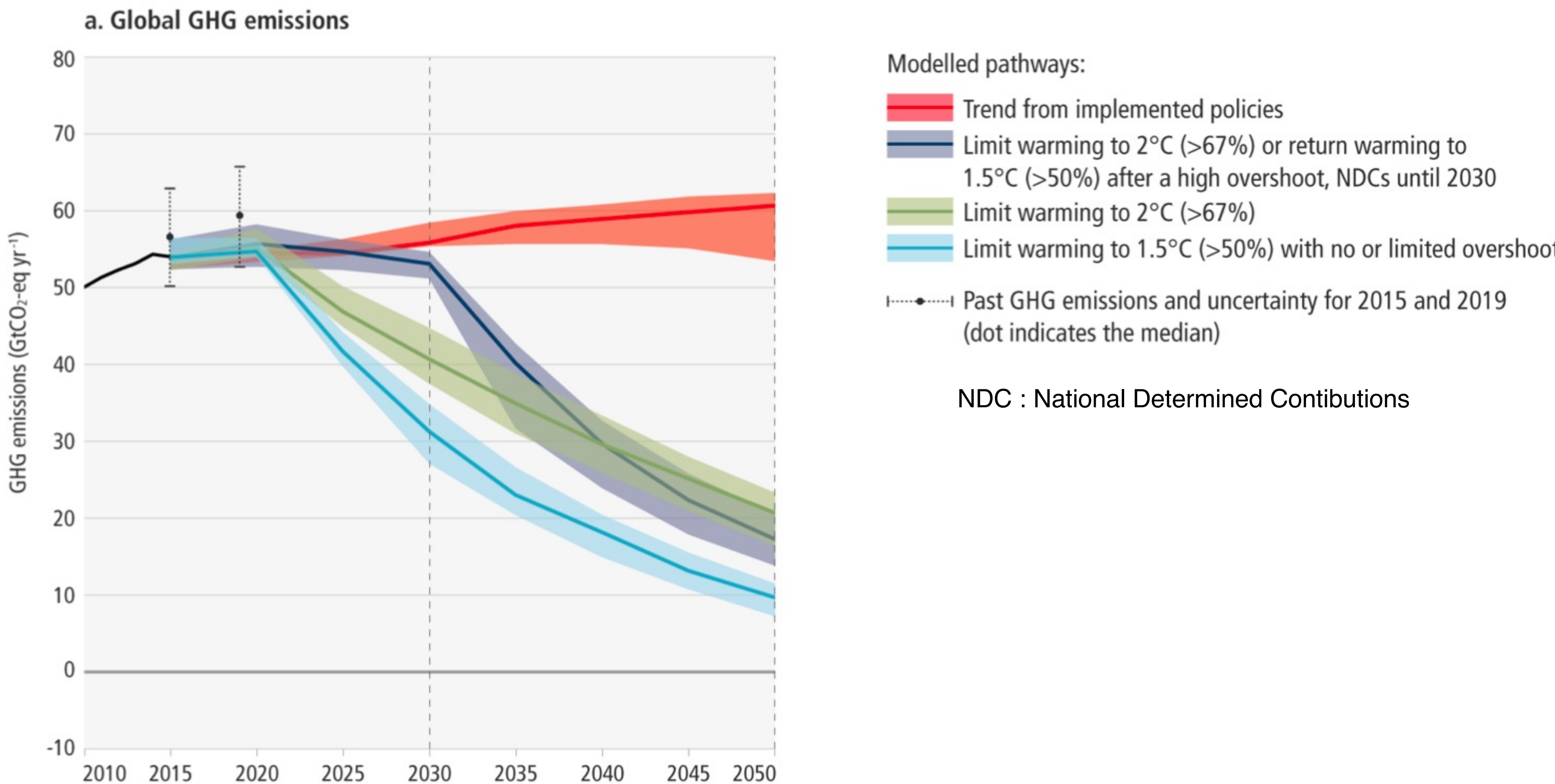

NDC : National Determined Contibutions

Soilutions are available: wind and solar have become much cheaper

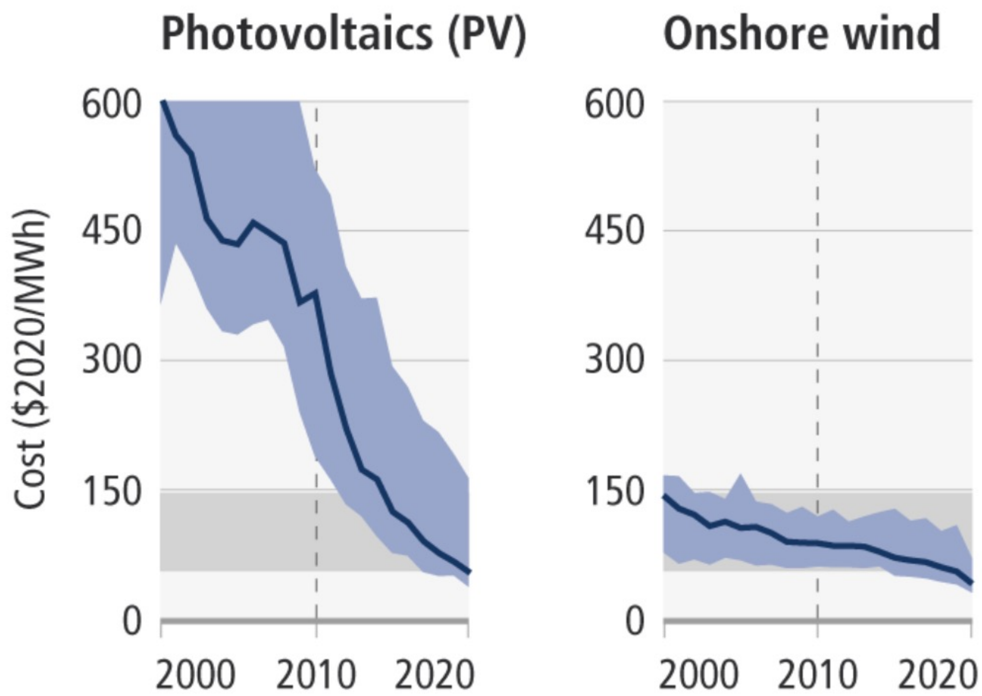

But energy storage remains a big issue. To compensate for the intermittency and annual oscillation of wind and solar power, about six months of storage of a country's energy consumption is needed. Sadly, although now cheaper to produce, batteries last only a few hours...

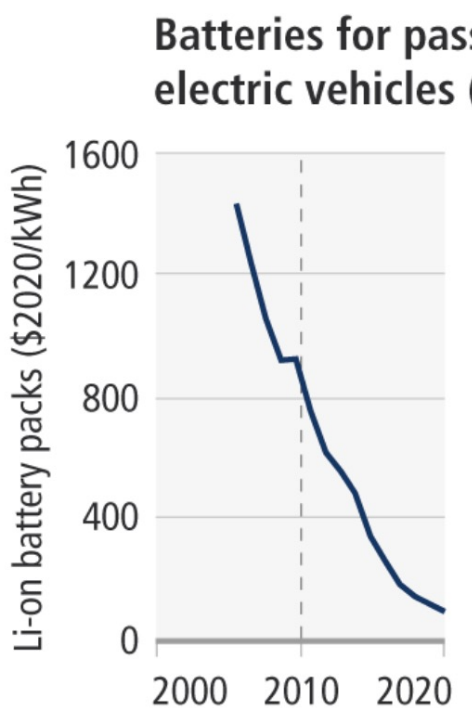

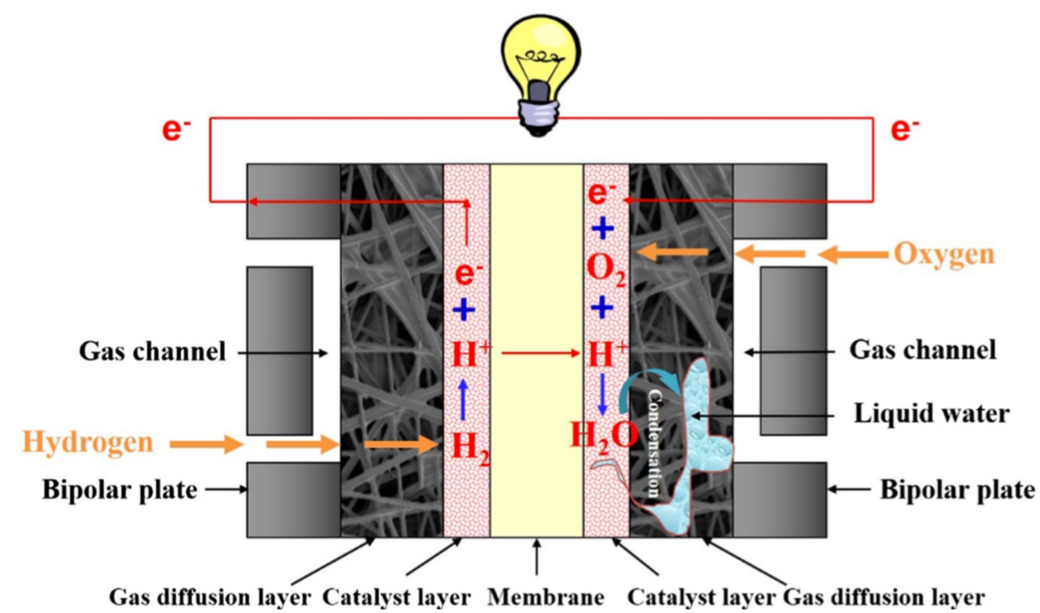

Fuel cell

The number 420 is thus connected to two of the main issues discussed in this lecture:

- Energy and climate : production, storage, usage, ocean-atmosphere interactions

- Respiratory disease transmission by aerosols.

Climate change and the emission reductions necessary to mitigate it are related to many natural phenomena and technologies.

Climat change and the emission reductions necessary to mitigate it are related to many natural phenomena and technologies.

An essential phenomenom is the ocean-atmosphere interface.

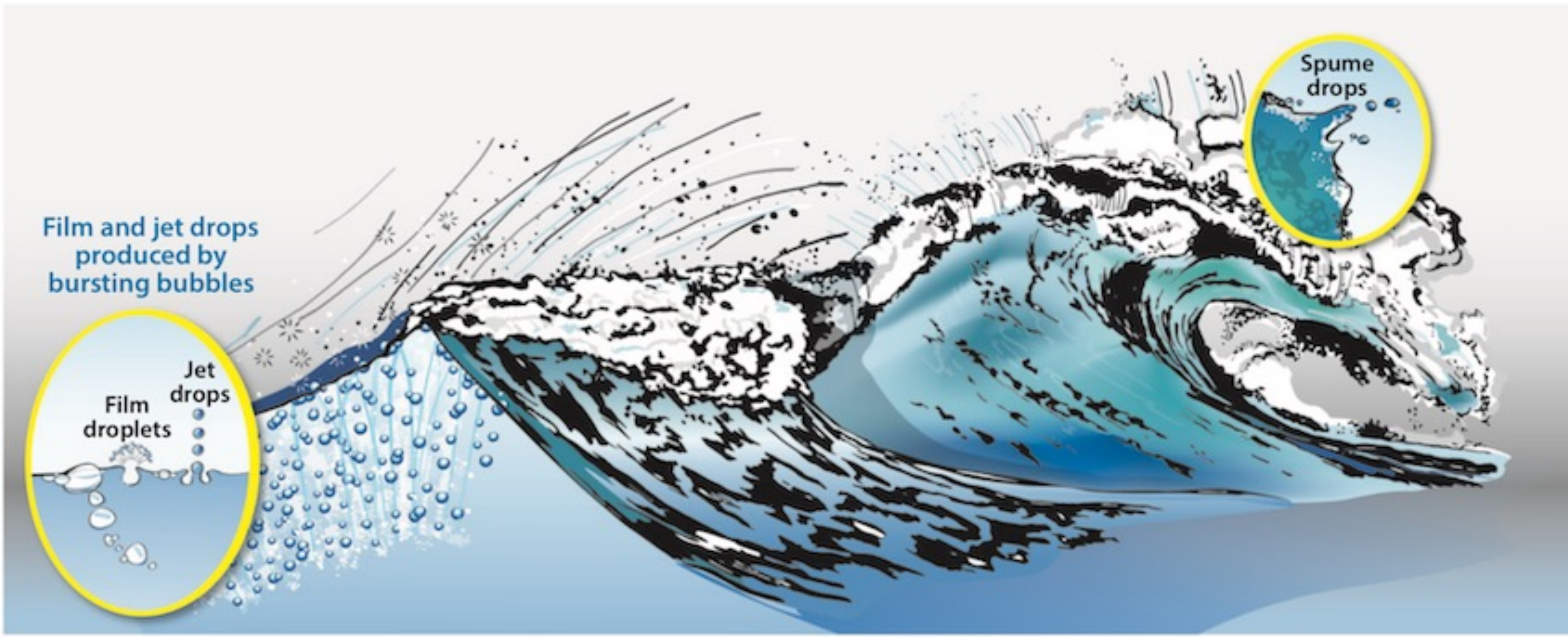

From Véron, ocean spray, 2015

Chemical and process engineering

Bubble Columns

From:http://p2pays.org/ref/16/15865.pdf

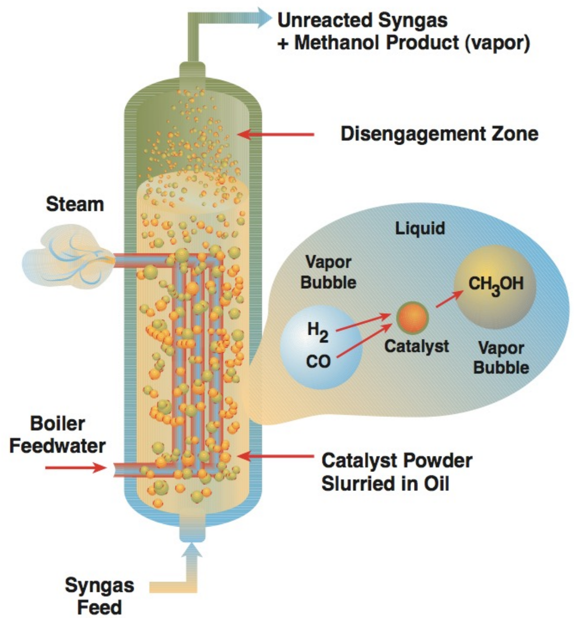

Liquid Phase Methanol (LPMEOH™) Process

Examples of Applications of Bubble Columns

Process	Methods and/or Reactants
Acetone	Oxidation of cumene
Acetic acid	Oxidation of acetaldehyde
	Oxidation of sec-butanol
	Carbonylation of methanol
Acetic anhydride	Oxidation of acetaldehyde
Acetaldehyde	Partial oxidation of ethylene
Acetophenone	Oxidation of ethylbenzene
Barium chloride	Barium sulfide and chlorine
Benzoic acid	Oxidation of toluene
Bleaching powder	Aqueous calcium oxide and chlorine
Bromine	Aqueous sodium bromide and chlorine
Butene	Absorption in aqueous solutions of sulfuric acid
Carbon Dioxide	Absorption in ammoniated brine
Carbone tetrachloride	Carbon disulphide and chlorine
Copper oxychloride	Oxidation of cuprous chloride
Cumene	Oxidation of phenol
Cupric chloride	Copper and cupric acid or hydrochloric acid
Dichlorination	Oxychlorination of ethylene
Ethyl benzene	Benzene and ethylene
Hexachlorobenzene	Benzene and chlorine
Hydrogen peroxide	Oxidation of hydroquinone
Isobutylene	Absorption in aqueous solutions of sulfuric acid
Phtalic acid	Oxidation of xylene
Phenol	Oxidation of cumene
Potassium bicarbonate	Aqueous potassium carbonate
Sodium bicarbonate	Aqueous sodium carbonate
Sodium metabisulphides	Carbon dioxide, aqueous sodium carbonate, and sulfur dioxide
Thiuram disulphides	Dithiocarbamates, chlorine, and air
Vinyl acetate	Oxidation of ethylene in acetic acid solutions
Water	Wet oxidation of waste water

After: S. Furusaki, L.-S. Fan, J. Garside**. The Expanding World of Chemical Engineering** (2^{nd} ed), Taylor & Francis 2001

Bubble Columns

From:http://p2pays.org/ref/16/15865.pdf

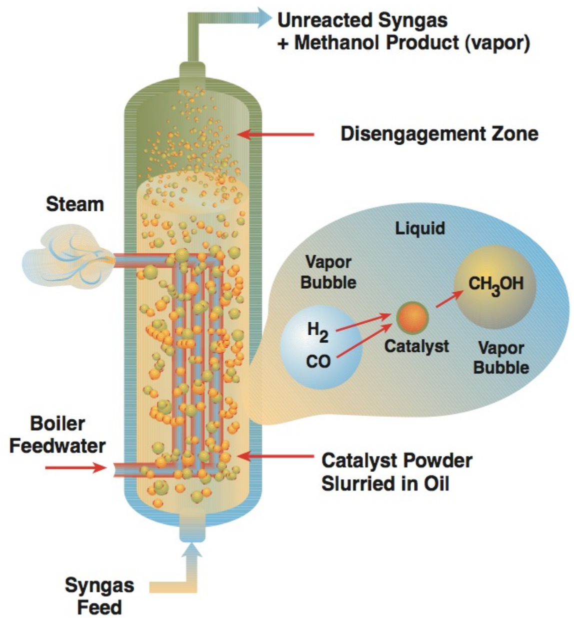

Liquid Phase Methanol ($LPMEOH^{TM}$) Process

Transform back CO into fuel

Examples of Applications of Bubble Columns

Process	Methods and/or Reactants
Acetone	Oxidation of cumene
Acetic acid	Oxidation of acetaldehyde
	Oxidation of sec-butanol
	Carbonylation of methanol
Acetic anhydride	Oxidation of acetaldehyde
Acetaldehyde	Partial oxidation of ethylene
Acetophenone	Oxidation of ethylbenzene
Barium chloride	Barium sulfide and chlorine
Benzoic acid	Oxidation of toluene
Bleaching powder	Aqueous calcium oxide and chlorine
Bromine	Aqueous sodium bromide and chlorine
Butene	Absorption in aqueous solutions of sulfuric acid
Carbon Dioxide	Absorption in ammoniated brine
Carbone tetrachloride	Carbon disulphide and chlorine
Copper oxychloride	Oxidation of cuprous chloride
Cumene	Oxidation of phenol
Cupric chloride	Copper and cupric acid or hydrochloric acid
Dichlorination	Oxychlorination of ethylene
Ethyl benzene	Benzene and ethylene
Hexachlorobenzene	Benzene and chlorine
Hydrogen peroxide	Oxidation of hydroquinone
Isobutylene	Absorption in aqueous solutions of sulfuric acid
Phtalic acid	Oxidation of xylene
Phenol	Oxidation of cumene
Potassium bicarbonate	Aqueous potassium carbonate
Sodium bicarbonate	Aqueous sodium carbonate
Sodium metabisulphides	Carbon dioxide, aqueous sodium carbonate, and sulfur dioxide
Thiuram disulphides	Dithiocarbamates, chlorine, and air
Vinyl acetate	Oxidation of ethylene in acetic acid solutions
Water	Wet oxidation of waste water

capture CO2

After: S. Furusaki, L.-S. Fan, J. Garside. **The Expanding World of Chemical Engineering** (2nd ed), Taylor & Francis 2001

Boiling

Nuclear power plant

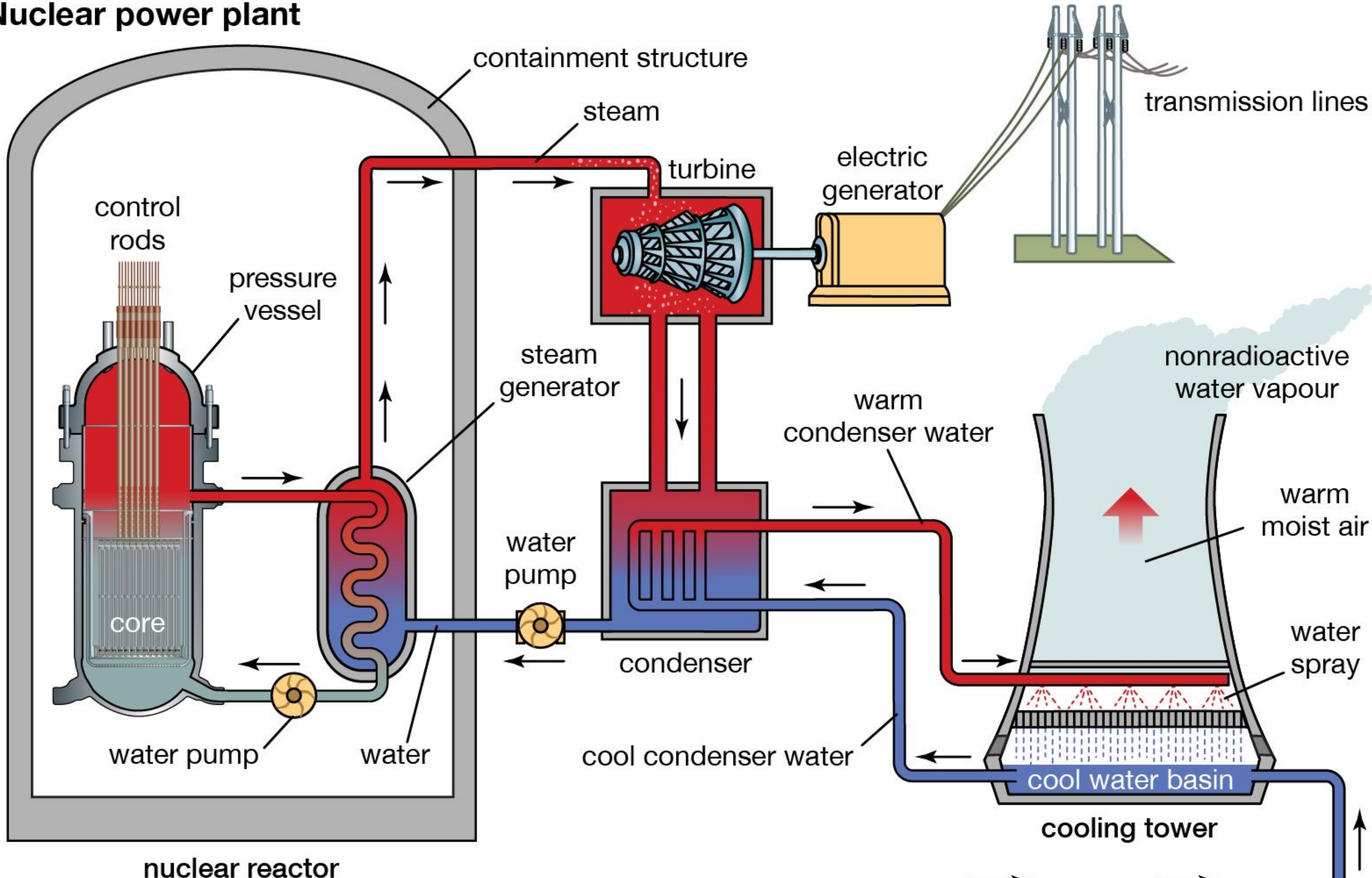

© 2013 Encyclopædia Britannica, Inc.

Boiling

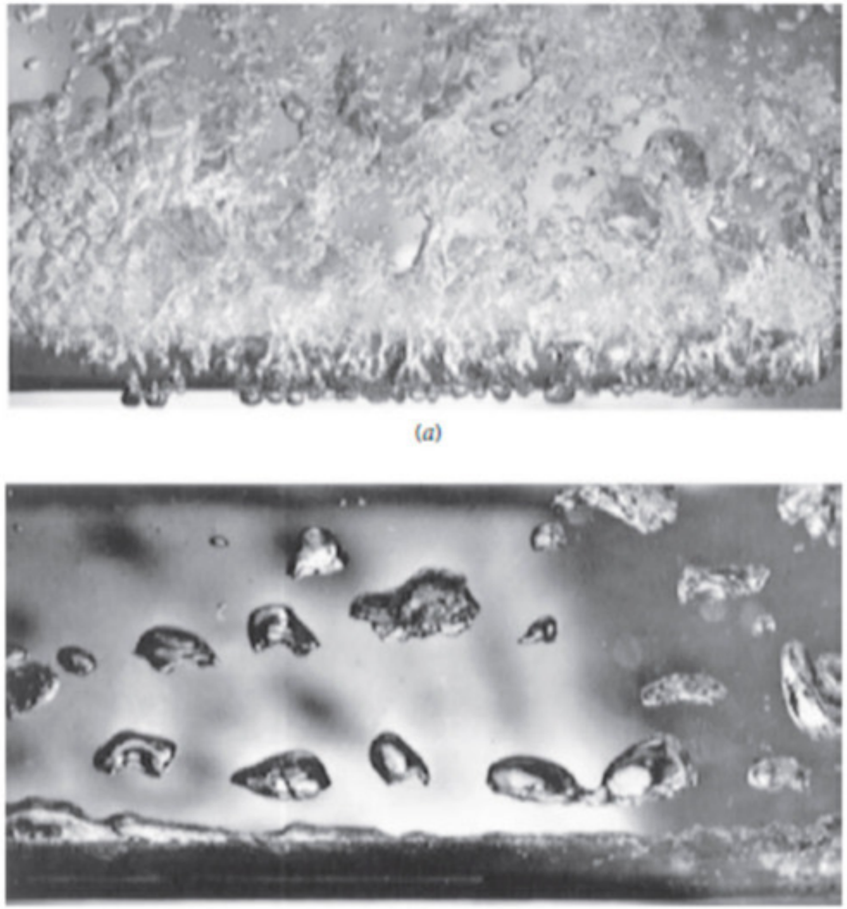
(a)
(b)

Bergman, T.L.; Incropera, F.P.; DeWitt, D.P.; Lavine, A.S. *Fundamentals of Heat and Mass Transfer*; John Wiley & Sons: Hoboken, NJ, USA, 2011.

Fuel cells

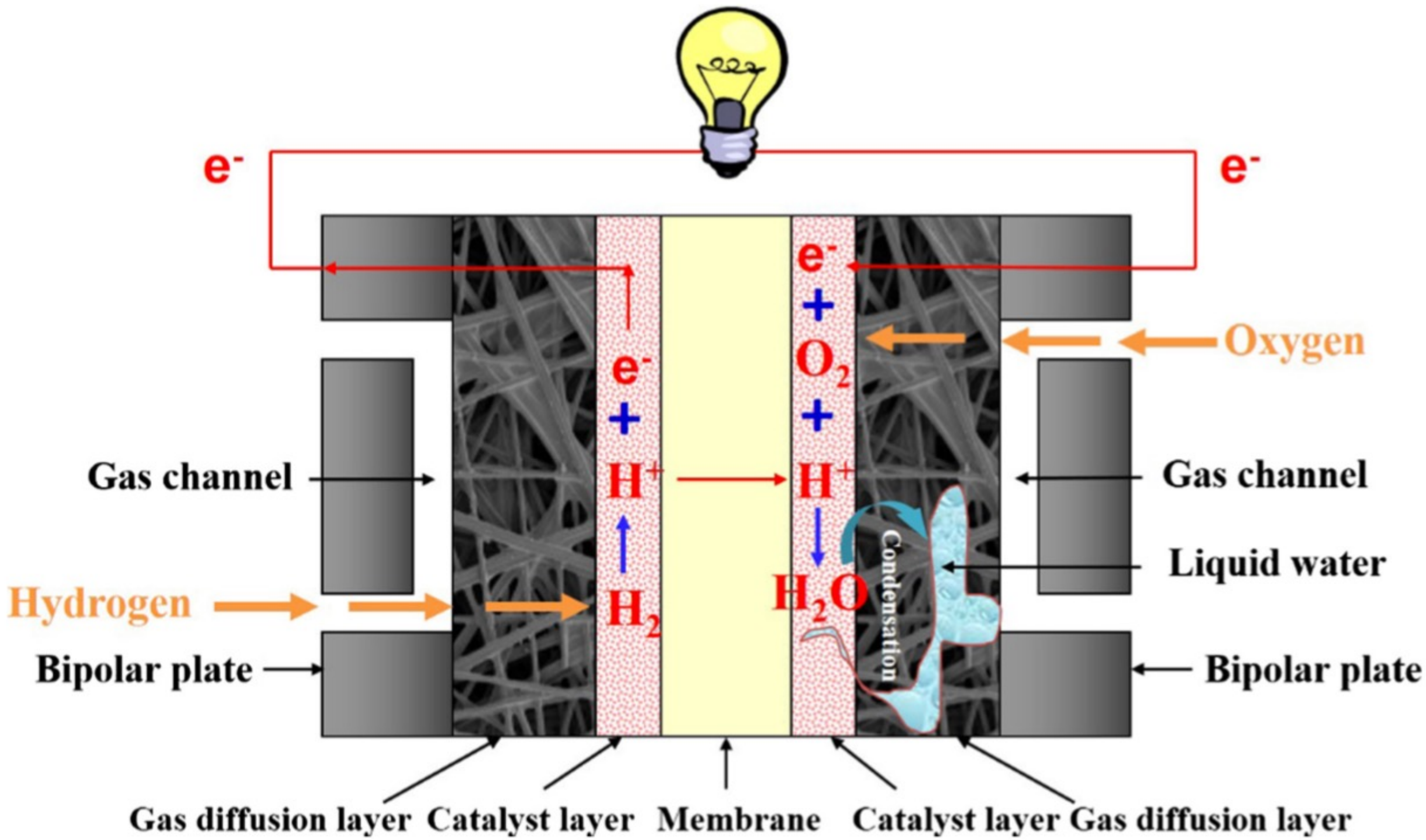
e-
e-
e-
+
O2
+
H+
H2O
Condensation
e-
+
H+
H2
Oxygen
Gas channel
Liquid water
Bipolar plate
Gas channel
Hydrogen
Bipolar plate
Gas diffusion layer
Catalyst layer
Membrane
Catalyst layer
Gas diffusion layer

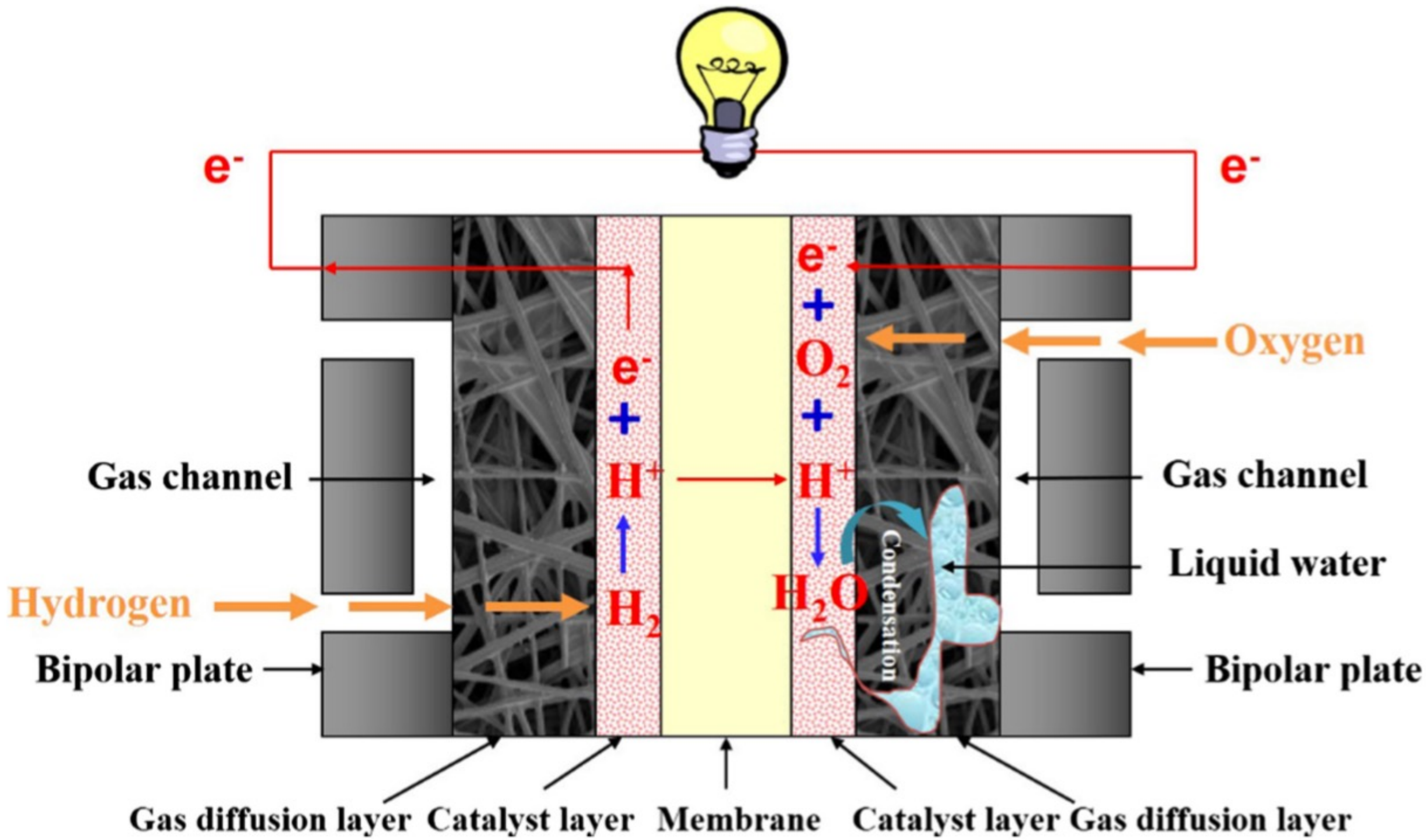

need to evaporate the water in the cathode

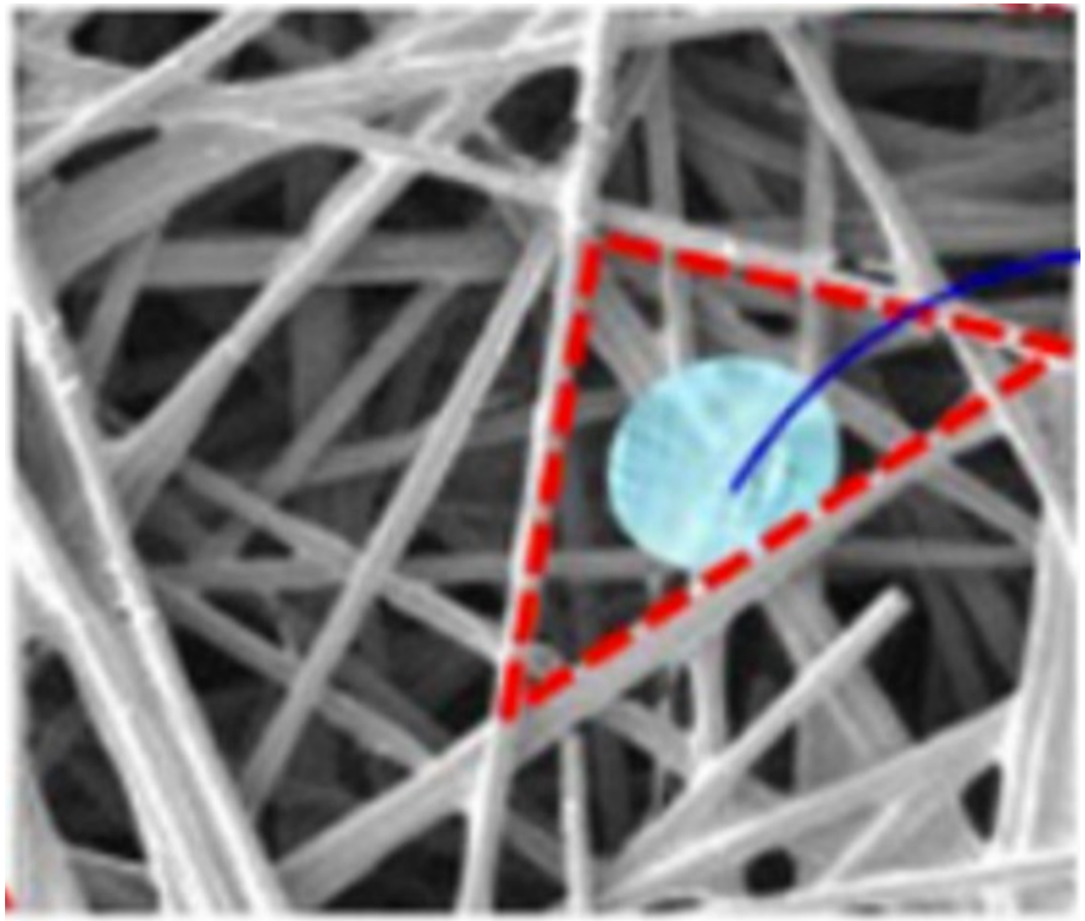

Simulation setup

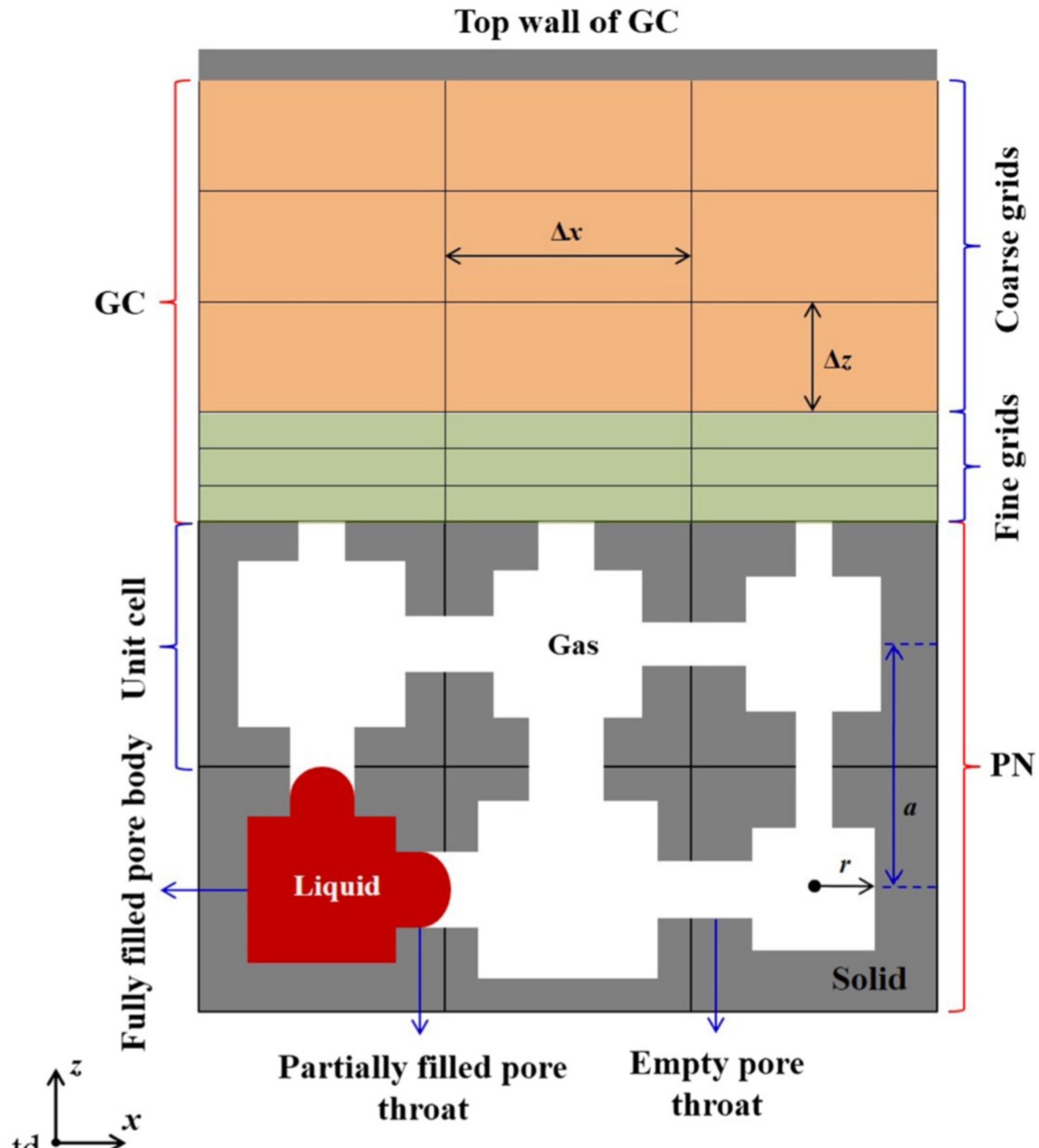

Covid and atomization

Recent motivation: respiratory disease transmission

A short history of epidemiology and droplets

- Pasteur thought that pathogens were transmitted by dust particules. (Hence vacuum cleaners, waxing floors etc.)

- Paradox: why mandatory masks and no mandatory vacuuming ?

- No paradox: masks and waxing floors at time 1918 influenza epidemic

- In 1930 Wells introduces the distinction between « droplets » and « aerosols » or « droplet nuclei ». Studies tuberculosis. Makes assumptions about the droplet size distribution. Introduces arbitrary 5 micron limit.

Origin of Bioaerosols

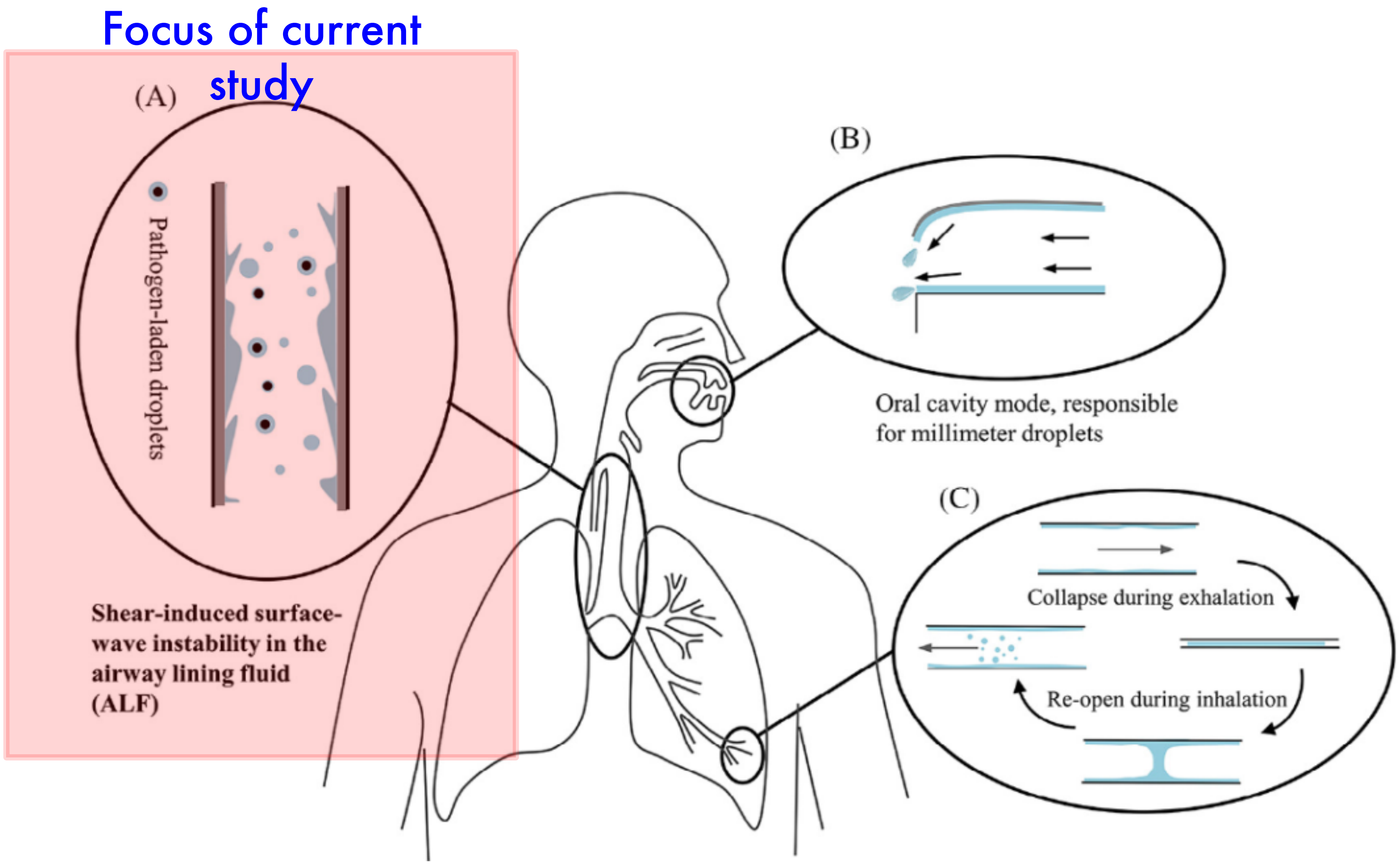

Jianjian Wei and Yuguo Li, *Am. J. Infect. Control* (2016)

Droplets generation during coughing/sneezing

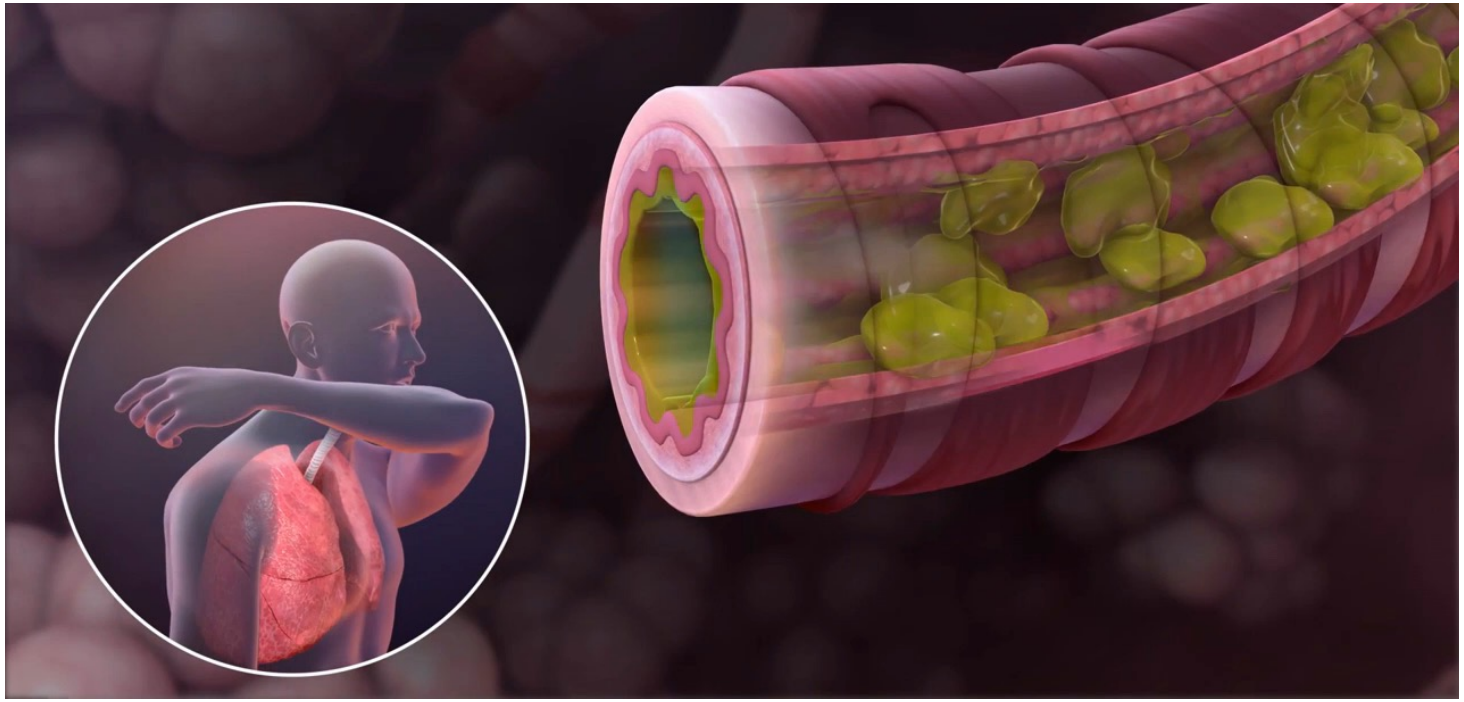

Video credit: Cystic Fibrosis Foundation

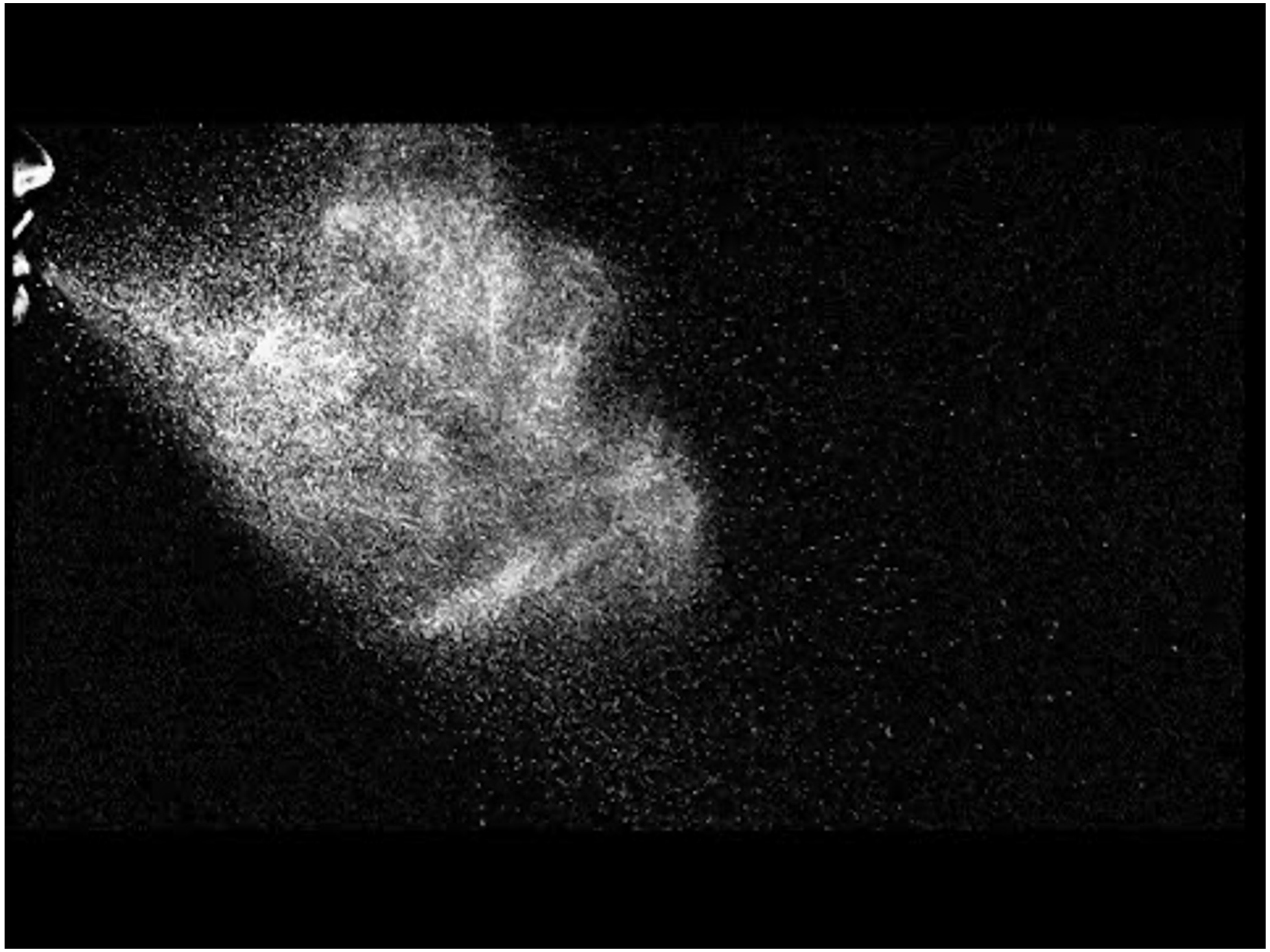

turbulent puff.

From *Bourouiba L. Turbulent gas clouds and respiratory pathogen emissions: potential implications for reducing transmission of COVID-19. Jama. 2020 Mar 26.*

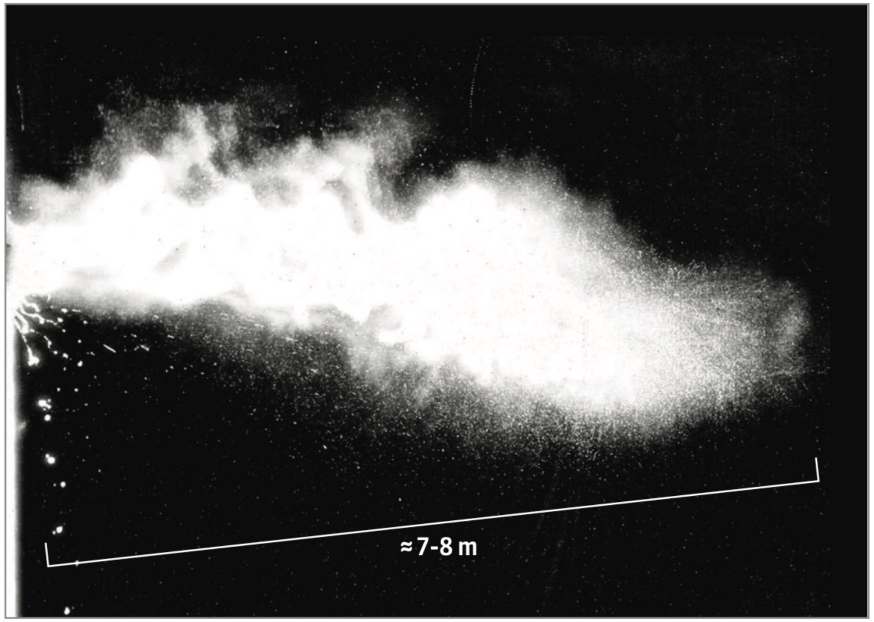

A turbulent puff created by a sneeze. The larger droplets (approx > 100 microns) fall to the ground in less than a meter. Smaller droplets are entrained into the turbulent puff. The image is from *Bourouiba L. Turbulent gas clouds and respiratory pathogen emissions: potential implications for reducing transmission of COVID-19. Jama. 2020 Mar 26.*

vidéo

The hotter turbulent puff can rise by natural convection and either stagnate near the ceiling or be entrained into the HVAC system and spread to other rooms.

Disease Transmission *via* Bioaerosols

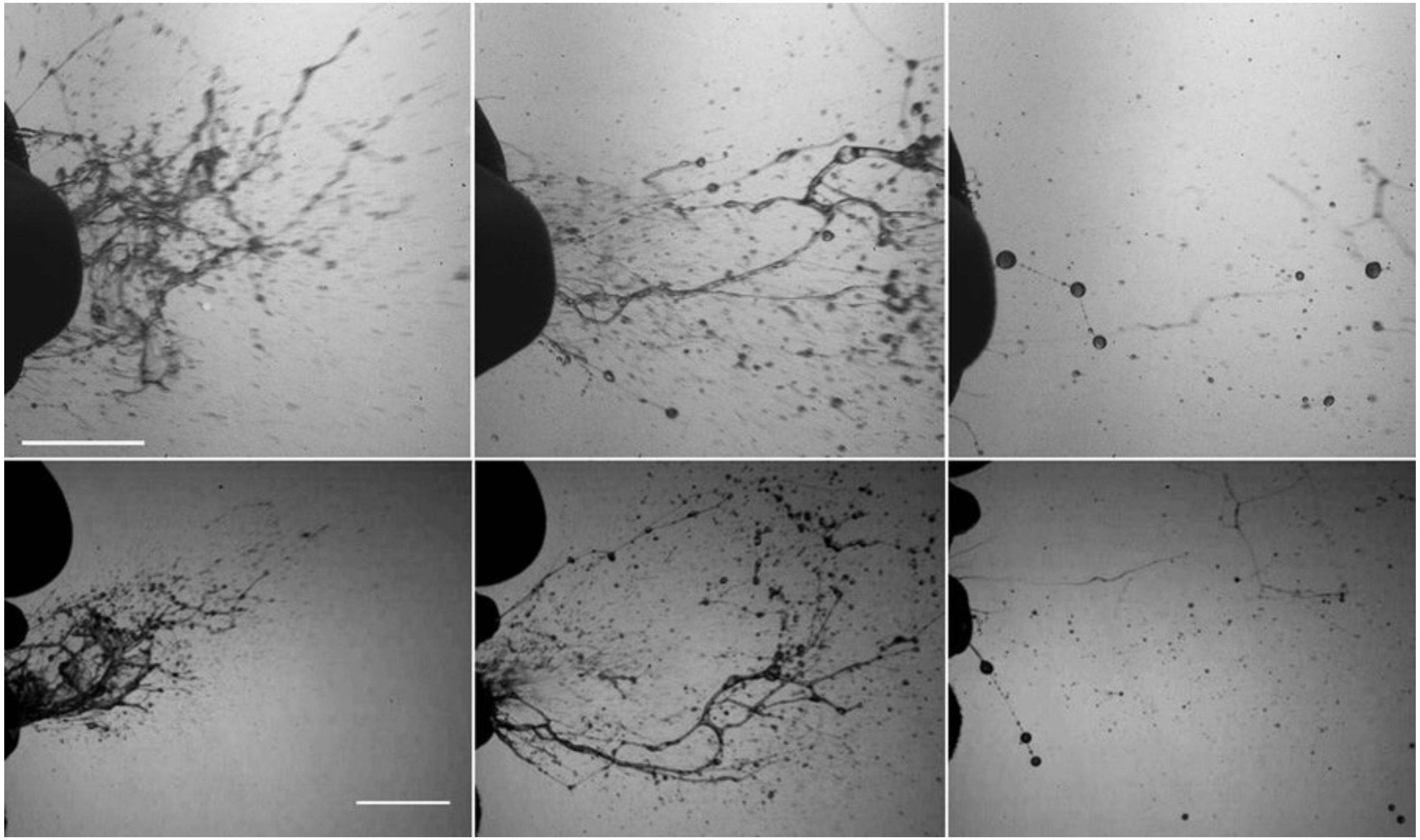

- Wide range of d !
- Viscoelastic !

Scharfman, et al. *Experiments in Fluids* (2016)

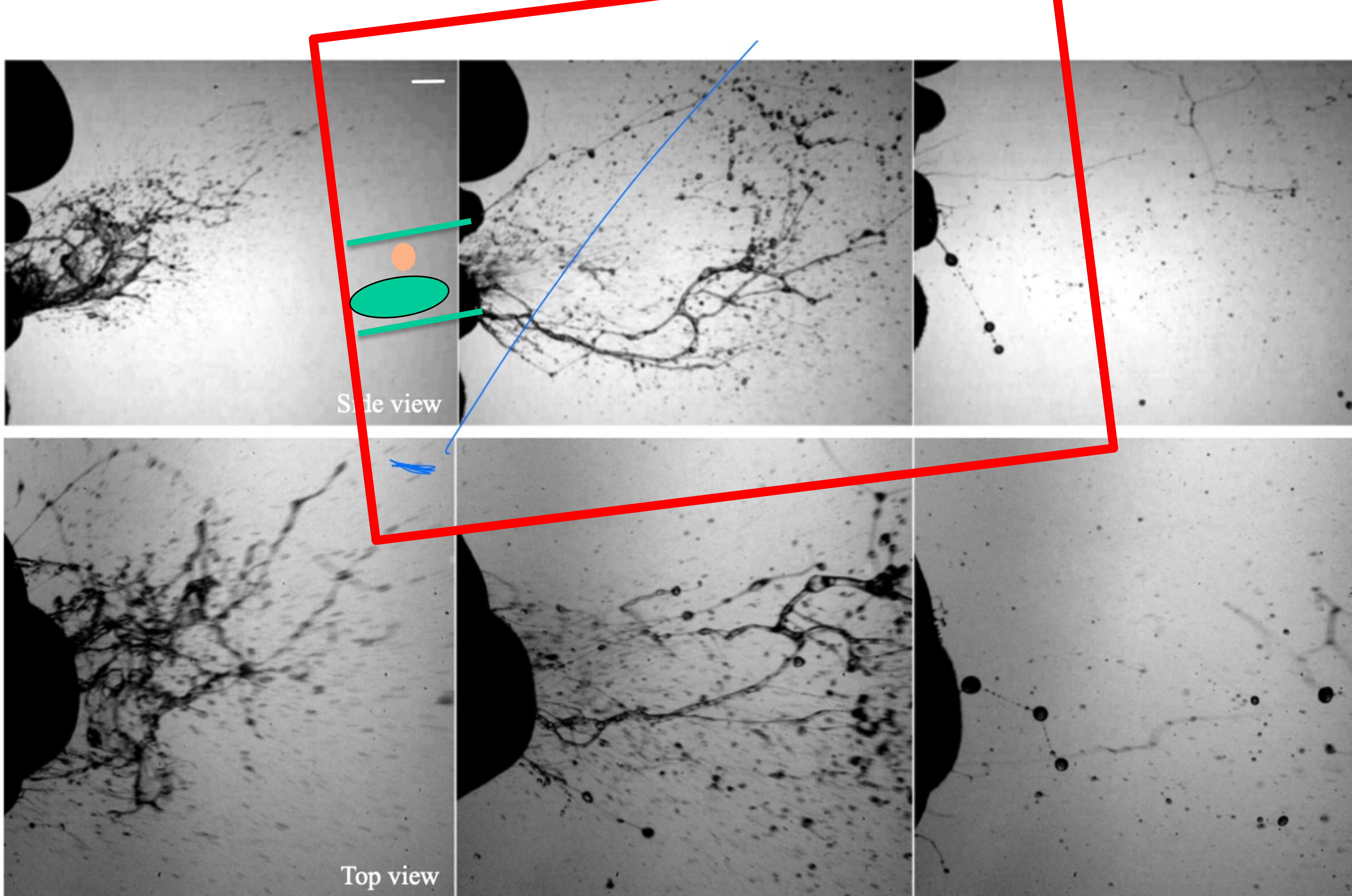

Zoom on the boxed region. Model the mouth and the airways.

Question: what is the size of the droplets in the atomisation process ?

First experimental answer from Duguid (1946) … Hard to do better since

SORBONNE UNIVERSITÉ
CRÉATEURS DE FUTURS
DEPUIS 1257

Pareto N(d) ~1/d^2 fit

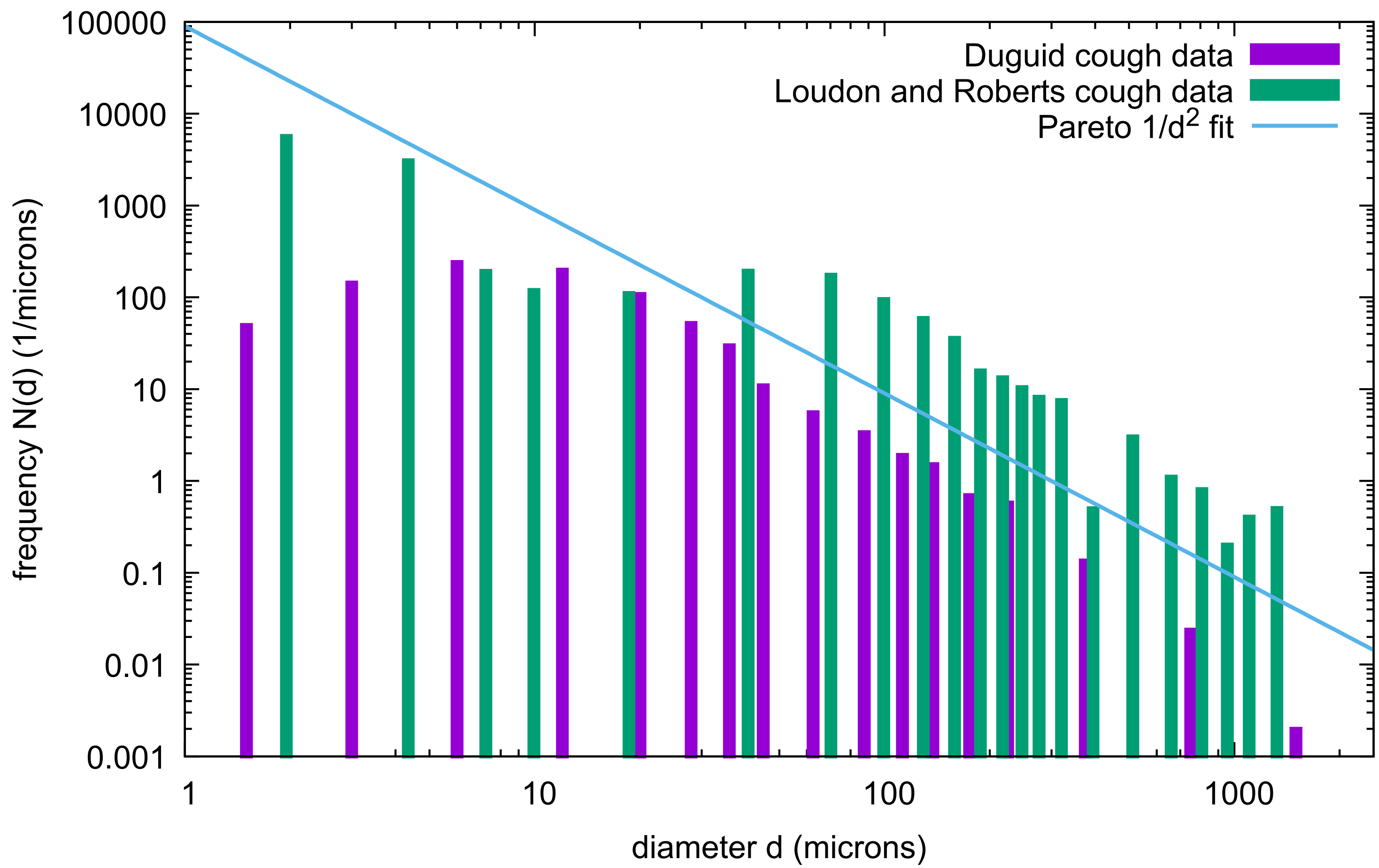

Droplet size distribution in human aerosols

First experimental answer from Duguid (1946) … Hard to do better since

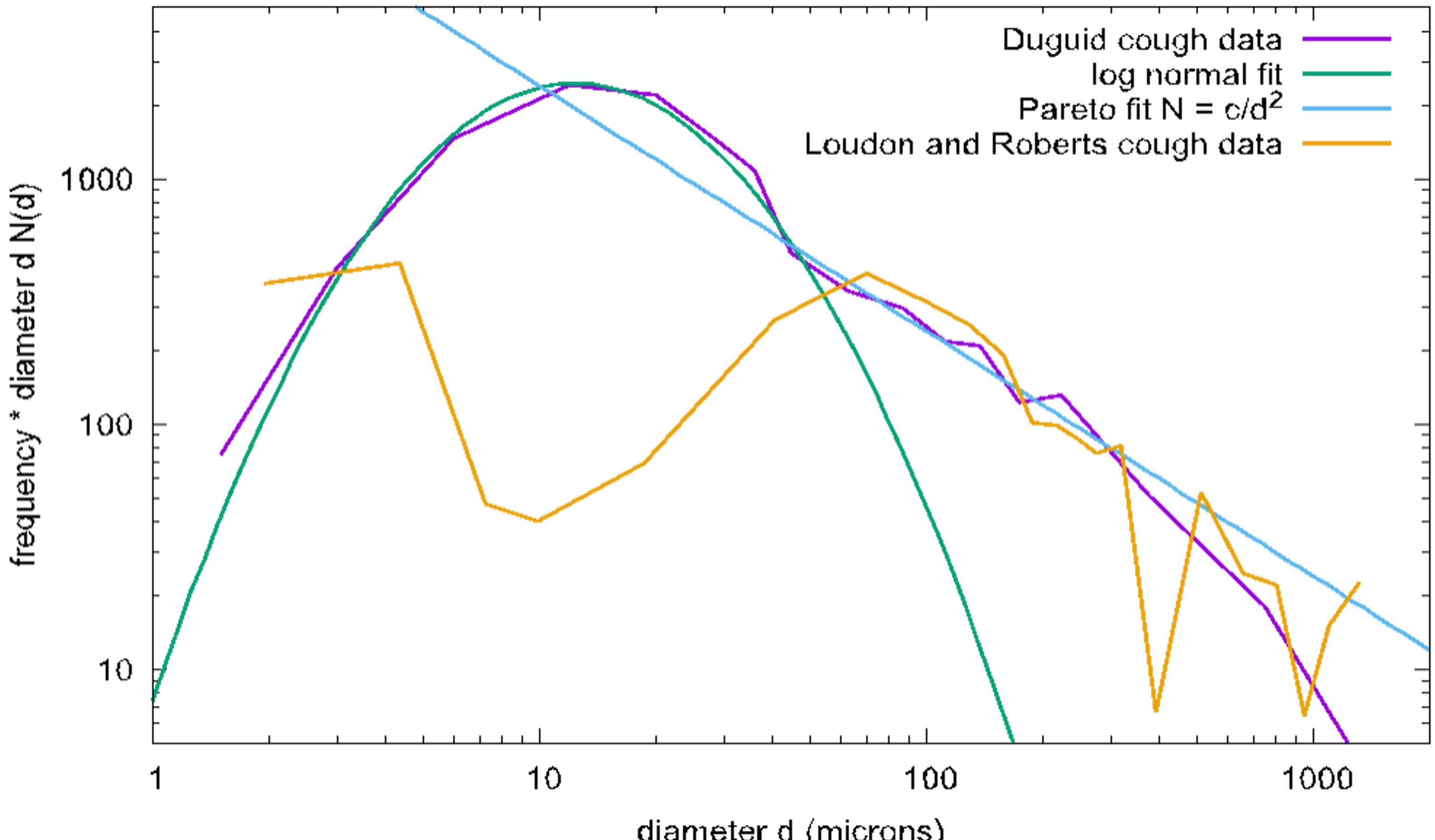

Pareto fit $N = C/d^2$

Log-normal fit : $N(d) = \frac{B}{d} \exp\left[-\frac{(\ln d - \hat{\mu})^2}{2\hat{\sigma}^2}\right]$

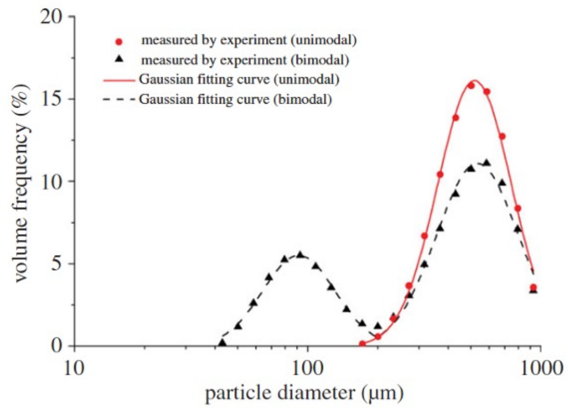

Figure 4. Measured data and fitting curves of two sample sneezes (unimodal and bimodal distributions, respectively). (Online version in colour.)

« Characterizations of particle size distribution of the droplets exhaled by sneeze » by Z.Y. Han, W.G. Weng and Q.Y. Huang, J R Soc Interface 10: 20130560 (2013).

Why does this differ from the previous (and next) plots ?

- volume frequency or volume weighted:
d^3 N(d) → depresses small d
- not a log in ordinate … However, bimodal …

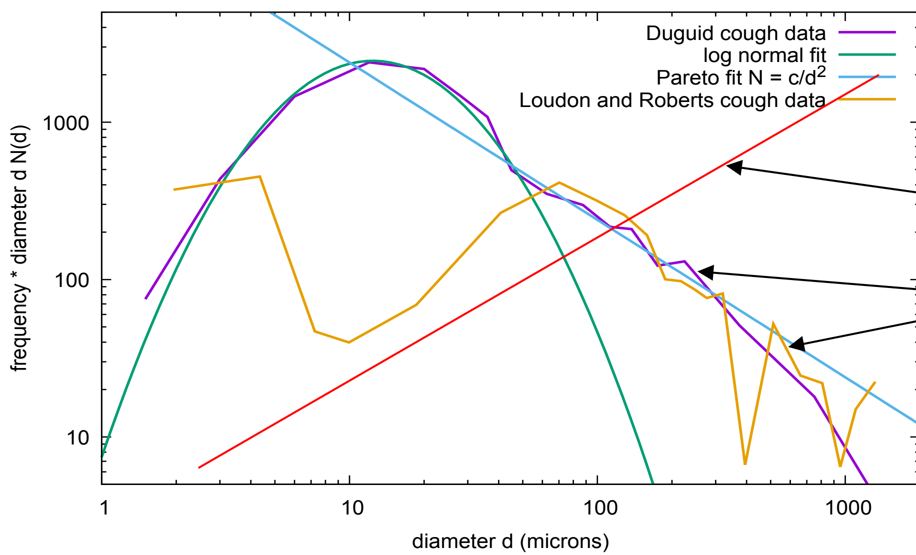

Go back to previous LN coord plot.

Volume weighted Pareto→ d^3 N ~ d

Loudon also bimodal

Cough Machine (with D. Lohse, P. Kant)

Flow meter connected to pressurized vessel via a solenoid valve

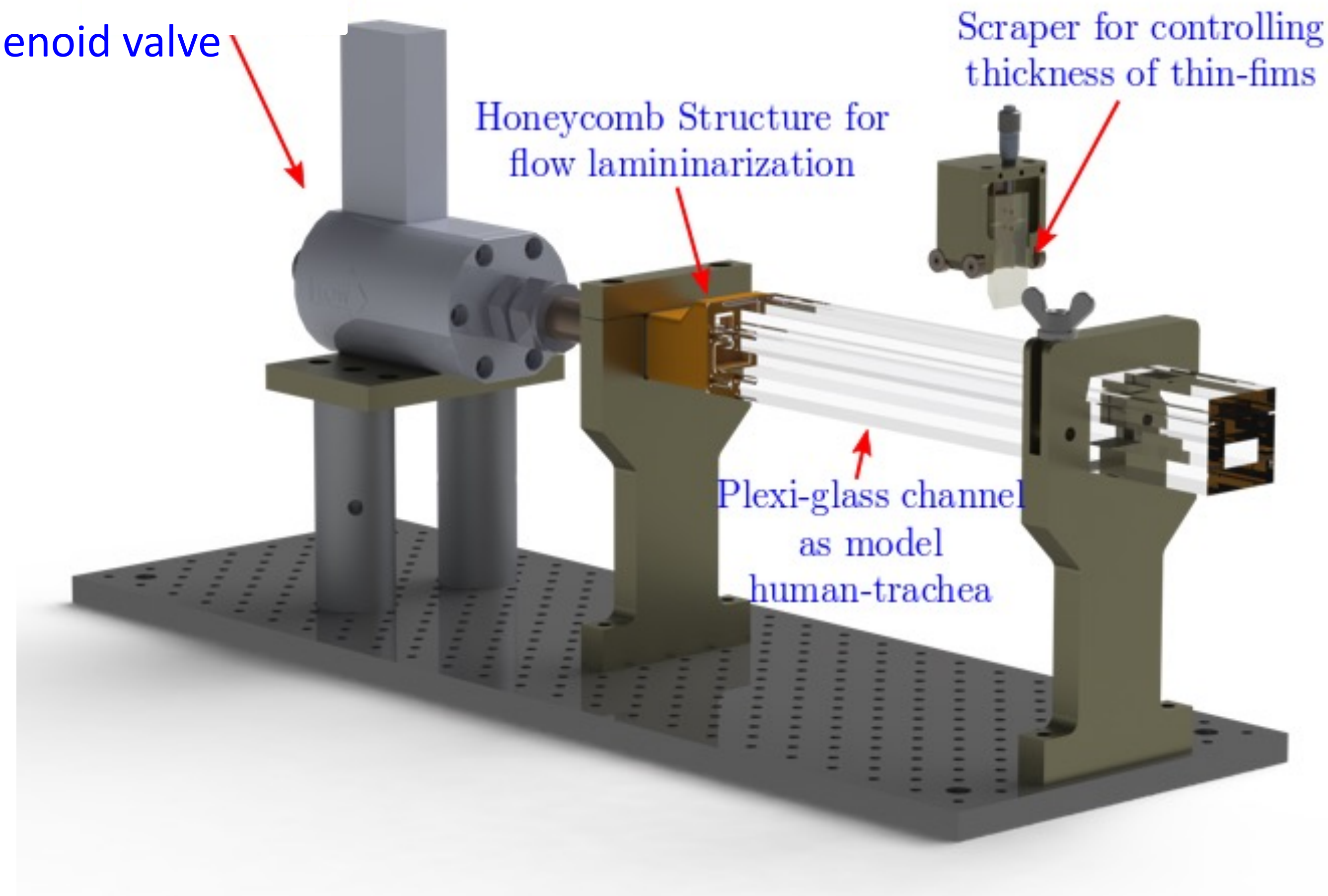

Cross-section 2 cm x 1cm

Experimental Parameters

- Liquid film : water-glycerol mixture
- Liquid viscosity : 2 – 100 10^{-3} kg m^{-1} s^{-1}
- Surface tension : 62 – 72 mN/m
- Flow velocity : 10 - 30 m/s

Droplet Generation

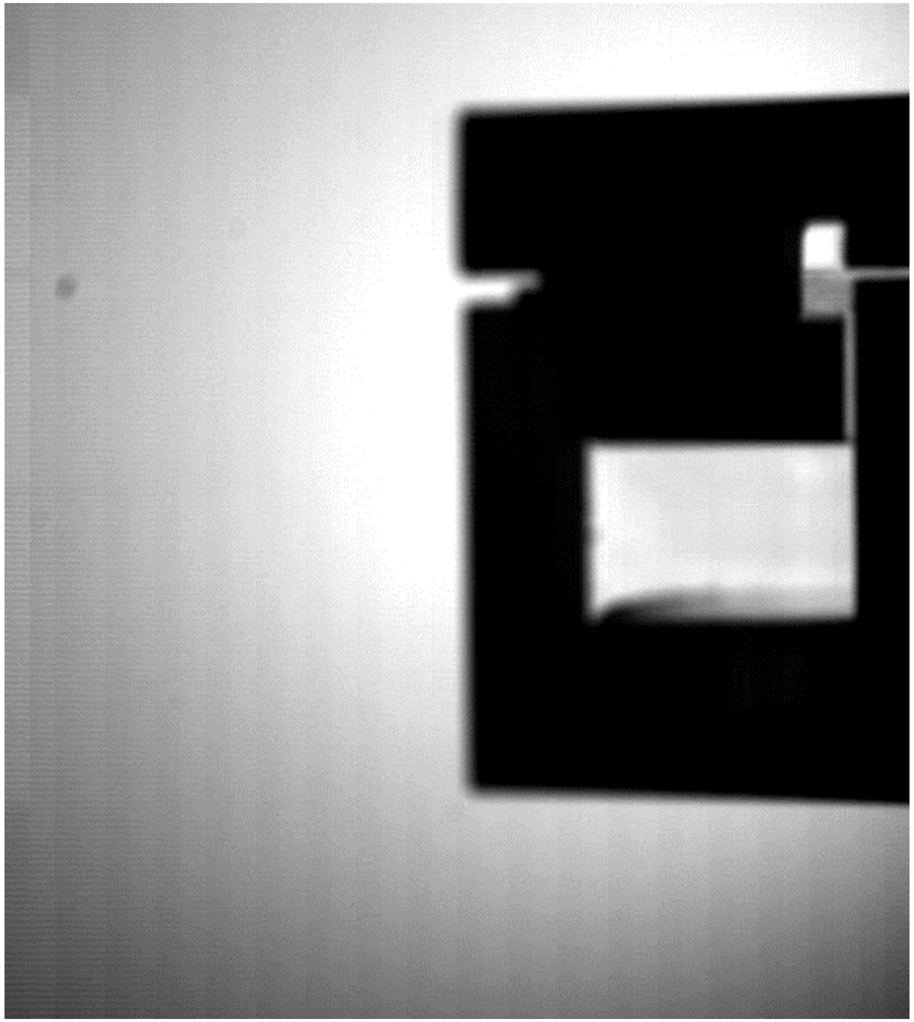

- Fine droplets are produced deeper in the channel
- Larger droplets form at the exit

Film Thickness $\mathcal{H}_{\mathrm{f}} = 1 \ \mathrm{mm}$
Mean Flow Velocity $U \sim 29 \ \mathrm{m/s}$

Experimental configuration

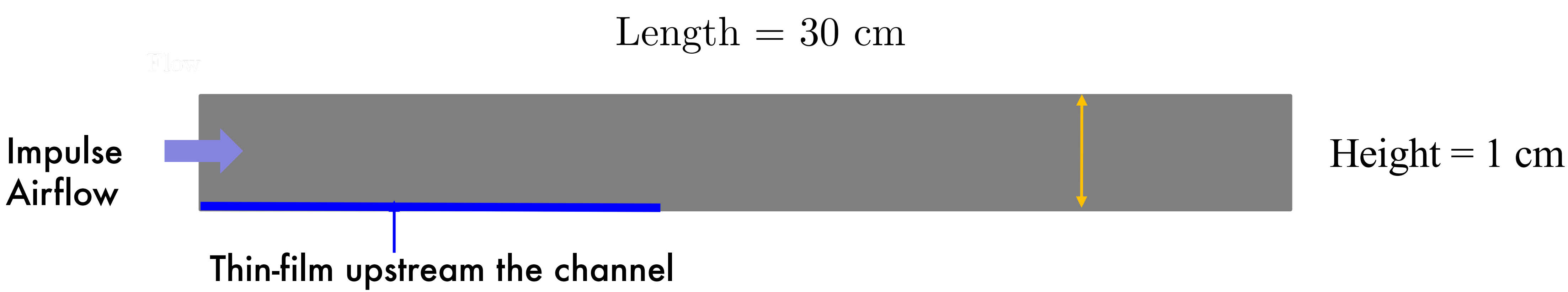

Atomization of a sheared-film

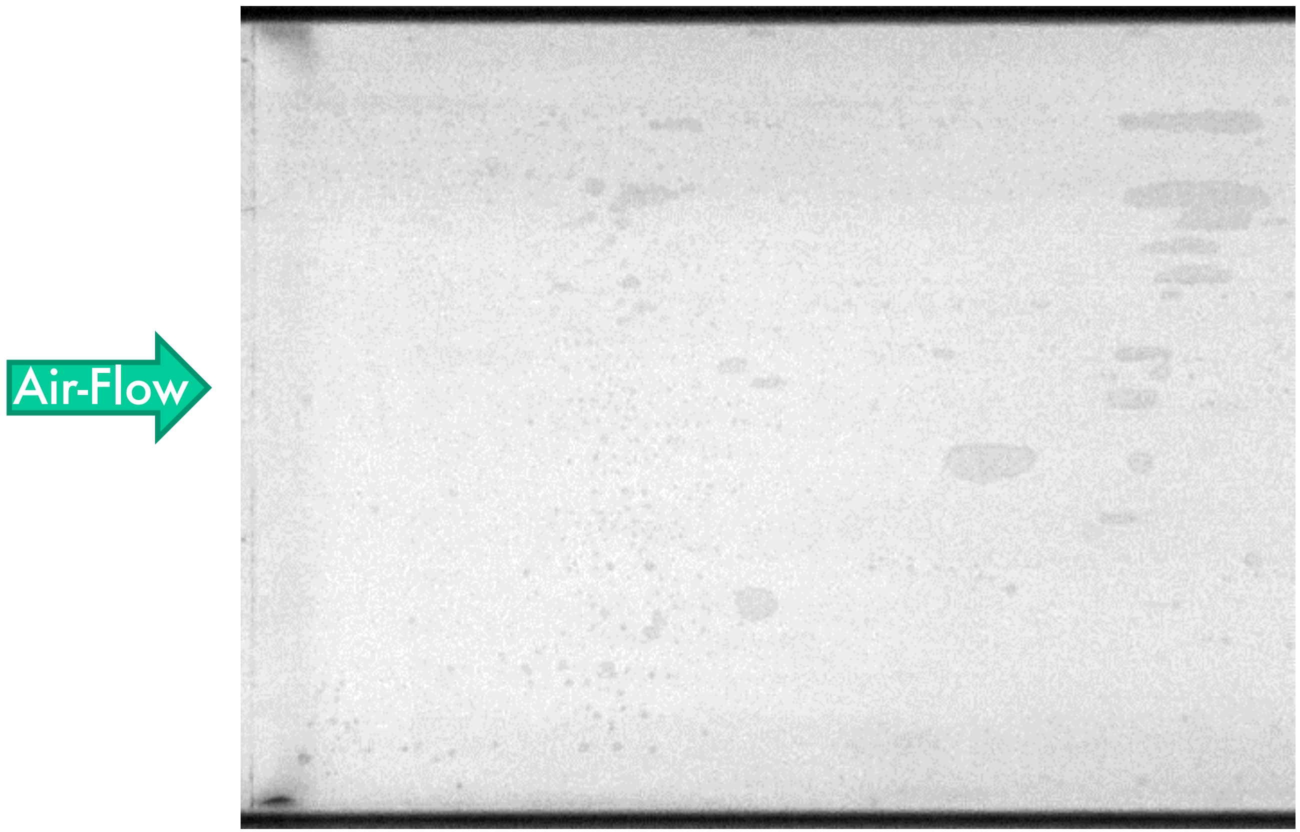

Top View

Film Thickness $\mathcal{H}_{\mathrm{f}} = 1 \ \mathrm{mm}$
Mean Flow Velocity $U \sim 15 \ \mathrm{m/s}$

`*Bag-mediated*' atomization of thin-film

Bag rupture mechanism

Example - 1

Example - 2

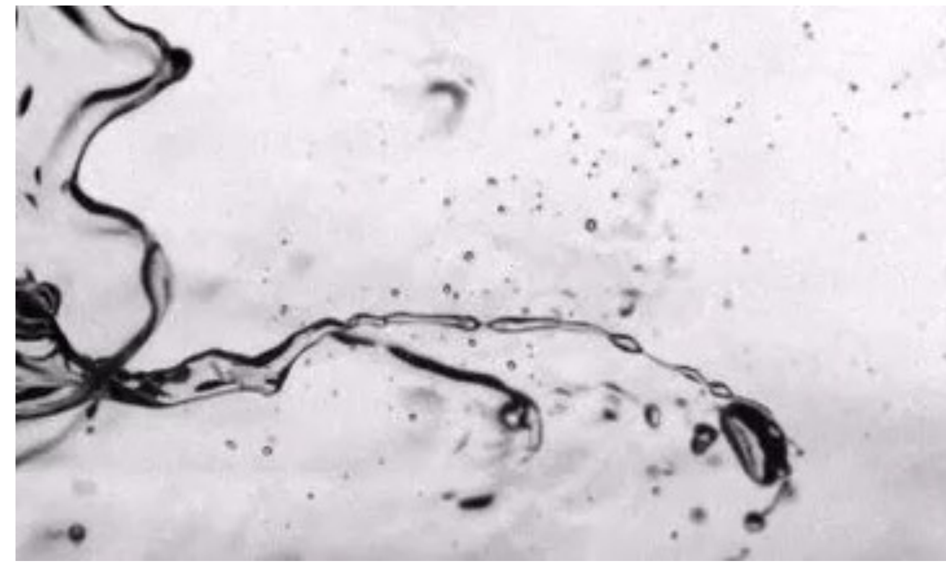

Bag rupture mechanism: Weak Spots

Example - 1

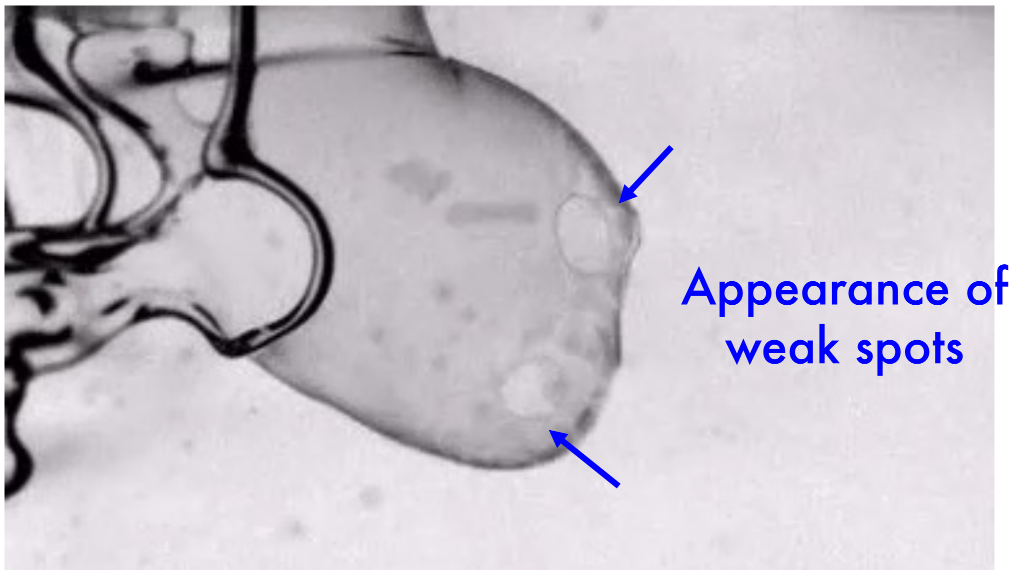

Example - 2

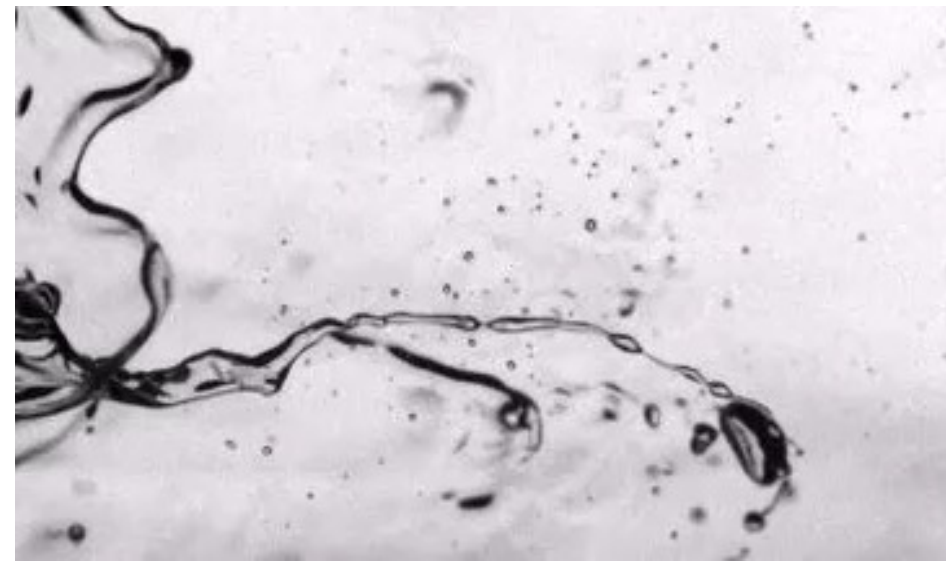

Unstable motion of retracting sheet generates small droplets $d \leq 50\,\mu\text{m}$

Bag rupture: Appearance of Weak Spots

Example - 1

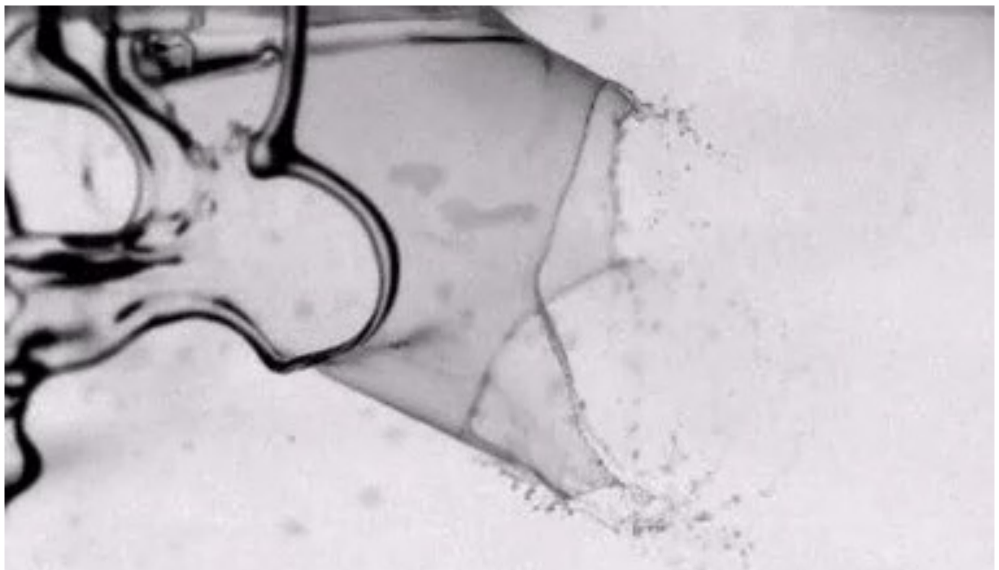

Example - 2

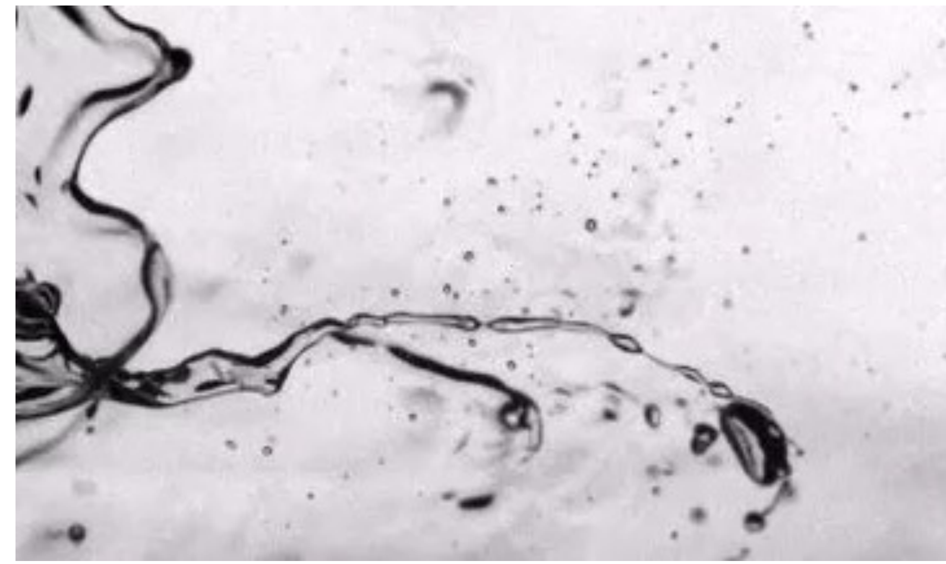

Finally the breakup of rim creates larger droplets

$d > 200\,\mu\mathrm{m}$

Thickness ?

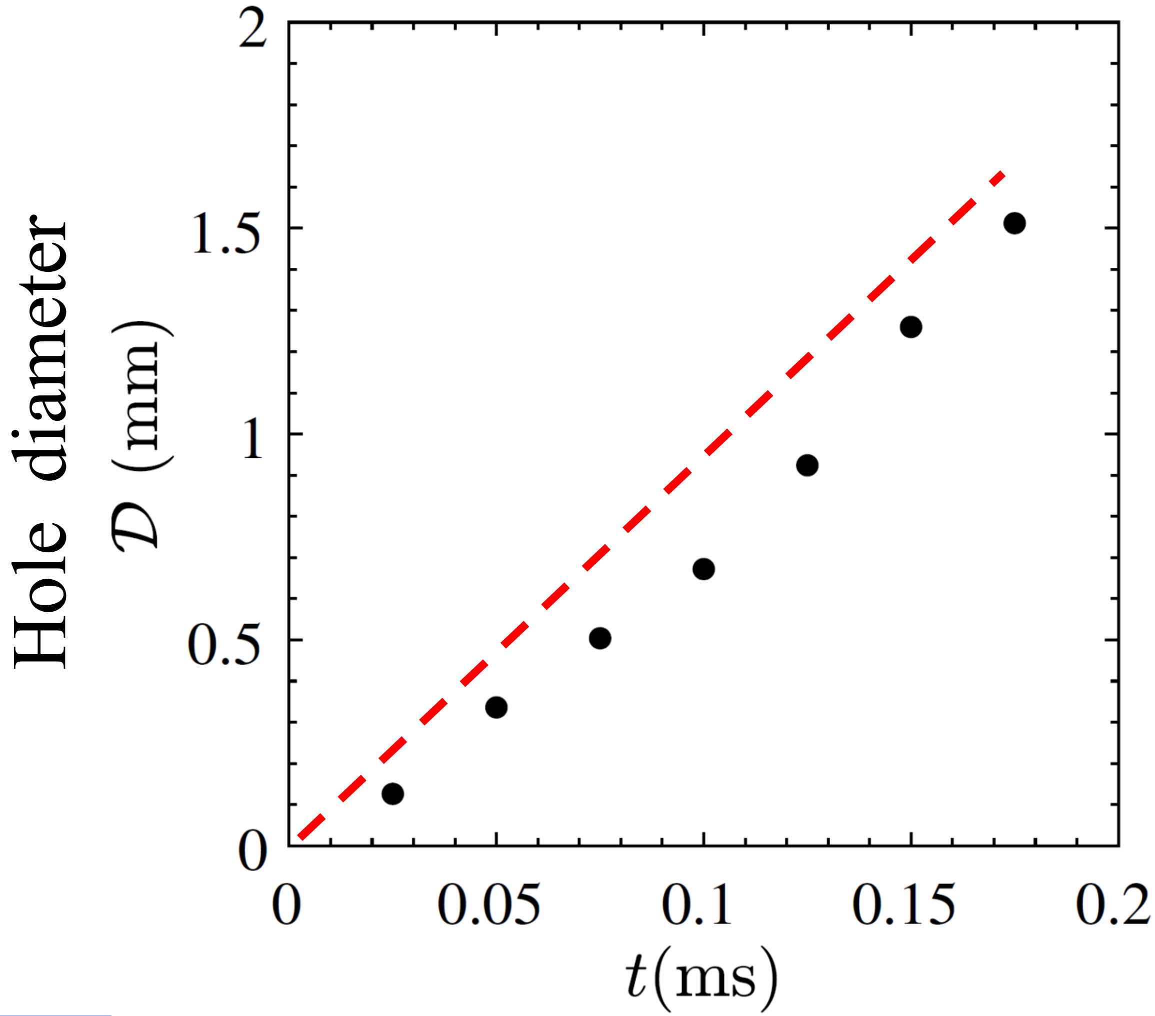

$$V_{\mathrm{retract}} = \left(\frac{2\,\sigma}{\rho\, h_{\mathrm{bag}}}\right)^{1/2}$$

By measuring retraction velocities we estimate bag thickness at the instant of rupture

Droplet Size Distribution

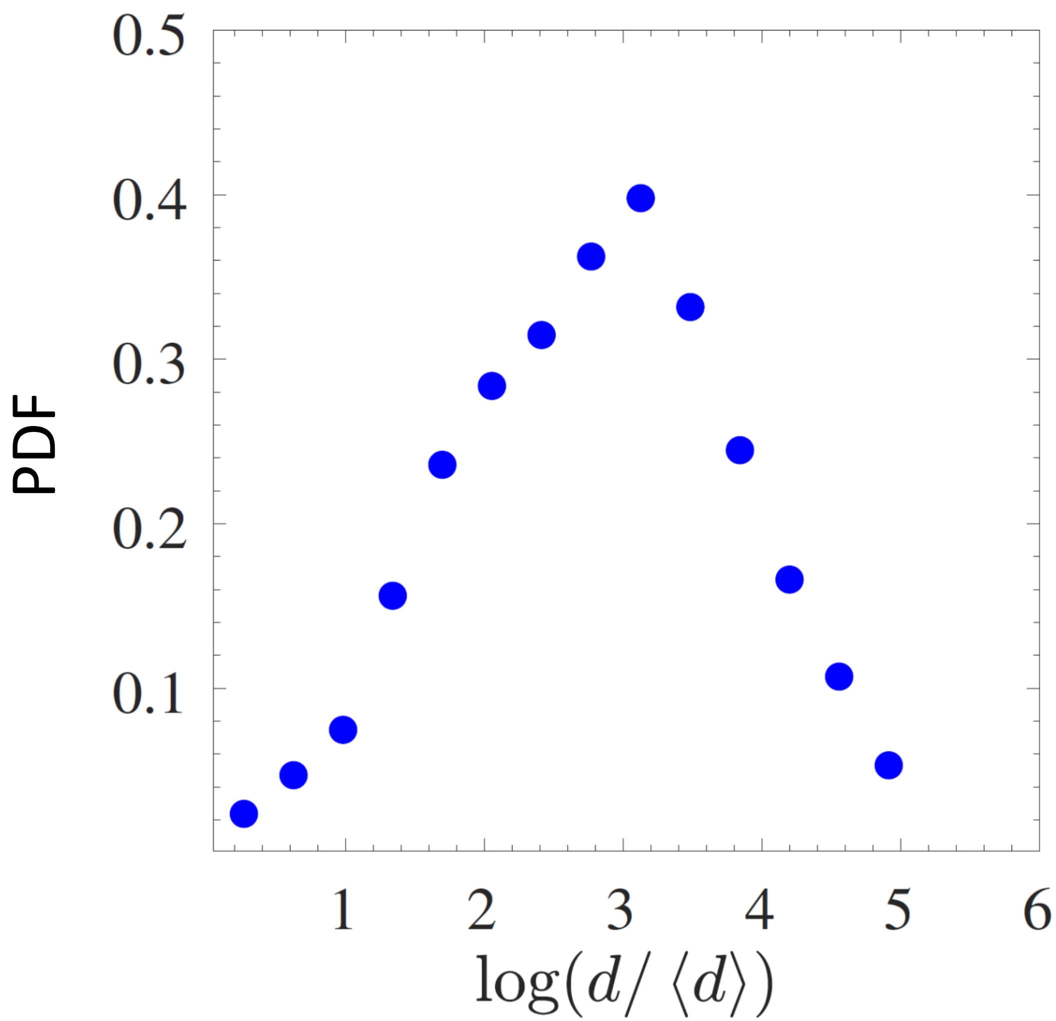

$\nu = 5$ cst

Droplet size distribution : Log-normal

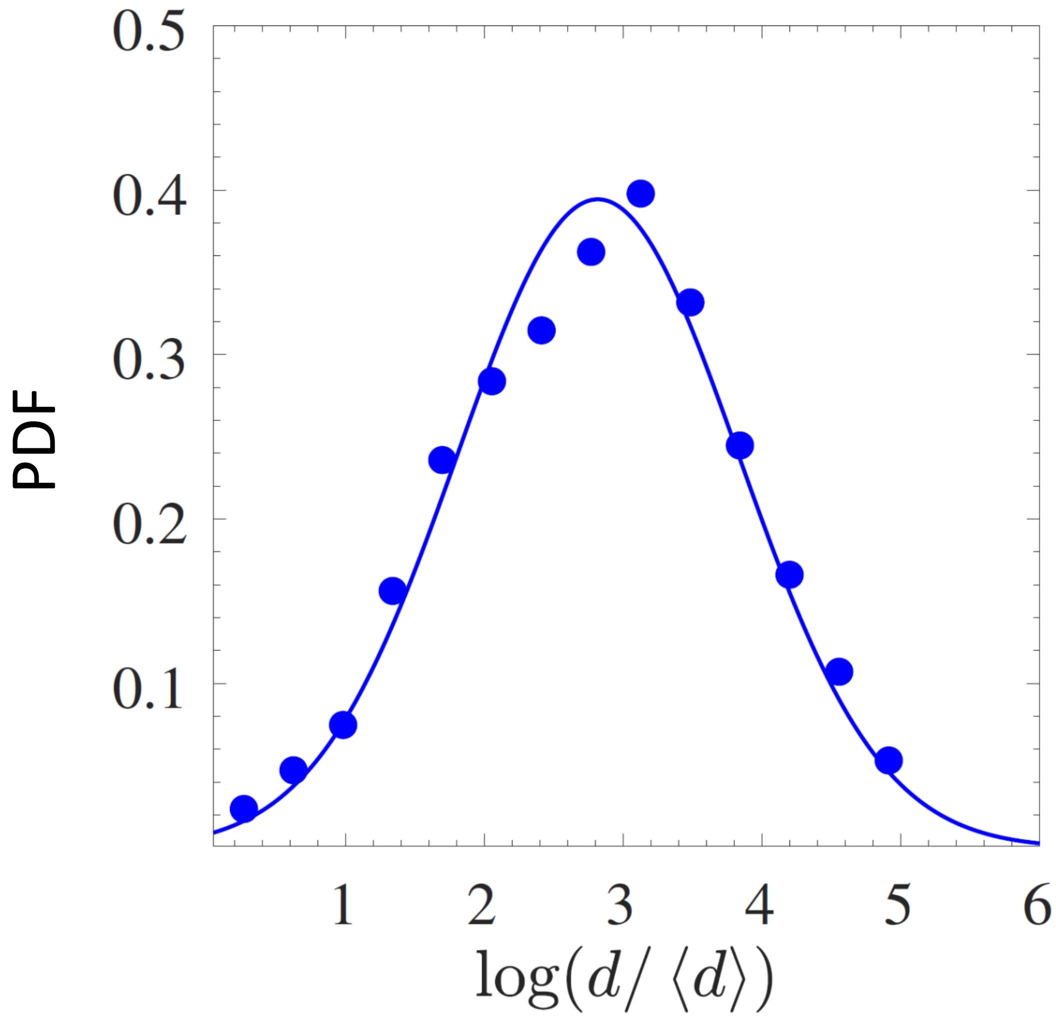

$\nu = 5$ cst

Droplet size distribution : Influence of viscosity

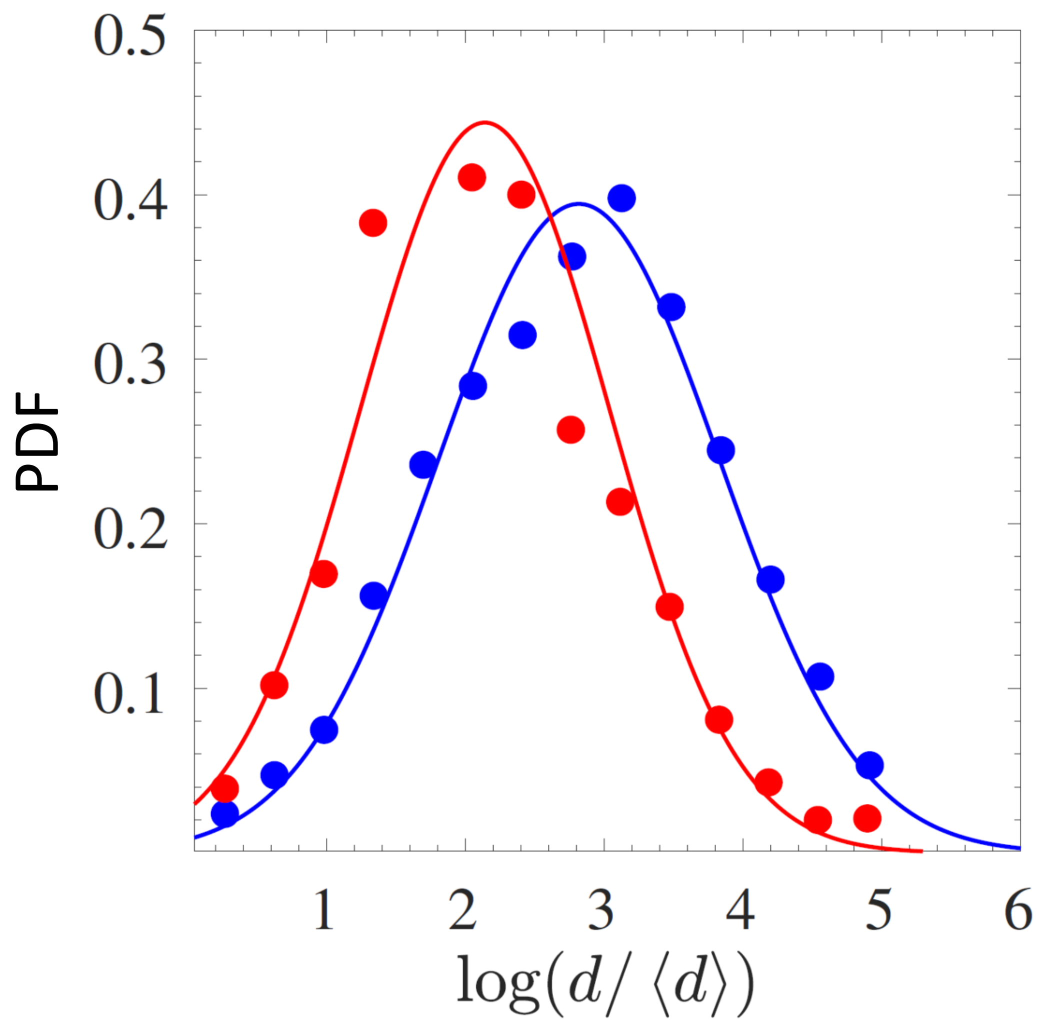

$\nu = 5$ cst
$\nu = 75$ cst

Influence of viscosity: Deeper and Wider bags

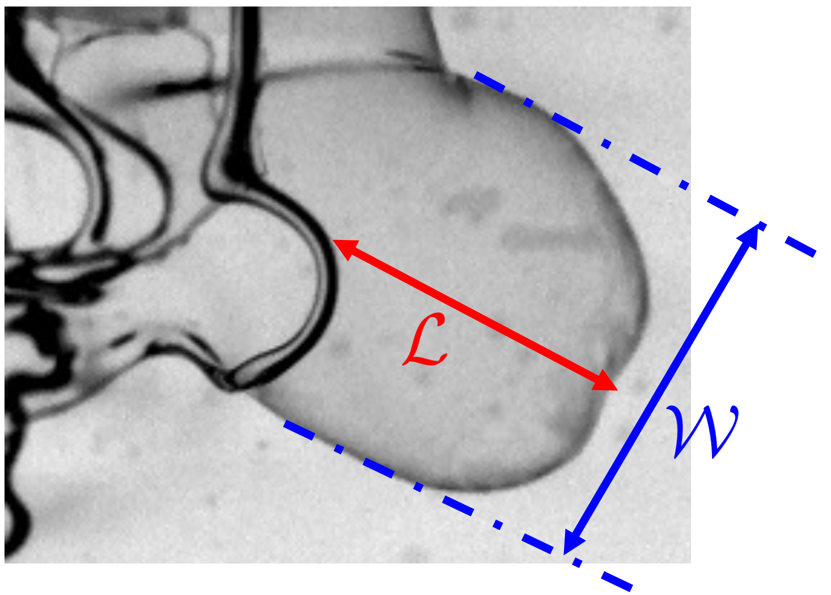

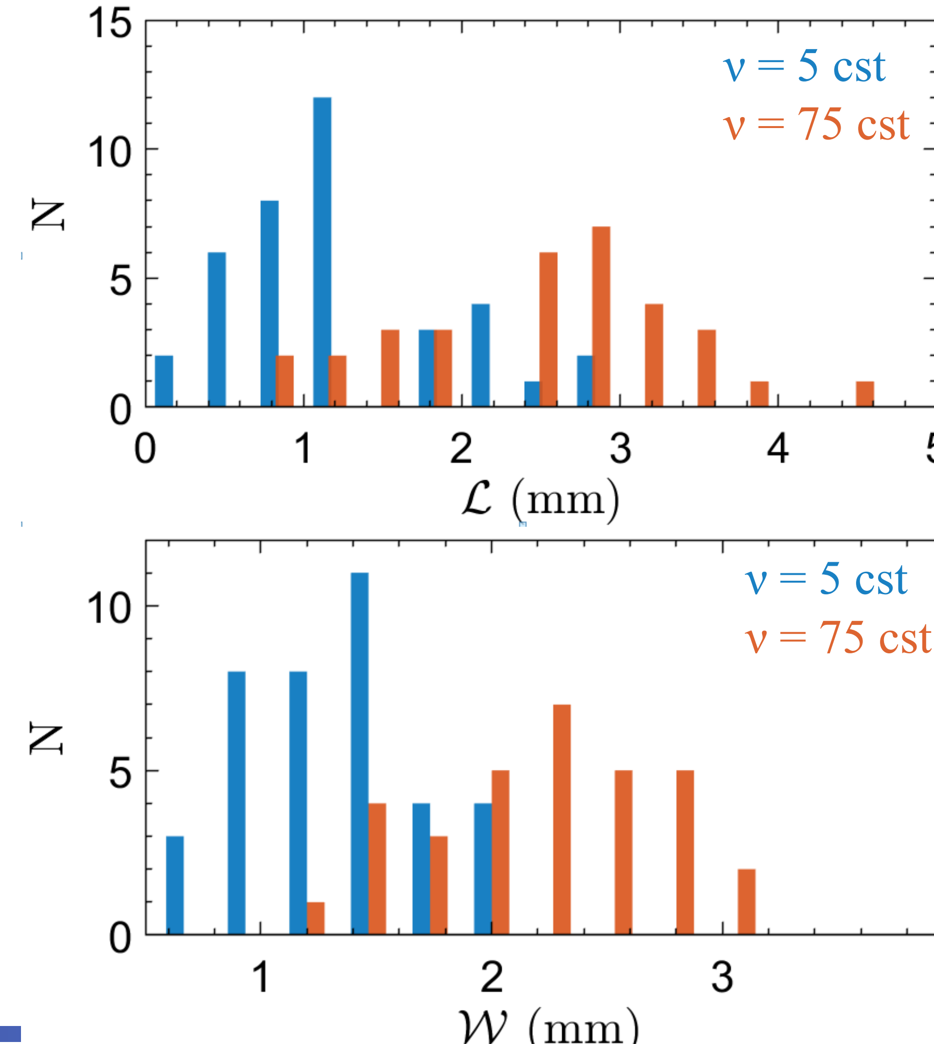

Influence of viscosity: Bag thickness

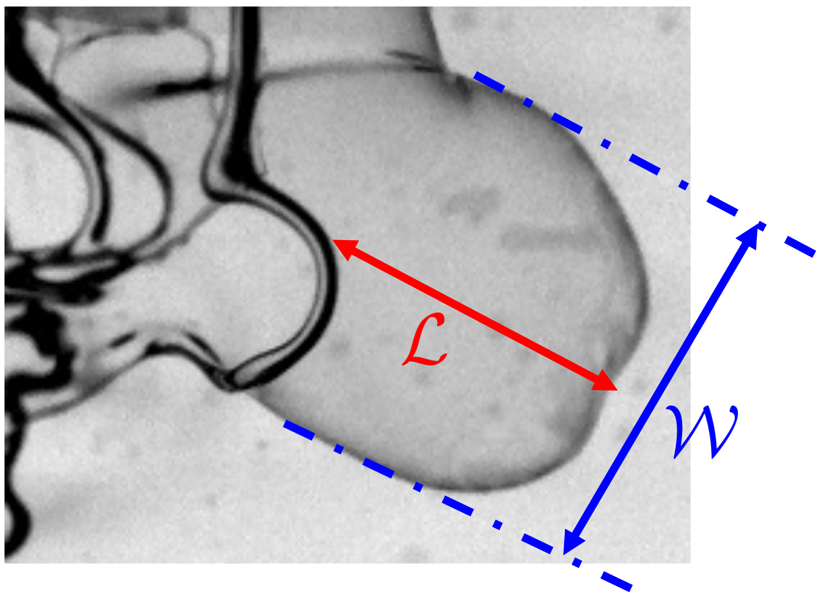

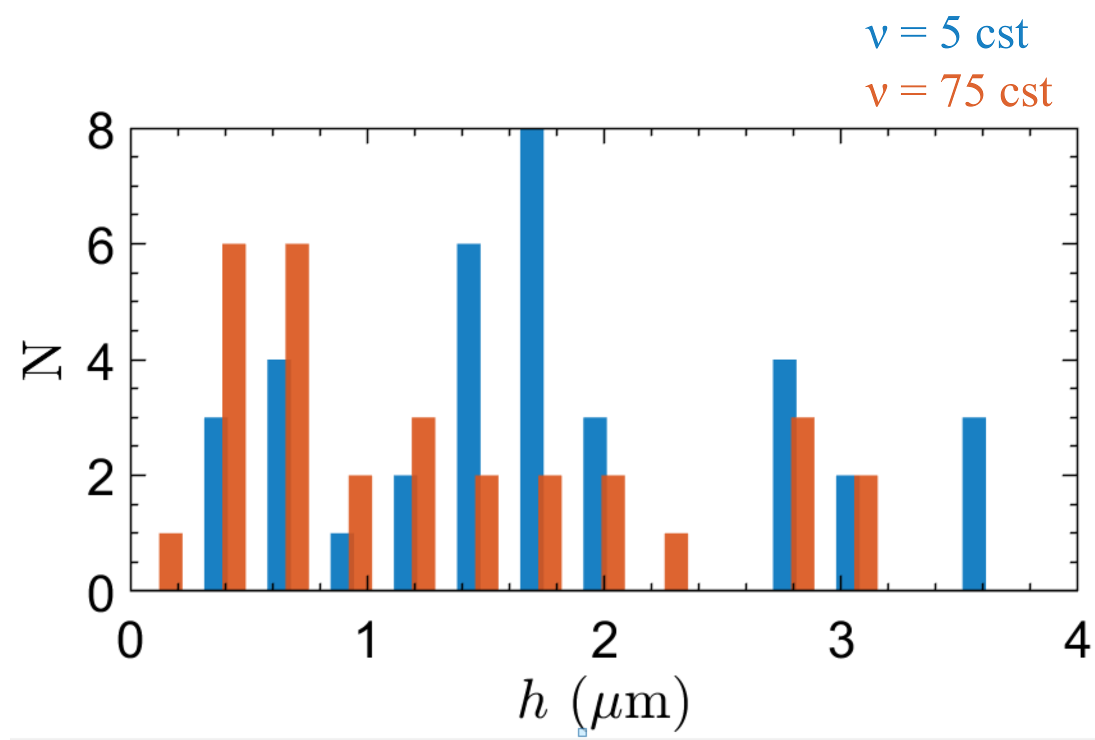

Experimental Conclusion

Viscosity promotes formation of deeper, wider and thinner bags, thus smaller droplets are generated.

Numerics of cough

with Cesar Pairetti

octree grid (basilisk code by S. Popinet)

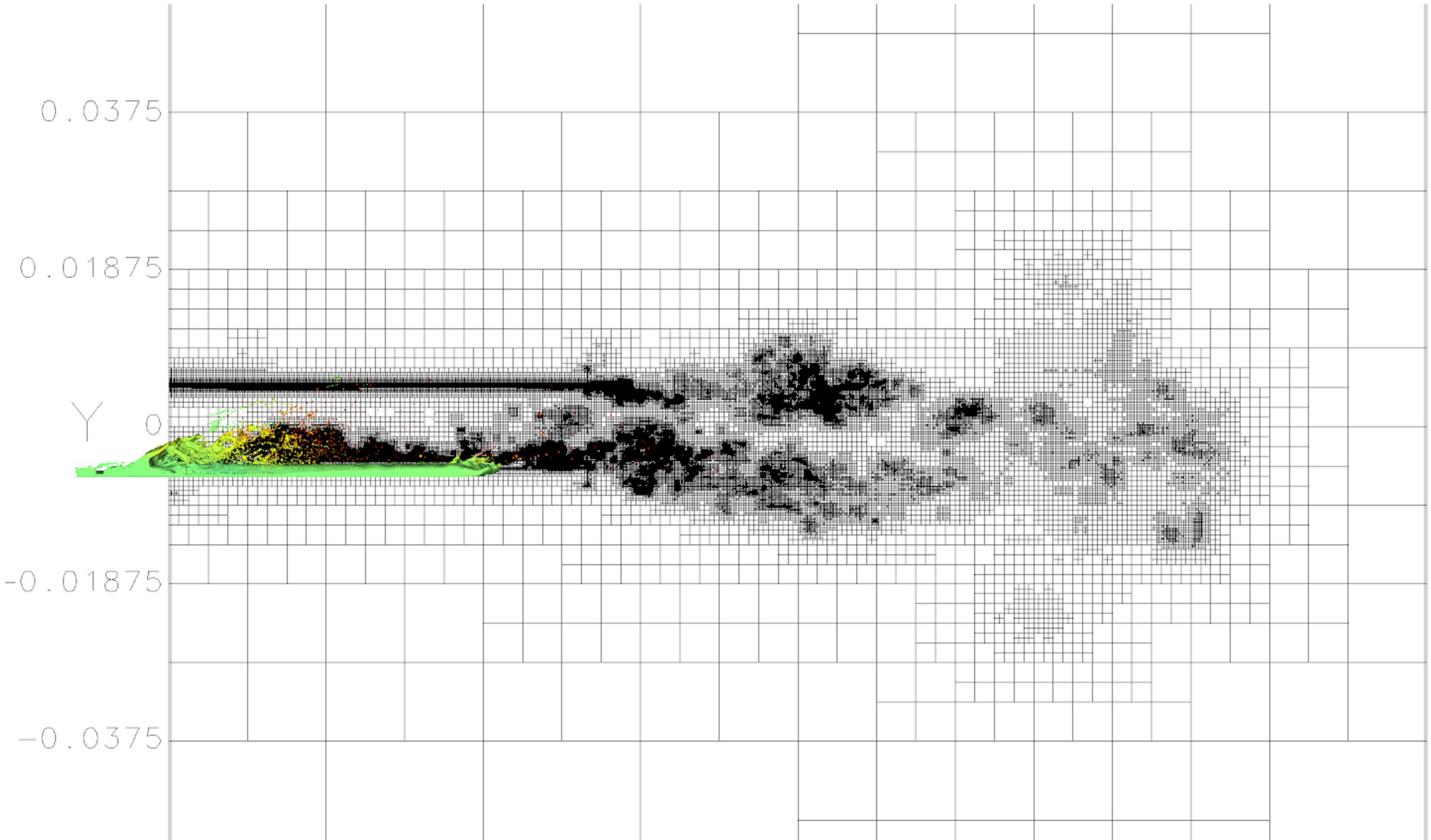

Sheet inflation and perforation regimes

The experimental setup allows to study more viscous configurations, closer to saliva properties (silicon oil experiments). Air velocity during sneeze can also be smaller.

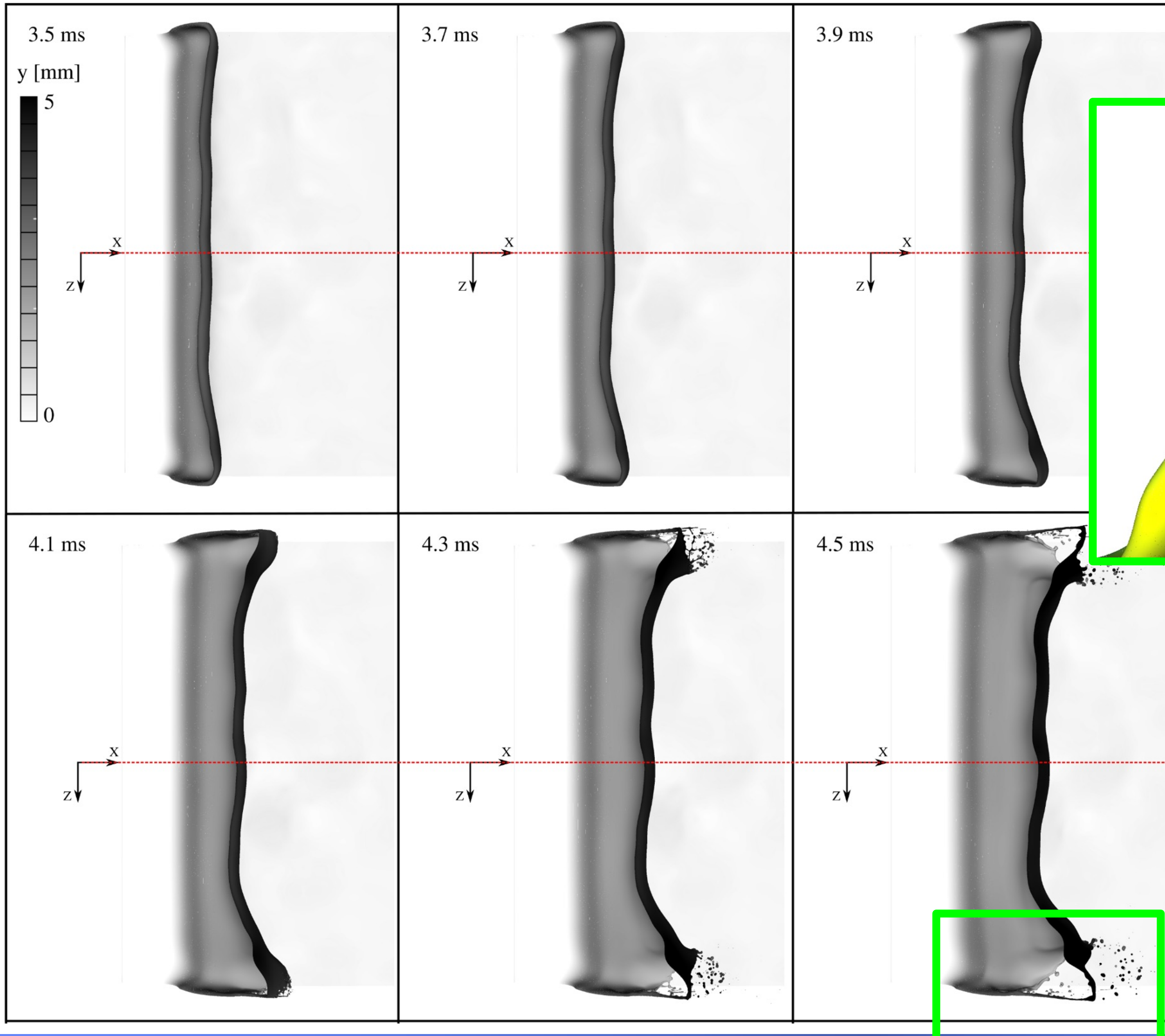

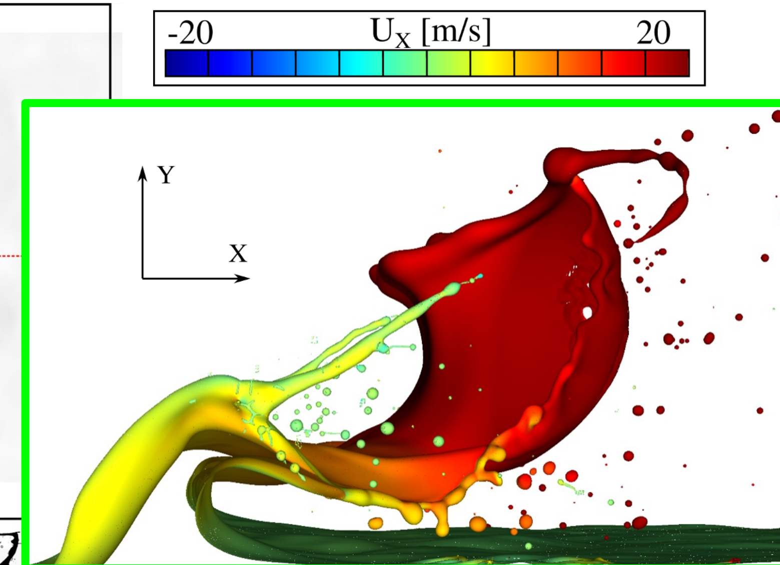

Laminar flow

U= 15 m/s

$$We_a = \varrho_a U^2 l_y / \sigma = 40$$
$$Re_a = \varrho_a U l_y / \mu_a = 9{,}700$$
$$Re_l = \varrho_l U h / \mu_l = 300$$

The liquid sheet close to the side wall deforms faster, thinning rapidly until perforation. The hole expansion forms ligaments that eventually fragment.

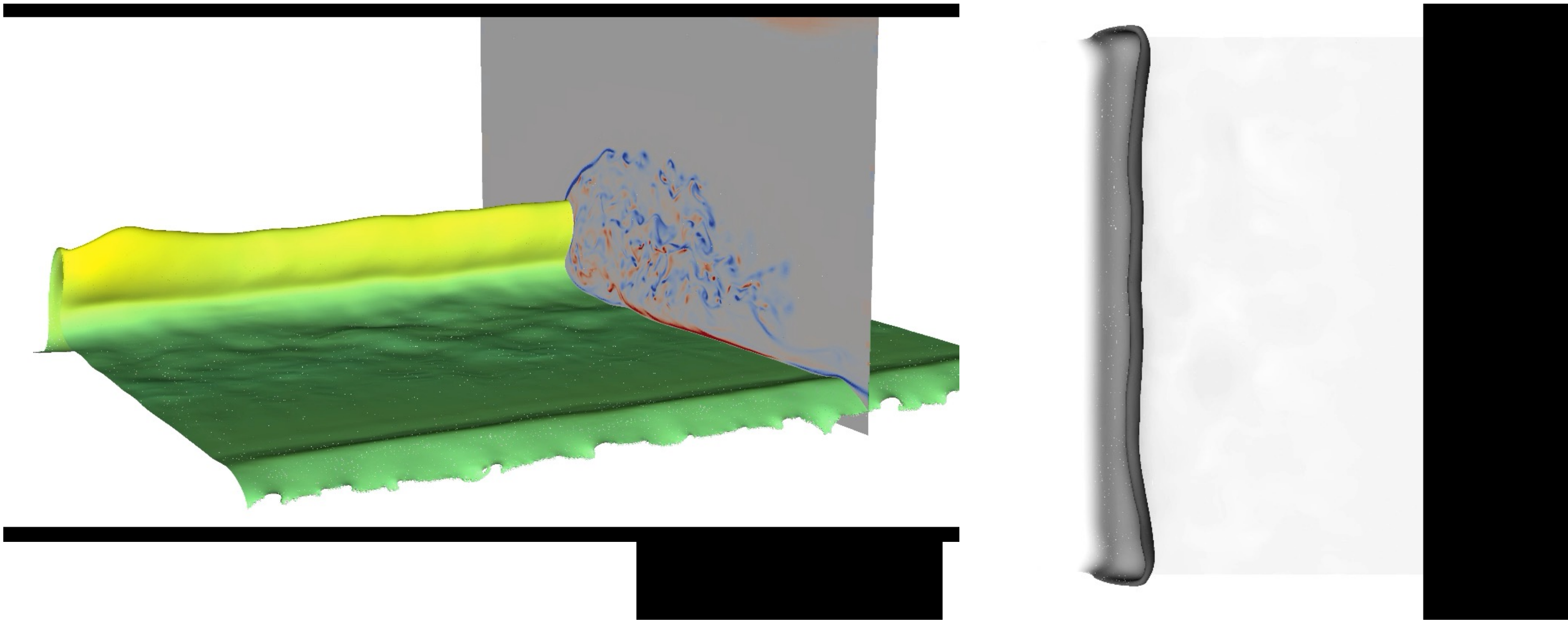

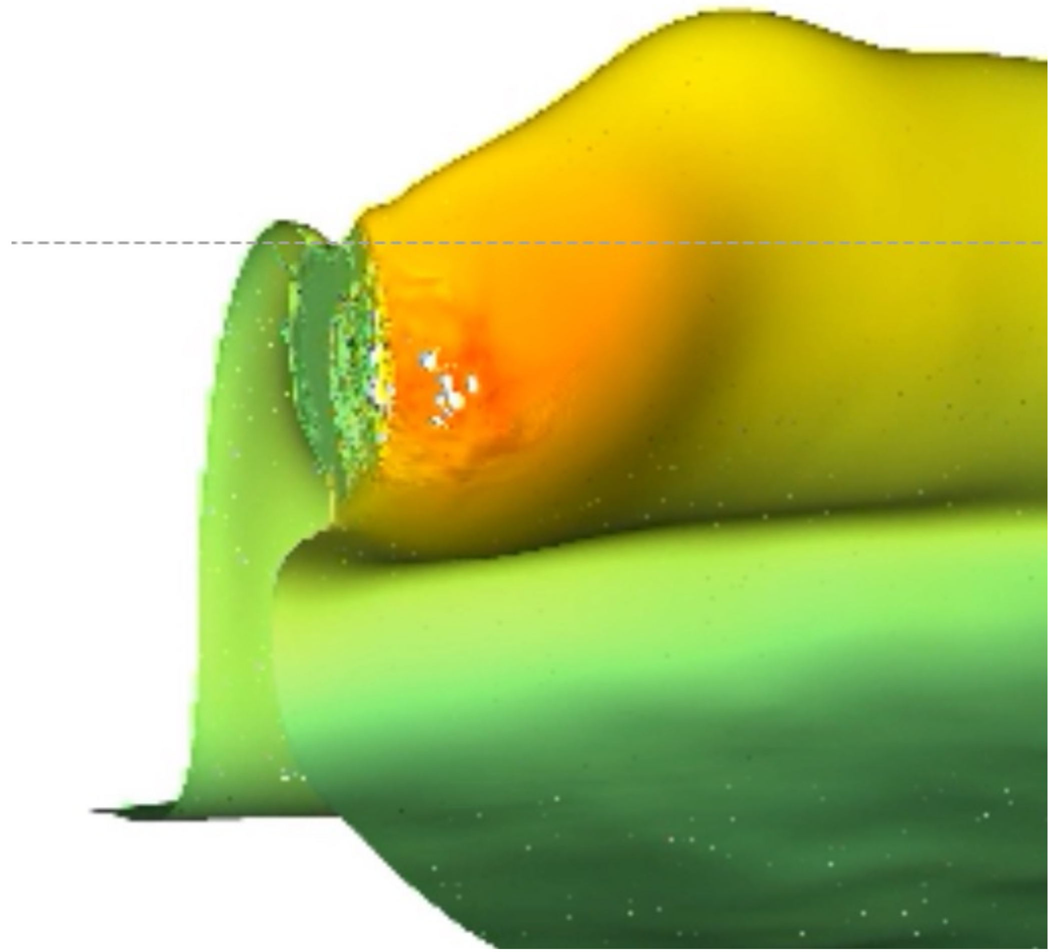

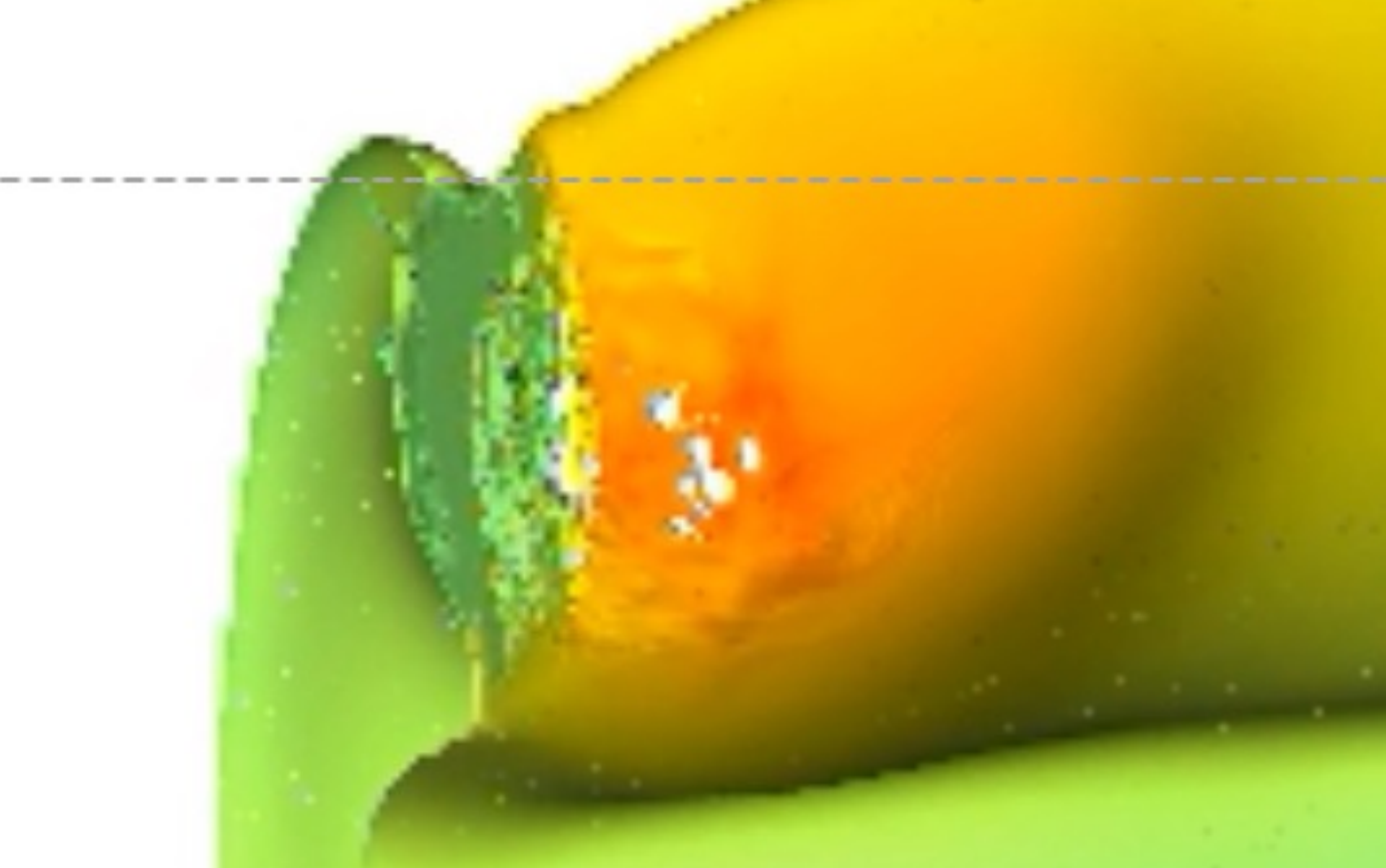

Distribution of droplet sizes. Most refined simulation seems converged for d > 4 Δx_min. The slope fitting Pareto shows some real cough experiments (Xie et. al. 2009), *but small drops are over-predicted. → no log normal seen.*

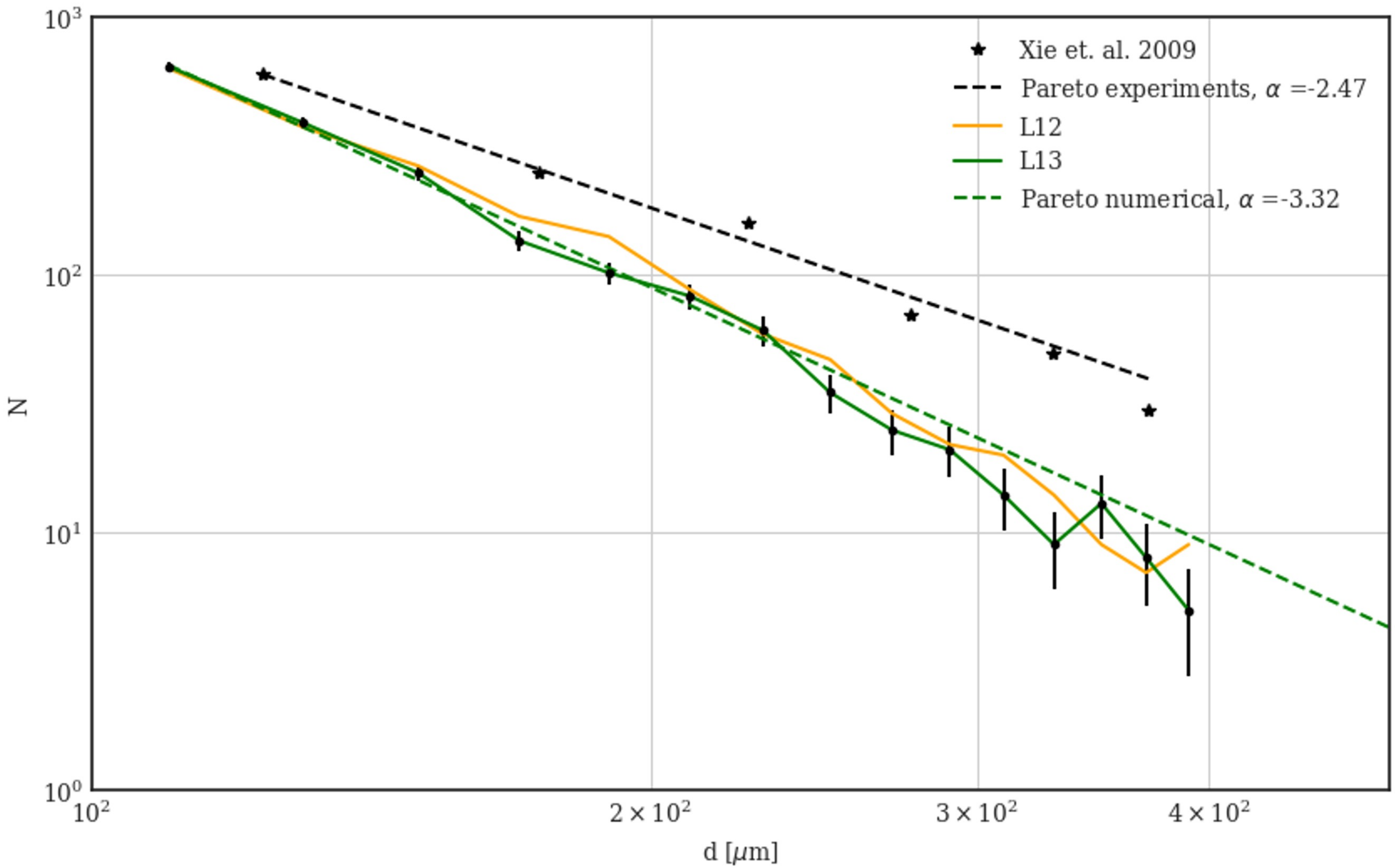

Ligament formation is similar to experiment.
We still need more computer power to determine the droplet size.

Beyond cough : atomization in general has progressed at an amazing pace

In 2004 about 5 million grid points

Bianchi Scardovelli Zaleski SAE

+ Berlemont, Hermann, Desjardins, Le Chenadec & Pitsch, Ashgriz, Sirignano ...

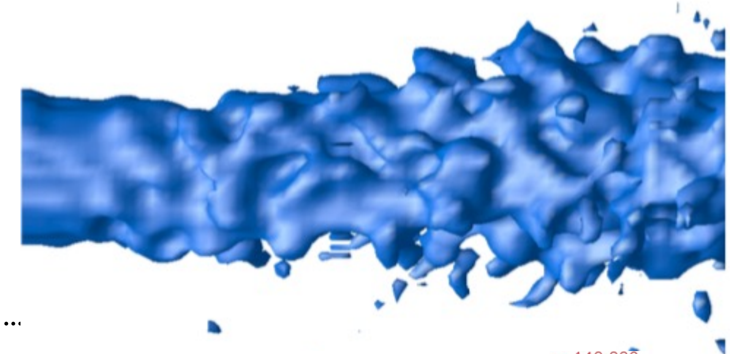

In 2010 about 6 billion grid points.
2 million CPU hours on 5760 cores.

Shinjo & Umemura. IJMF 2010

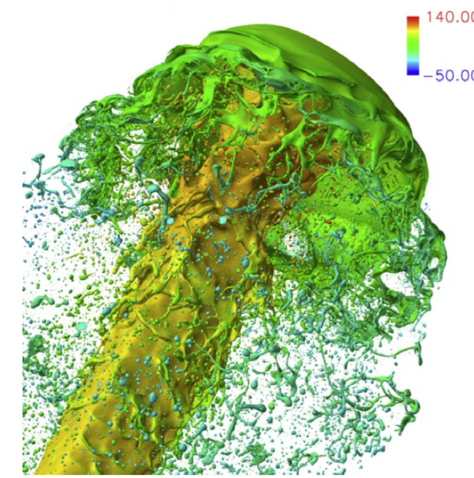

In 2016 adaptive simulation
« equivalent » to 64 billion grid points
10 thousand CPU hours on 1356 cores.

S. Popinet http://basilisk.fr/src/examples/atomisation.c

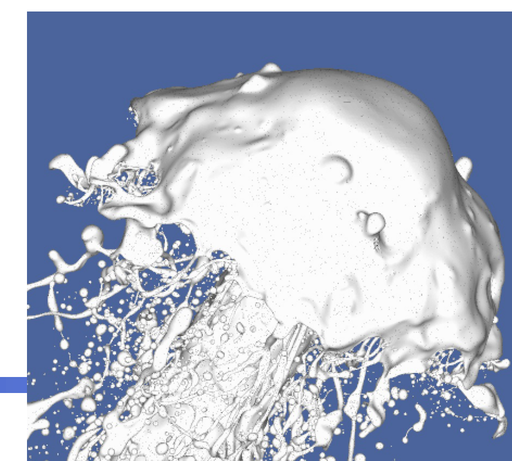

In 2021 the equivalent of 4 trillion grid points was reached by my students Y. Kulkarni and R. Villiers.

How ?

How ?

- 1 Compute an evolving surface : computational geometry

- Solve

  2 the Navier-Stokes or Stokes equations with

  3 surface tension

and

  4 variable viscosity and density

1. Compute surface evolution

it is a kind of computational geometry

Why is it difficult to follow evolving surfaces ?

- geometrical complexity (curved surfaces, how they cut – change topology)

- numerical stability issues of the most obvious methods.

- accuracy issues (high accuracy is needed: surface tension effects depend on the third derivative of the interface position.)

1. Compute surface evolution

Two formulations:

1) express surface velocity:

$$V_S = \mathbf{u} \cdot \mathbf{n}.$$

2) Use the characteristic function χ=1 in phase 1 and χ=0 in phase 2.

$$\partial_t \chi + \mathbf{u} \cdot \nabla \chi = 0.$$

The Piecewise Linear Interface Reconstruction Volume-of-Fluid method

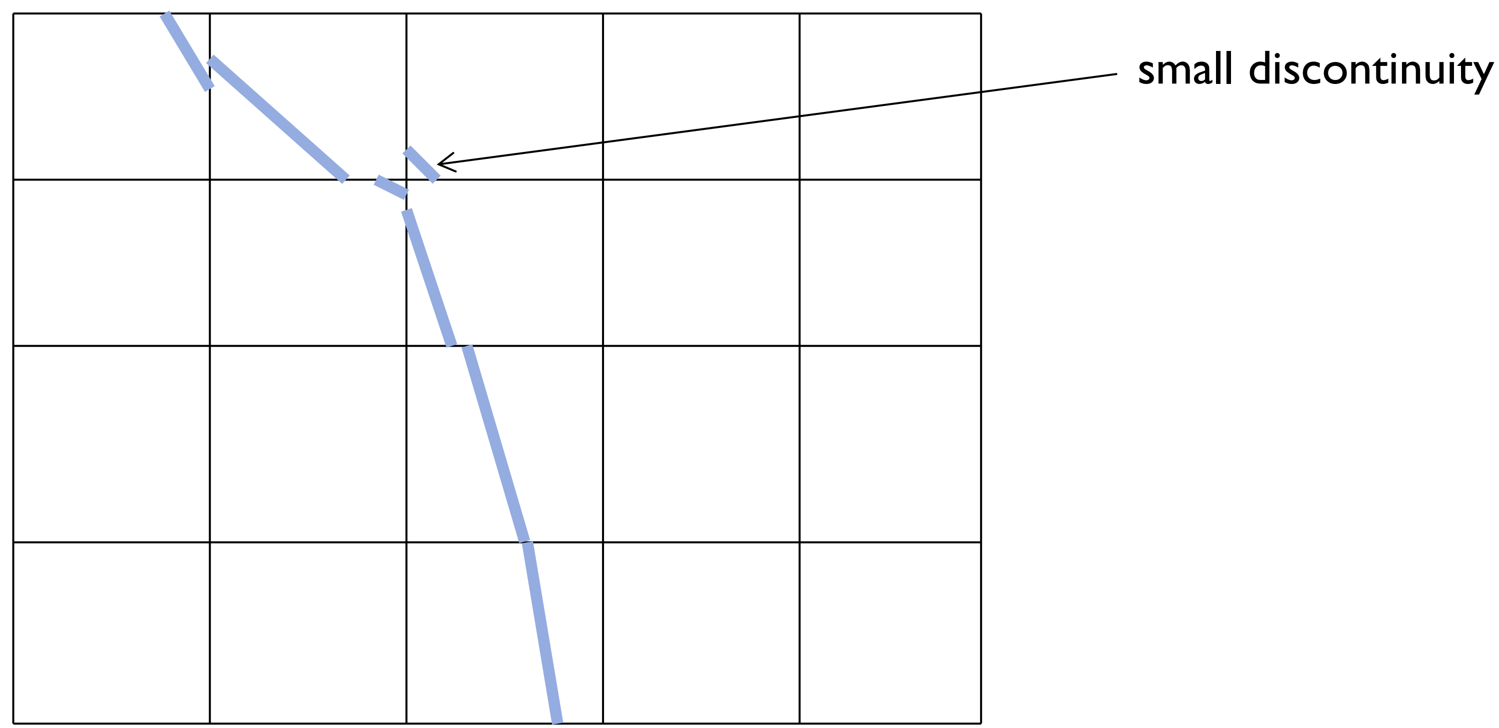

Cij = Volume of « fluid » in cell ij. We consider a relatively accurate version of VOF which may be considered « tracking » rather than « capturing ».

Two kinds of VOF methods:

- « off the shelf » methods for hyperbolic PDE / gas dynamics. (OpenFoam, JADIM etc. .)

- methods involving geometric operations (Surfer, Gerris, Basilisk, ParisSimulator)

Conclusions: excellent results obtained by VOF methods

Variable density

- use momentum-conserving methods (Rudman, Raessi and Bussman, Le Chenadec, Berlemont, Ménard etc..) : Advect the momentum near the interface using the same scheme used for the VOF color function.

- use extrapolation methods (Sussman et al., Xiao, Dianat & Mc Guirk) : extrapolate the liquid velocity field in gas nodes.

- combine above methods with flux limiters.

- filtering

need other ideas: for instance, doing a falling rain drop of 1,5 mm is already very difficult and requires 200 grid points / diameter.

An example of a difficult high Re flow: raindrops

The problem has large air/water density ratio + surface tension.

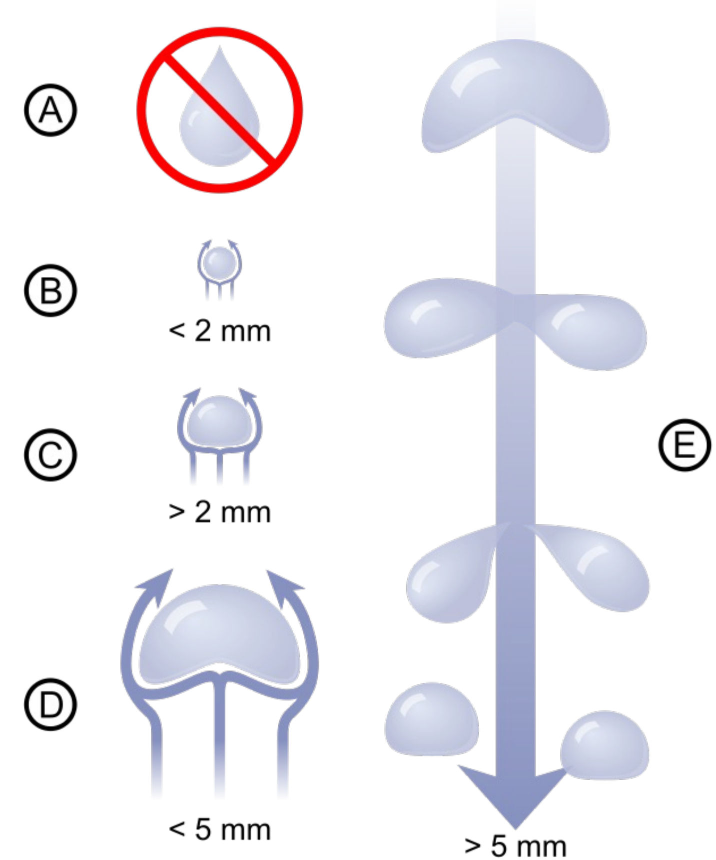

diameter d=8 mm

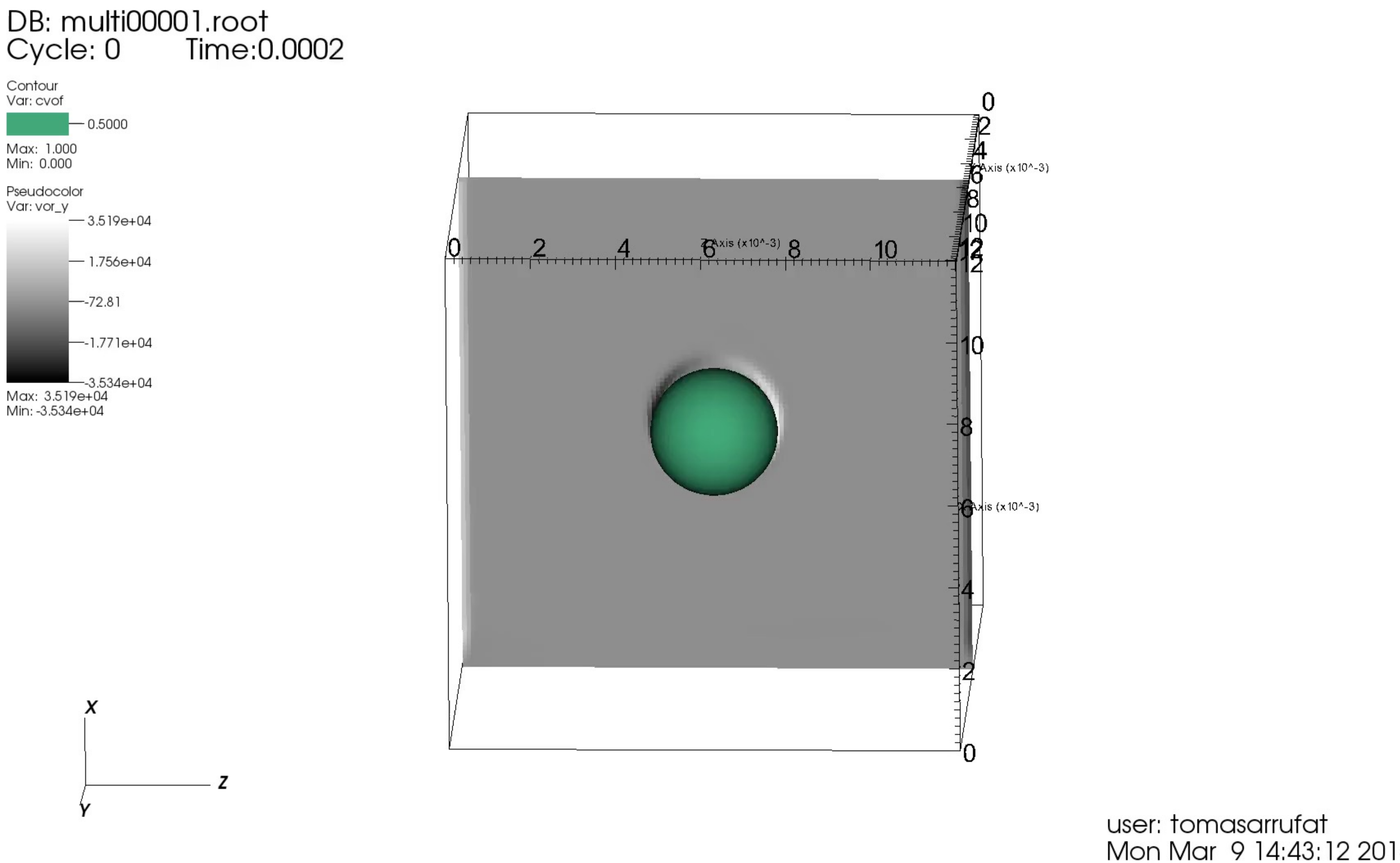

Intermede: CFD in the movies

Antz

Back to experimental science / engineering

Grenoble experiment

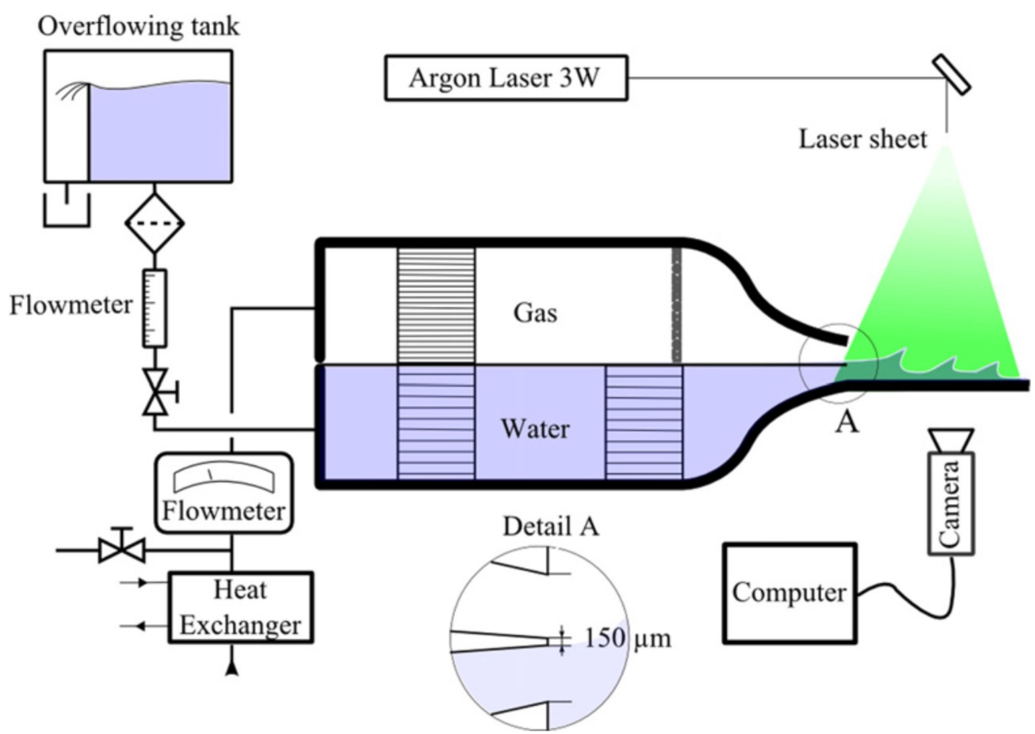

Descamps et al, 2008
Matas et al., 2011
Jérôme et al, 2013
Fuster et al, 2013
Ling et al 2015

and Hopfinger, Lasheras, Cartellier, Villermaux, Hoepffner, Popinet, Boeck, Rossi ...

2D simulations of the planar « Grenoble » setup.

The Grenoble quasi 2D experiment set up

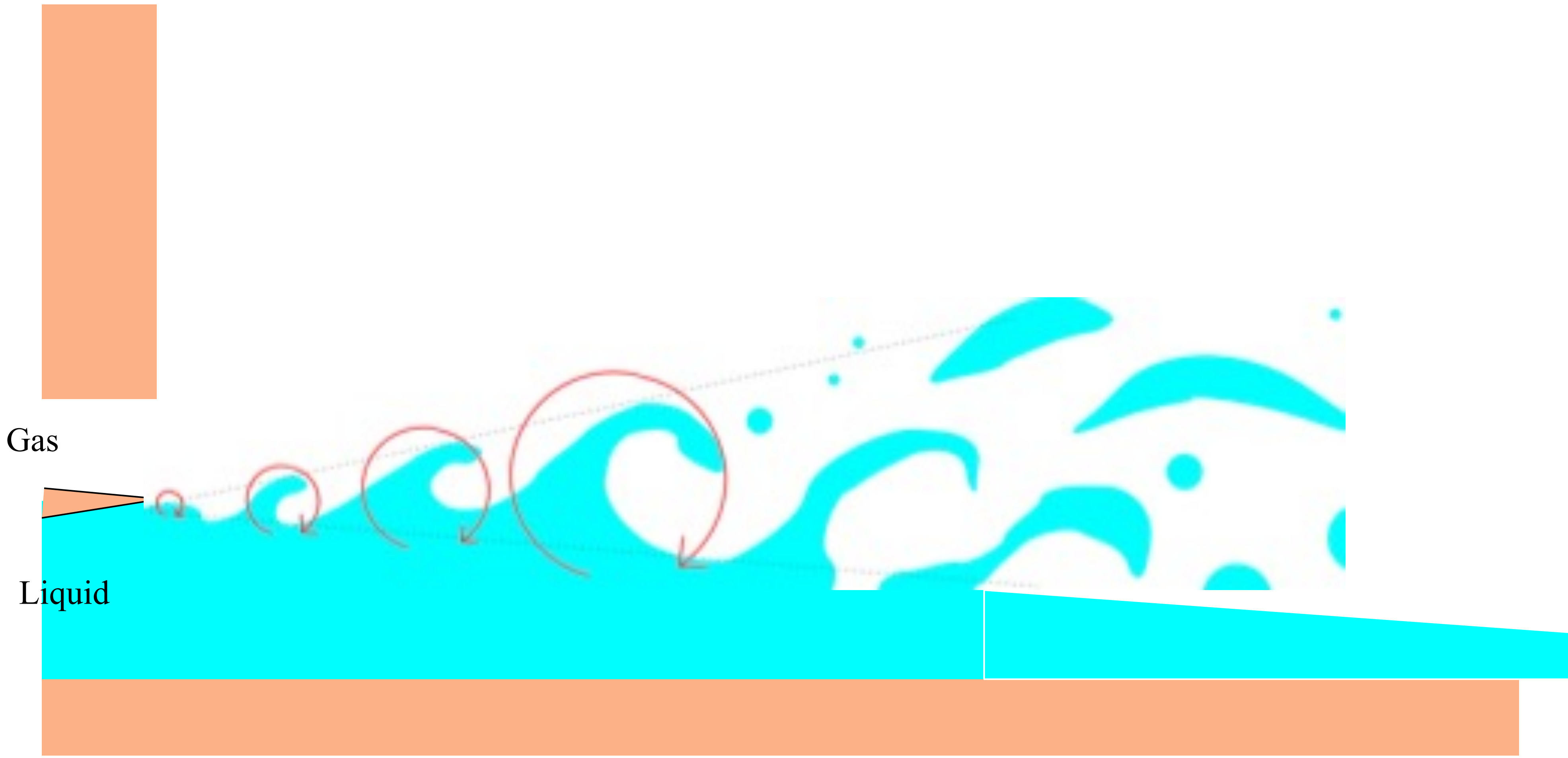

Atomizing 3D flows:

In 2015, real air-water parameters in ambient conditions were still too hard for a 3D detailed simulation.

Thus we designed a *synthetic case*. Parameters are chosen so that there is significant droplet production while avoiding exceedingly large Reynolds and Weber numbers to allow converged simulation.

At the time this project started, we did not have a good octree parallelising code, so « ParisSimulator » was developped by Gretar Tryggvason, Stanley Yue Ling, Daniel Fuster, Ruben Scardovelli and others.

Near perfect scaling

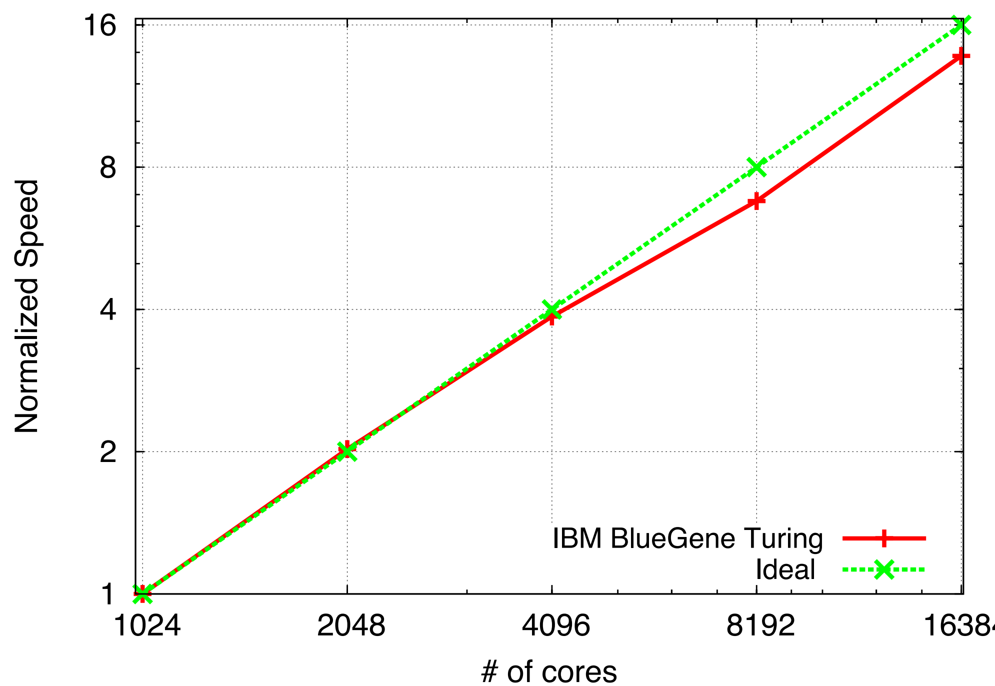

The trick ?

- regular grid
- simple local methods such as VOF
- simple linear algebra (either in-code multigrid Poisson solver or even simpler relaxation schemes)

"A20" synthetic case: dimensional values

	Density kg/m^3	Viscosity Pa-s	Surface Tension N/m	Jet Height H mm	Boundary Layer mm	Injection Velocity m/s
Gas	50	$5\ 10^{-5}$	0.05	0.8	0.1	10
Liquid	1000	10^{-3}		0.8	0.1	0.5

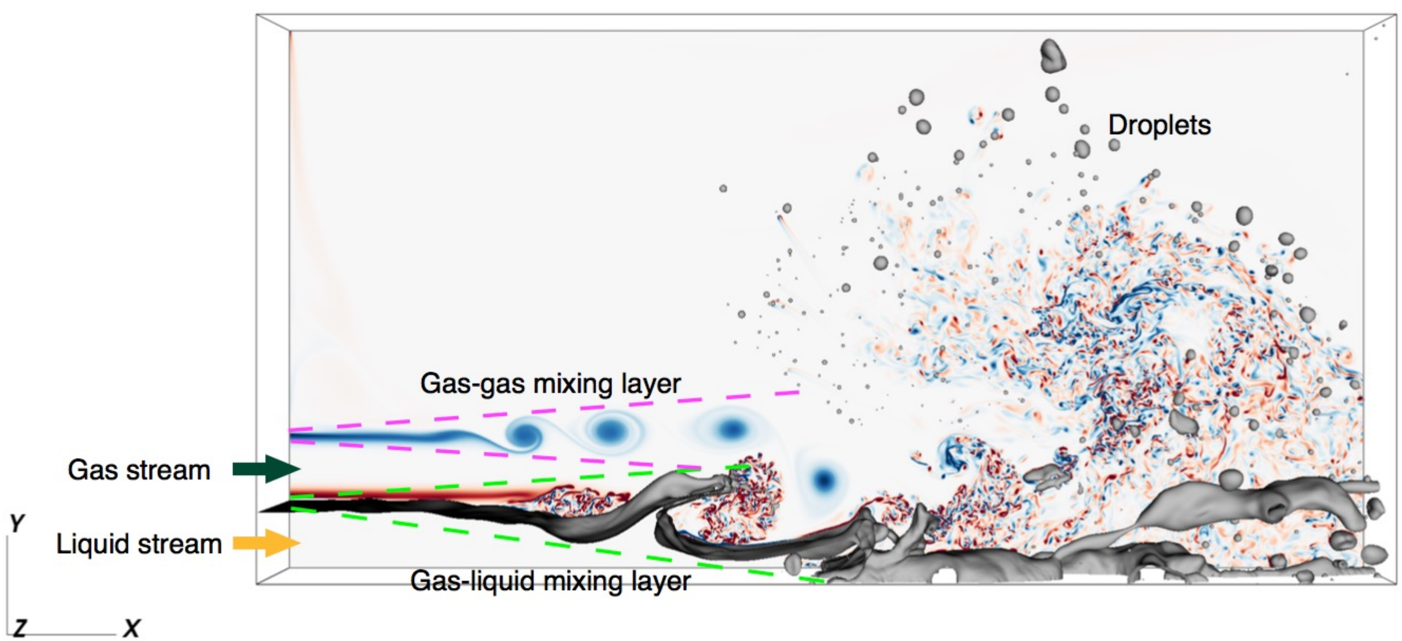

ParisSimulator Code

SORBONNE UNIVERSITÉ CRÉATEURS DE FUTURS DEPUIS 1257

"A20" synthetic case: dimensionless values

M	$Re_{g,\delta}$	$Re_{g,H}$	$We_{g,\delta}$	r	m	v
$\frac{\rho_g U_g^2}{\rho_l U_l^2}$	$\frac{\rho_g U_g \delta}{\mu_g}$	$\frac{\rho_g U_g H}{\mu_g}$	$\frac{\rho_g U_g^2 \delta}{\sigma}$	$\frac{\rho_l}{\rho_g}$	$\frac{\mu_l}{\mu_g}$	$\frac{U_l}{U_g}$
20	1000	8000	10	20	20	20

Ga
N
Liqu

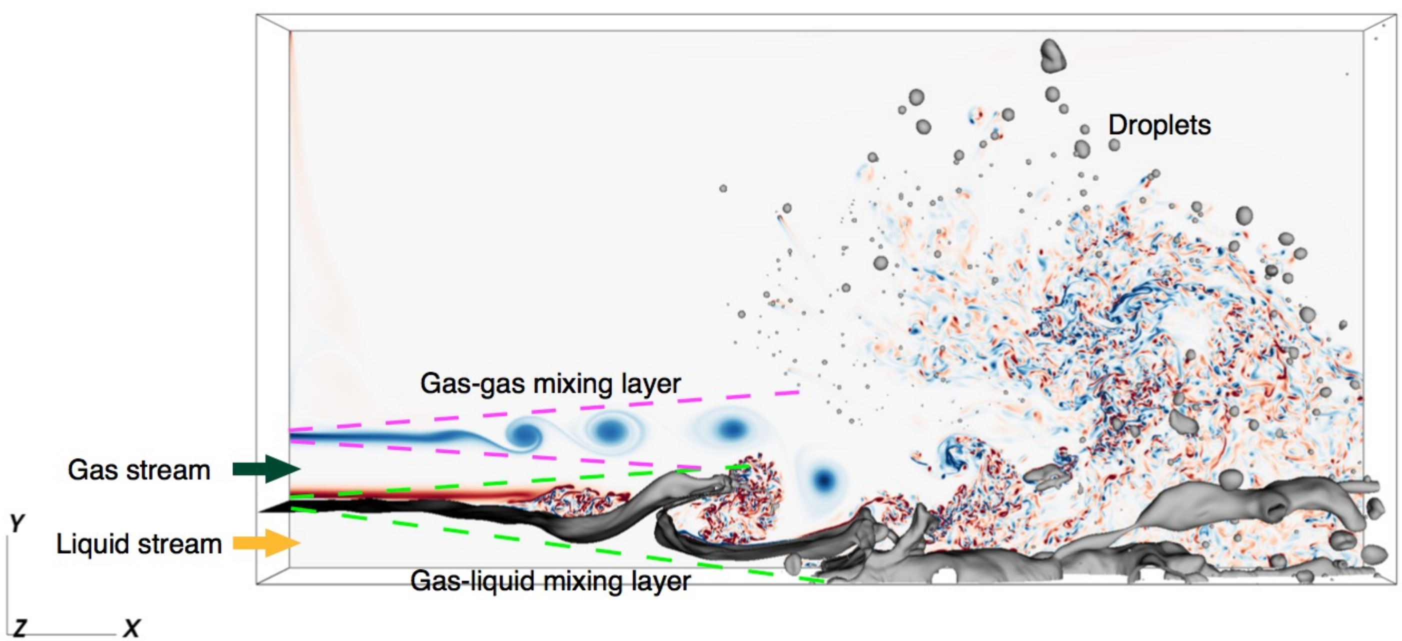

Grids

Domain: L_x=16 H, L_y=8 H,
L_z (various values, here 2 H) end-time: U_g t/H=400

Grids	h(μm)	H/h	# of cells	# of time steps	Total CPU time (hr)
M0	25	32	8.4 Million	$4.9\ 10^4$	$2.5\ 10^3$
M1	12.5	64	67 Million	10^5	$4.3\ 10^4$
M2	6.25	128	537 Million	$2.2\ 10^5$	$5\ 10^5$
M3	3.125	256	4 Billion	$4.5\ 10^5$	$20\ 10^6$

CPU time estimate based on performance on TGCC-CURIE machine.
Thanks to PRACE and HLRZ for their grants of CPU time.

Effect of mesh resolution.

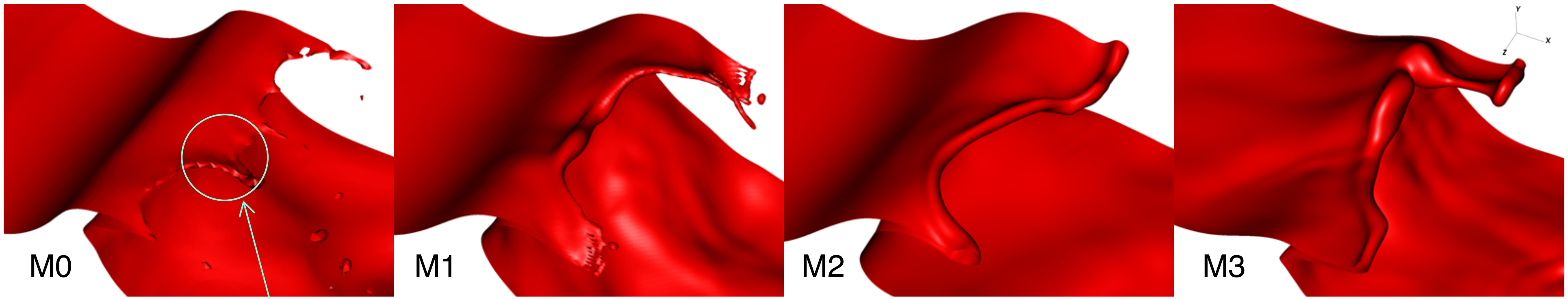

At low resolution, the tip of the sheet is « torn » in an irregular way.

At high resolution, the tip of the sheet ends in a nice Taylor-Culick rim.

Considerable CPU time can be gained by using adaptive grids.

In 2003 S. Popinet introduces Gerris, an octree code using the "forest of trees" parallelization method.

However massive parallelisation with Gerris was difficult.

Around 2016 Popinet releases a multiphase version of Basilisk, a new octree code with much better parallel performance. The forest of tree approach is replaced by space-filling curve

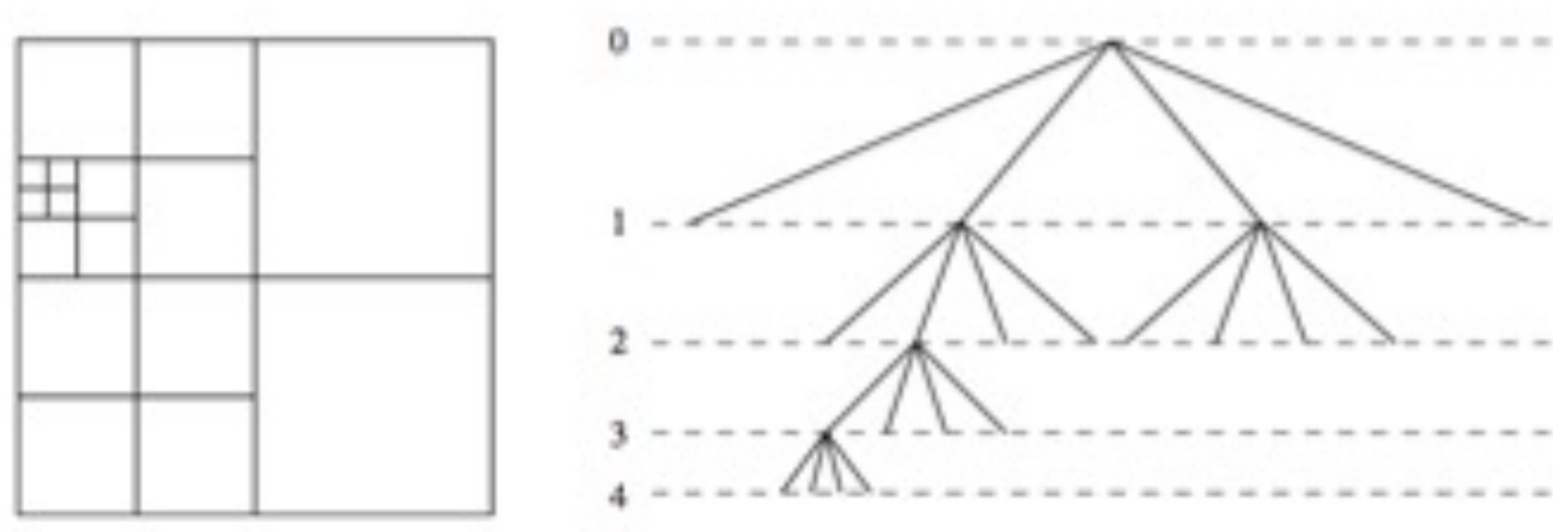

The octree grid

Memory accesses Cartesian/quadtree

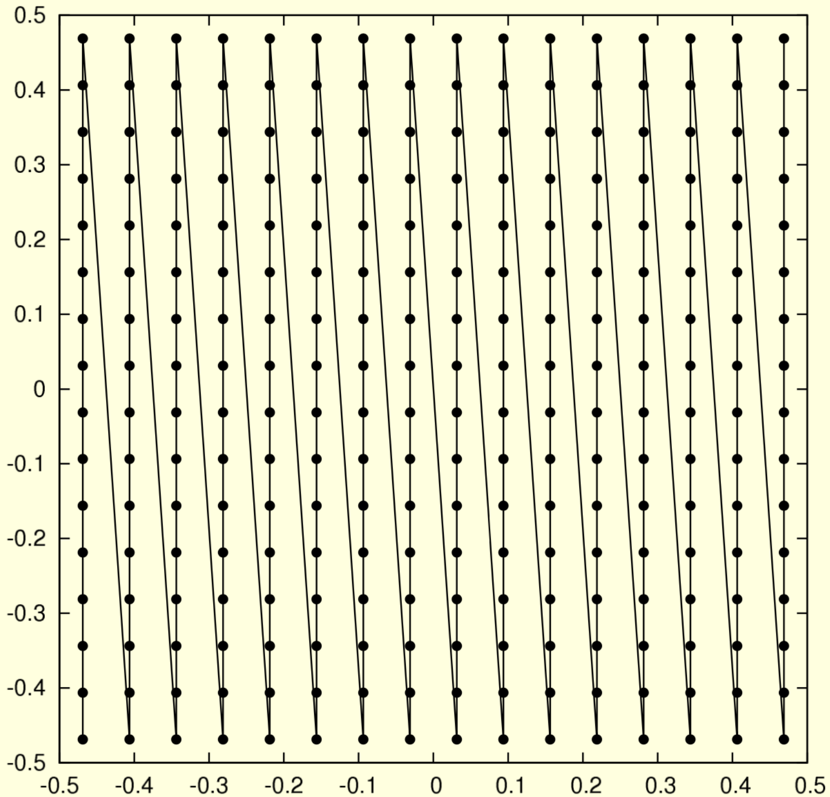

Cartesian, column by column

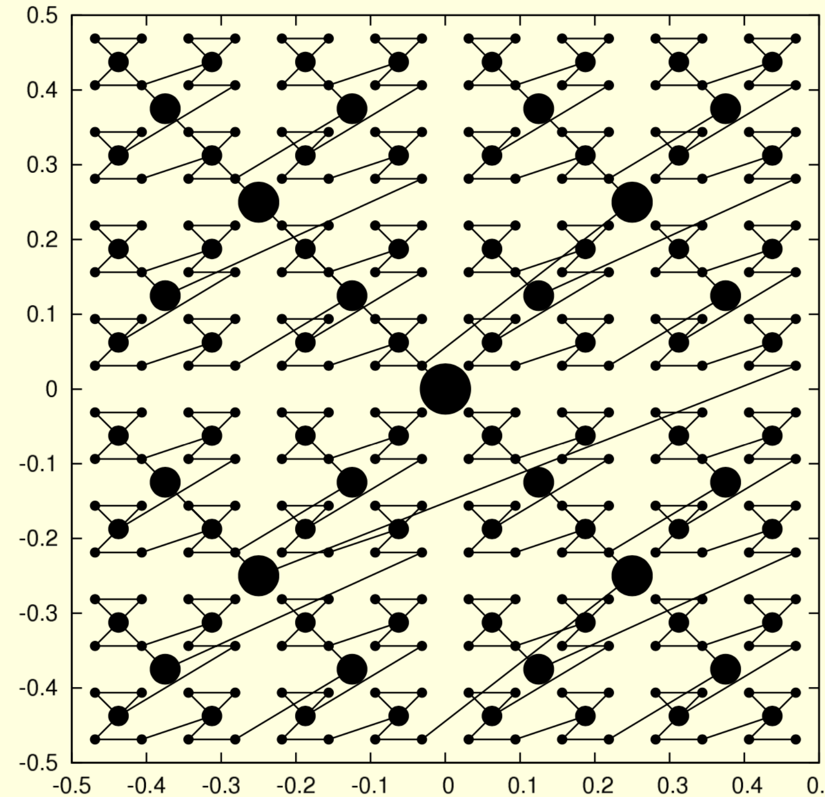

quadtree, Z-ordering

As a result, we have a very efficient, massively parallel, adaptive method. But:

Risks

Risks

Being given a very big computer


summit
IBM

Risks

Being given a very big computer and having to admit one is nowhere close to solving the problem.

Impossible problems

Impossible problems

Thin liquid sheets: too thin, nanometer scale
compared to meter scale experiments or industrial processes

Impossible problems

Thin liquid sheets: too thin, nanometer scale
compared to meter scale experiments or industrial processes

Pulsed jet case

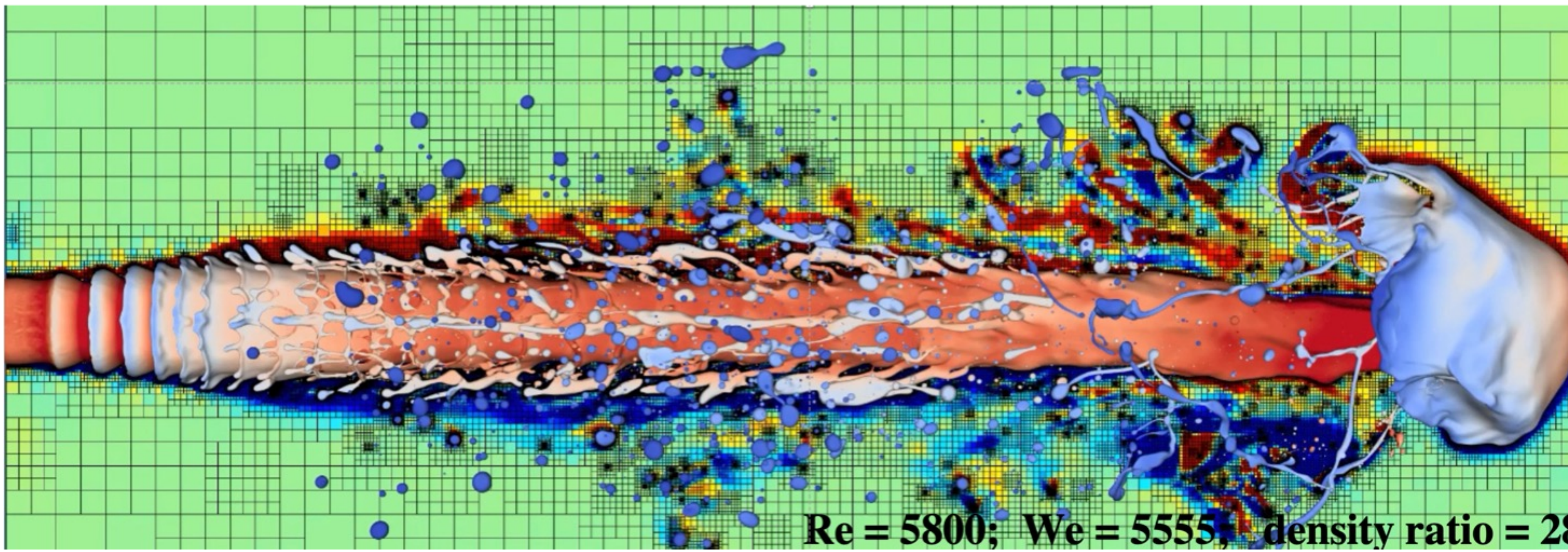
Re = 5800; We = 5555; density ratio = 28

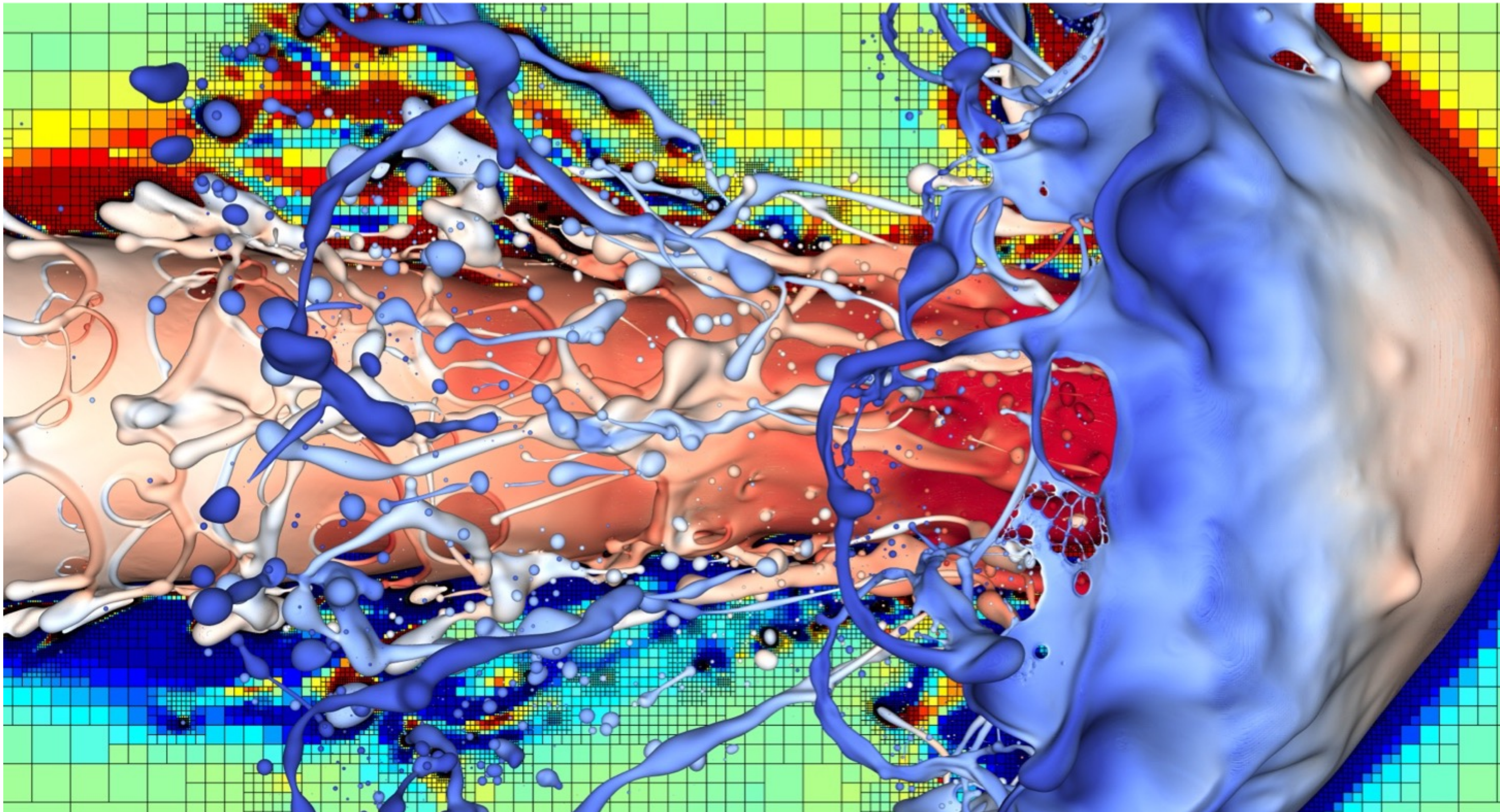

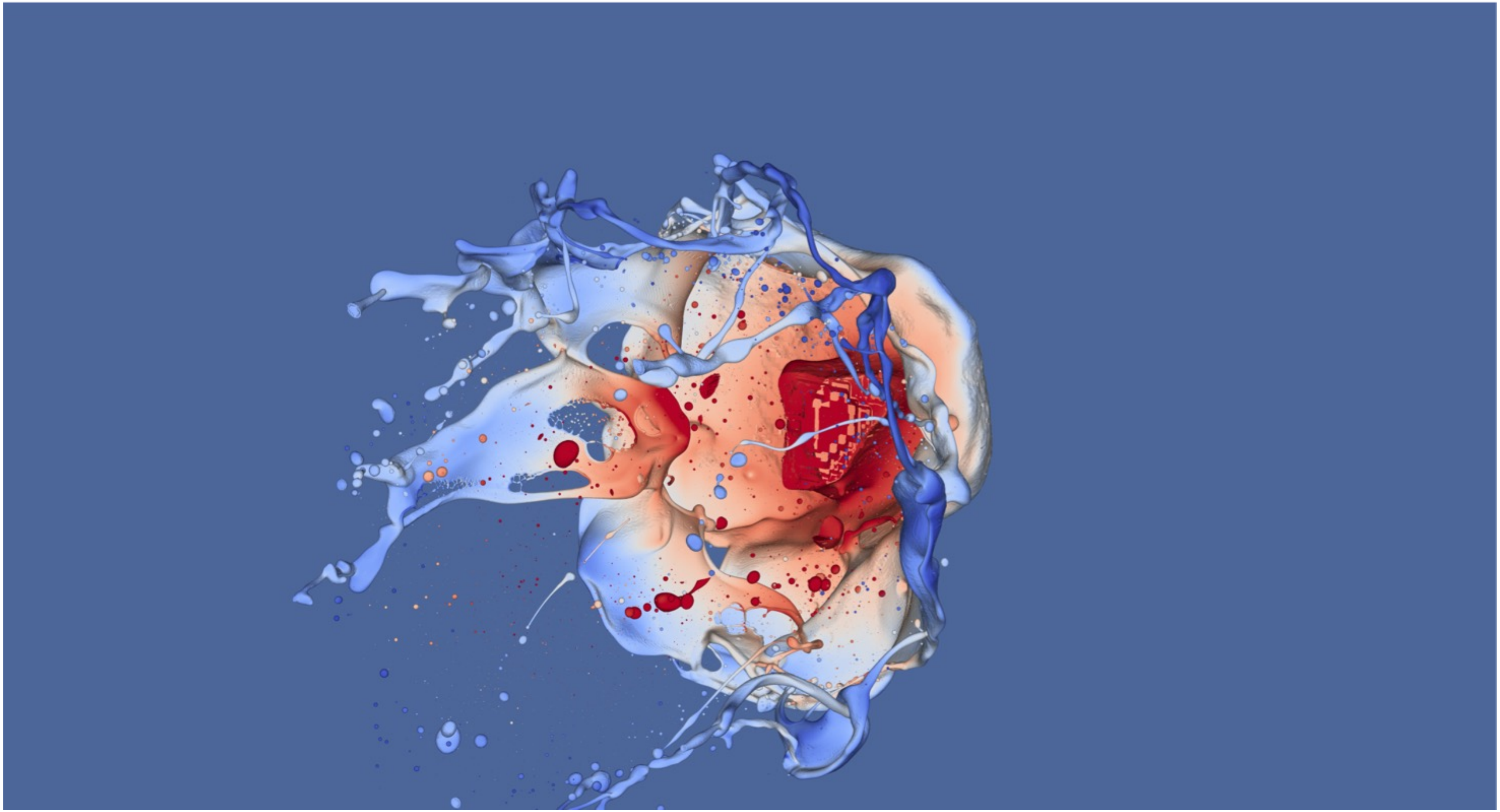

View of the mushroom head from behind

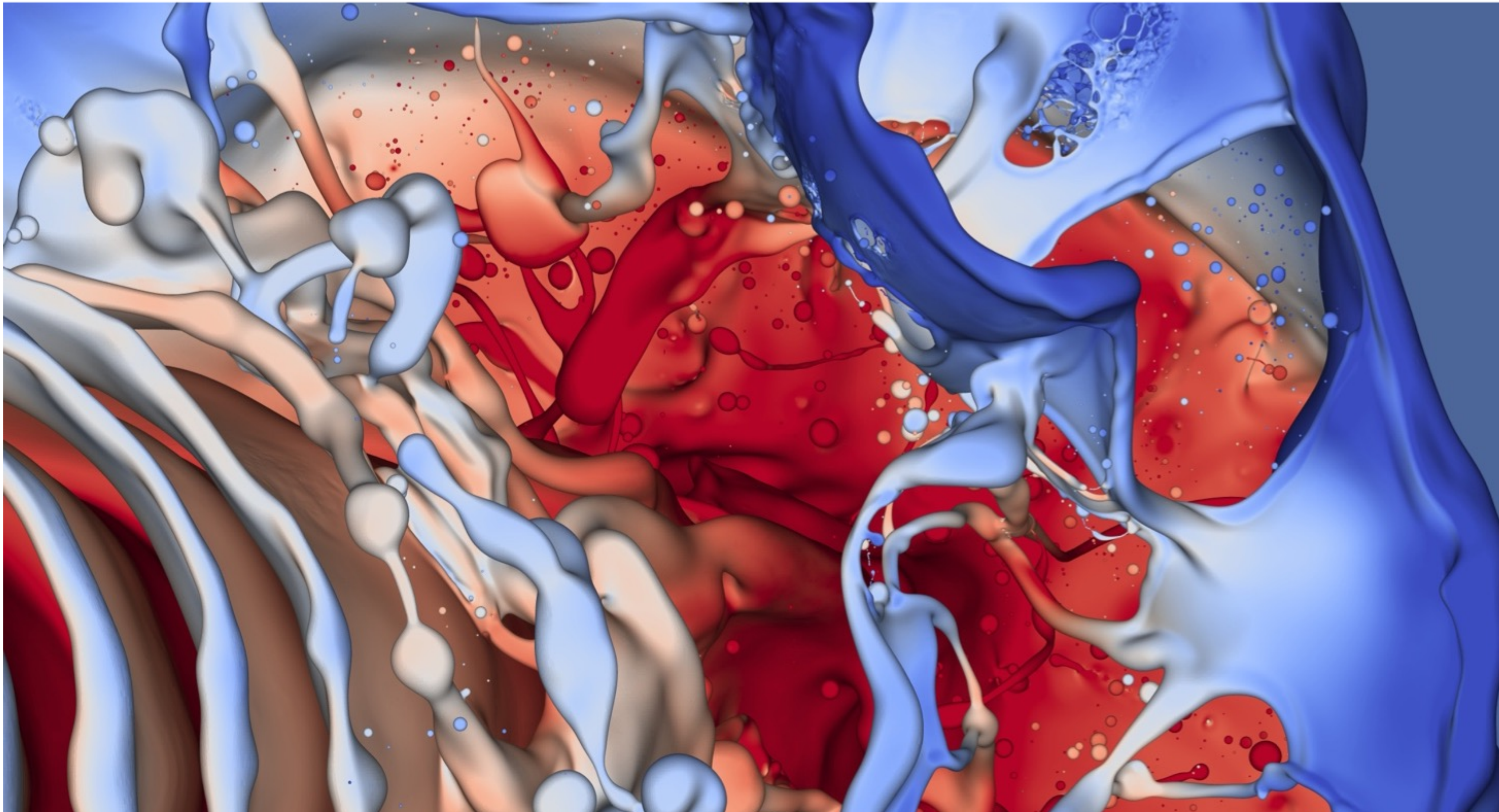

Further zoom on the mushroom head

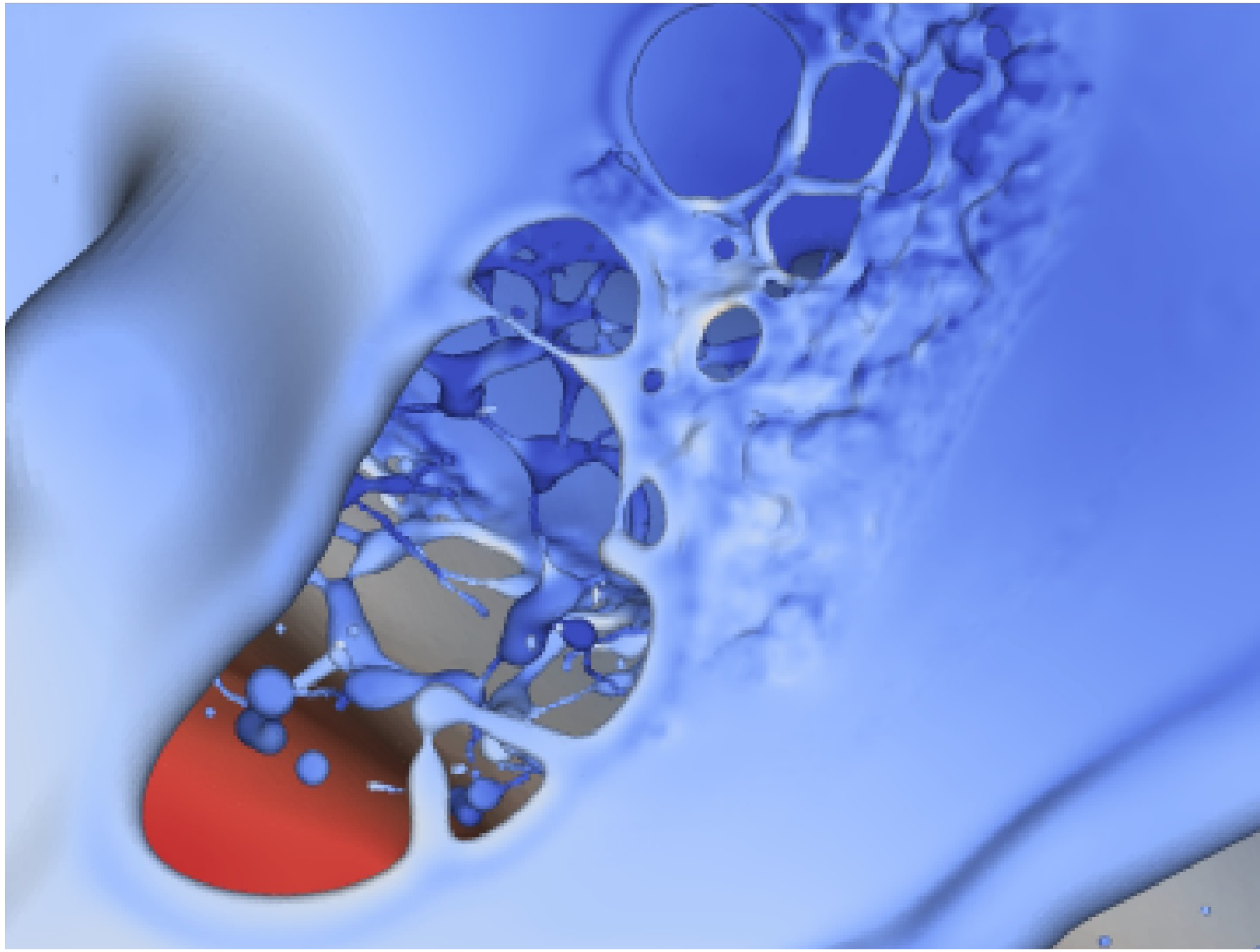

Further zoom : manifold death

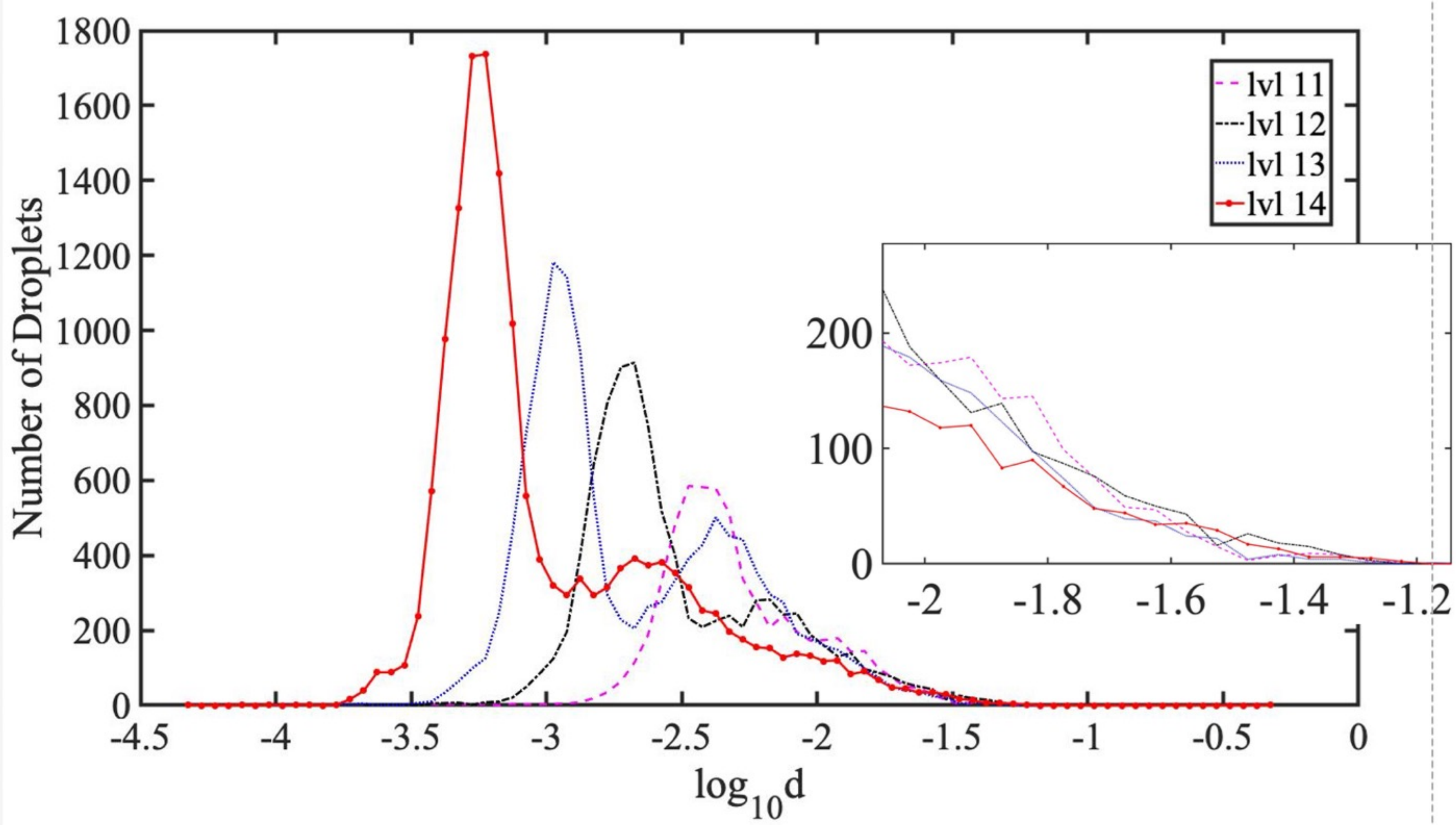

sequence of droplet size PDF with increasing resolution.

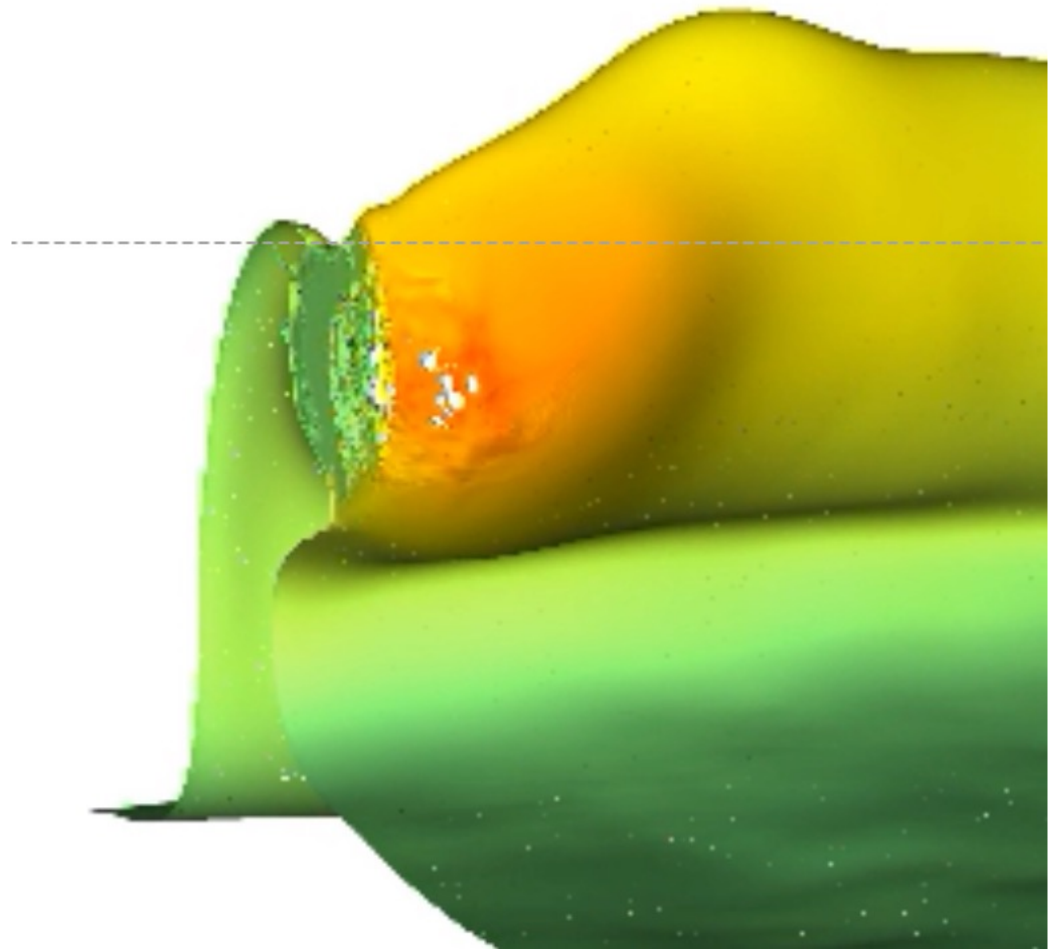

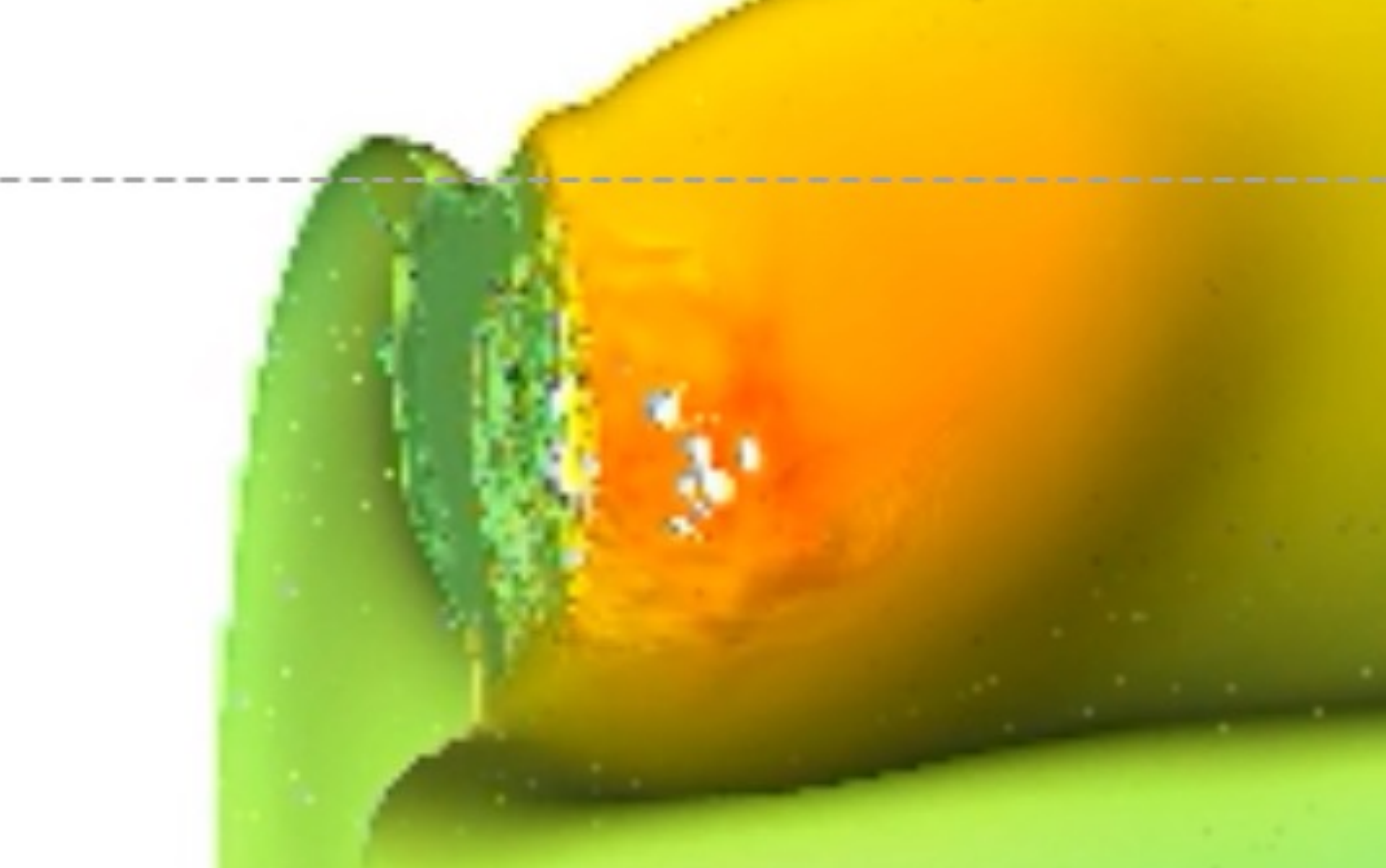

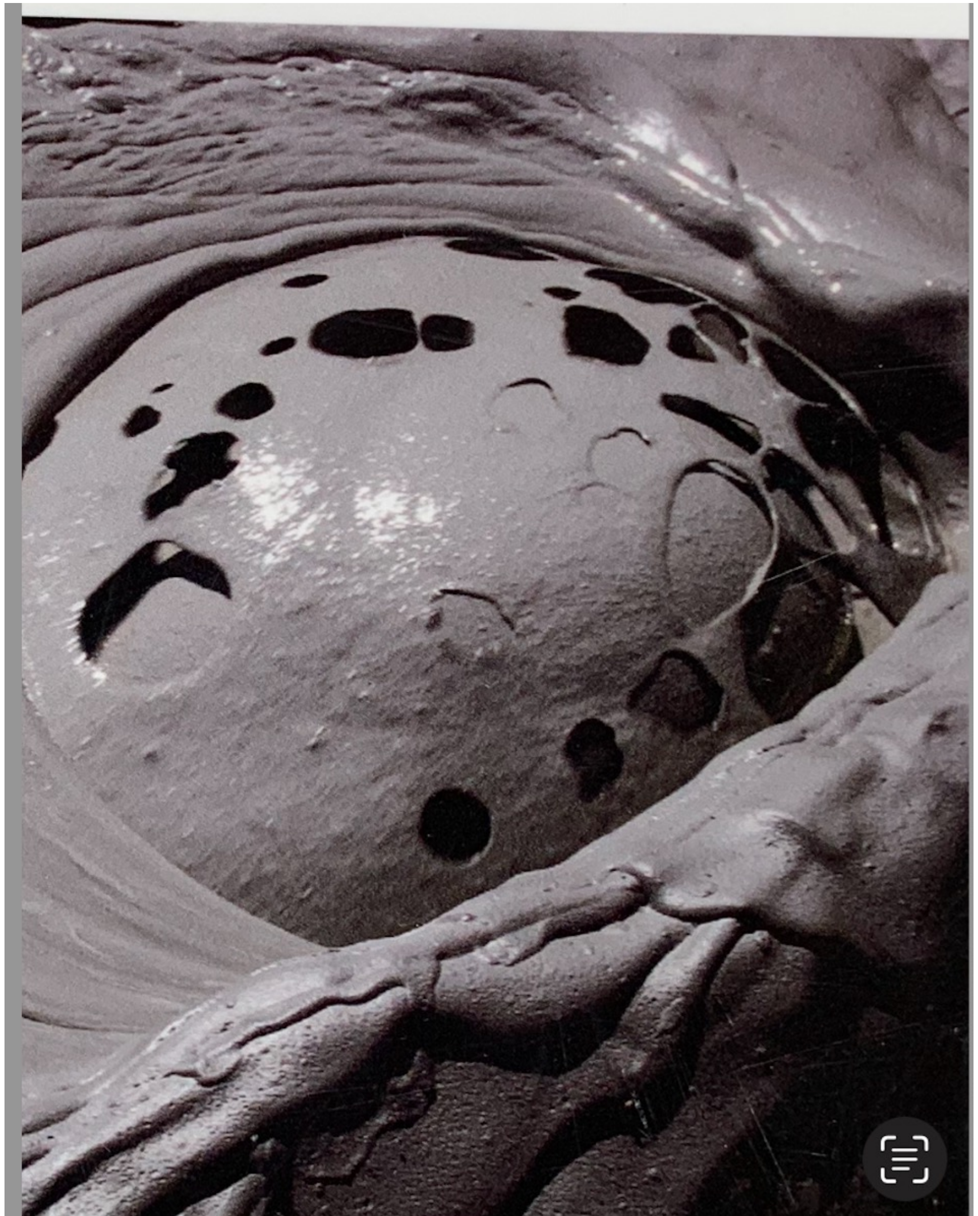

Real life is different

Mud volcano, Salse di Nirano

You can obtain something similar at high resolution

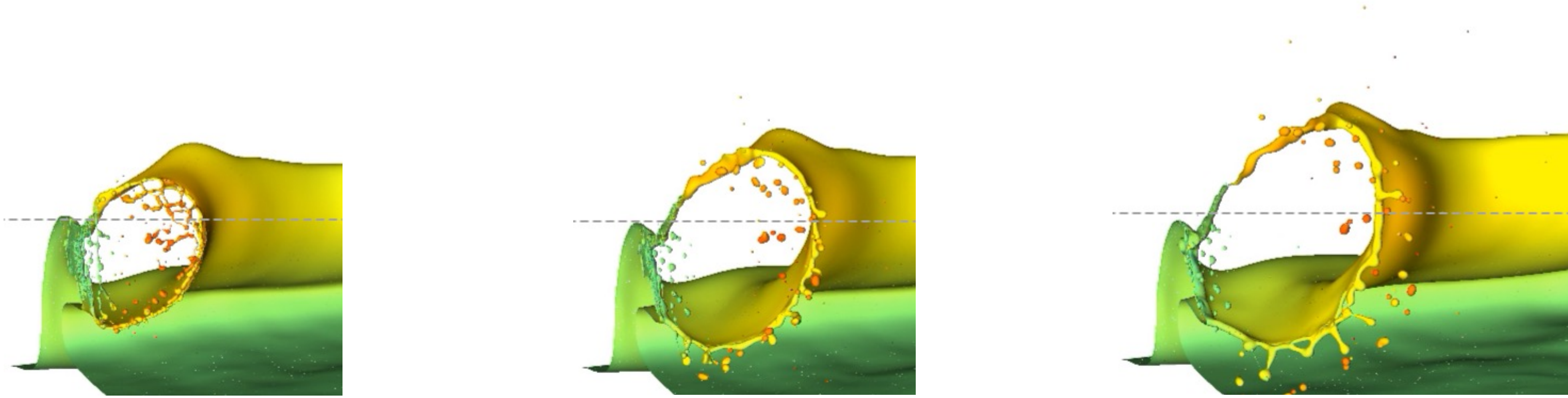

The expanding annular ring is killing the sheet (sheet = 2D manifold).
But it is imperfect: depends on grid size, and is unphysical at the initiation.

A possible solution : the "Manifold Death" procedure.

(with Leonardo Chirco)

In the last volume of Liu Cixin's trilogy, there are multiple intertwinned universes which are each manifolds of dimension D, with 1 < D < 14. War between advanced alien civilizations living in those universes results in each region after the other of any universe being destroyed by ennemy aliens. The alien weapon causes a region of dimension D to be "perforated". The weapon is a small element of dimension D-1 inserted in it.

Thus our 3D solar system is destroyed by an attack by a small post-it-sized thin sheet (2D manifold).

The lesson is that destruction of a D dimensional manifold is realized by a D-1 manifold, not a D-2 manifold. Thus a sheet (D=2) is destroyed by an expanding annular ring (D=1) not by a tiny point hole (D=0).

As a result we (Leonardo Chirco and I) call this topological transtion "Manifold Death" (MD). But the term "death" is also used for bursting bubbles.

**Remembrance of Earth's Past* (Chinese: 地球往事) trilogy, the whole series is normally referred to as *The Three-Body Problem*

What happens to thin sheets in multiphase flow simulations ?

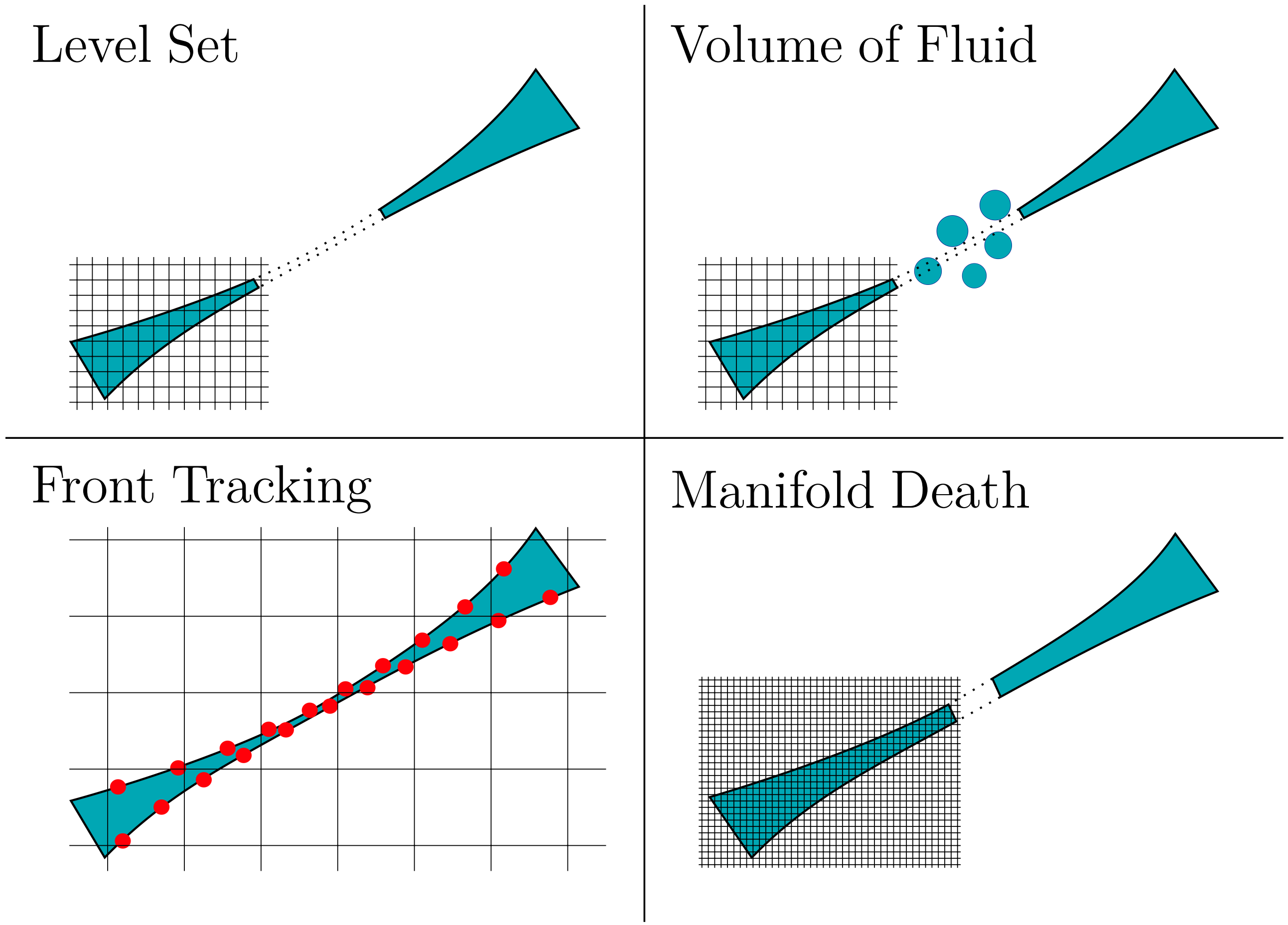

What happens to thin sheets in multiphase flow simulations ?

evaporates when
it reaches the grid size

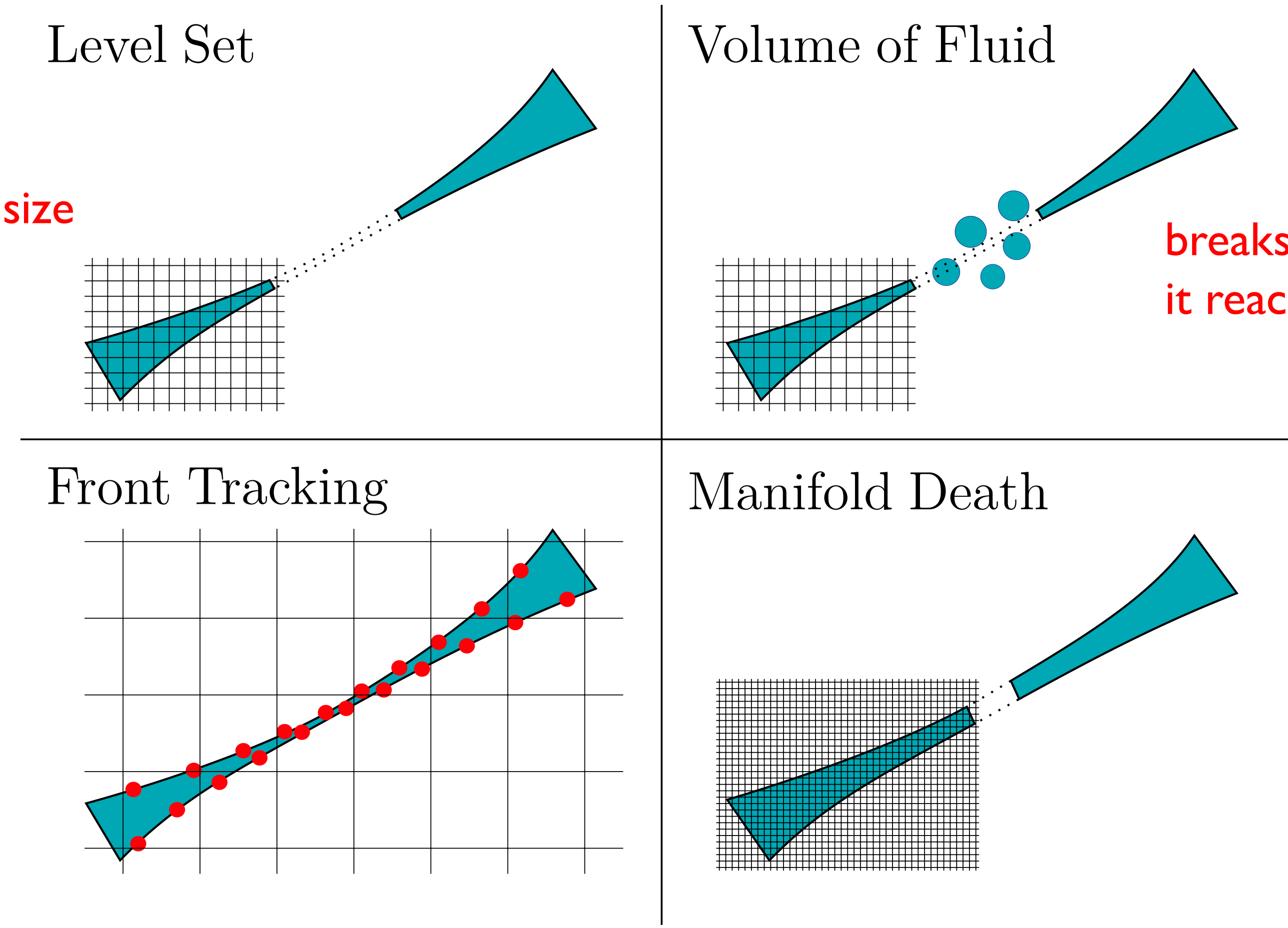

breaks into big droplets when
it reaches the grid size

What happens to thin sheets in multiphase flow simulations ?

evaporates when
it reaches the grid size

breaks into big droplets when
it reaches the grid size

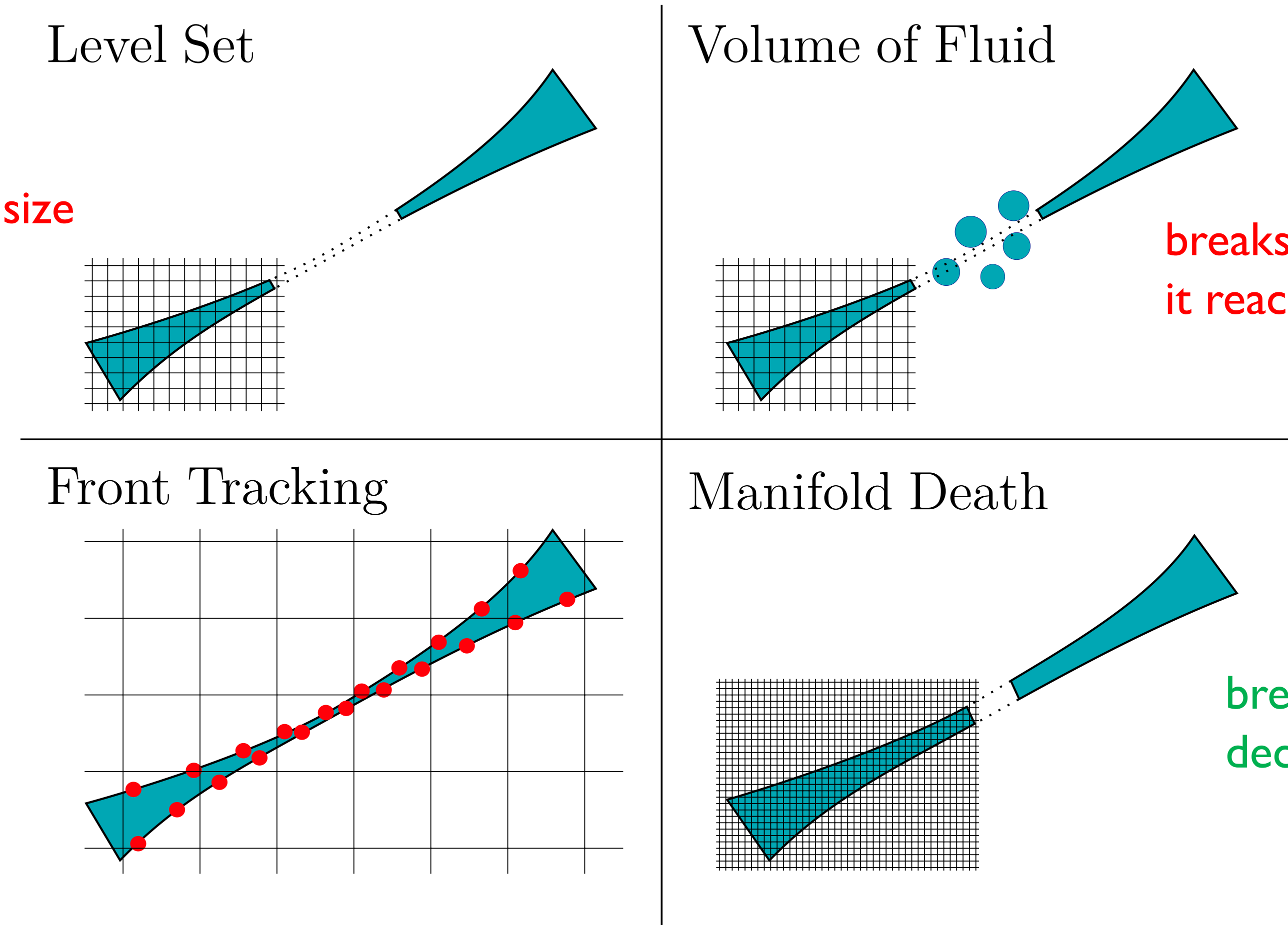

never breaks

breaks when we
decide.

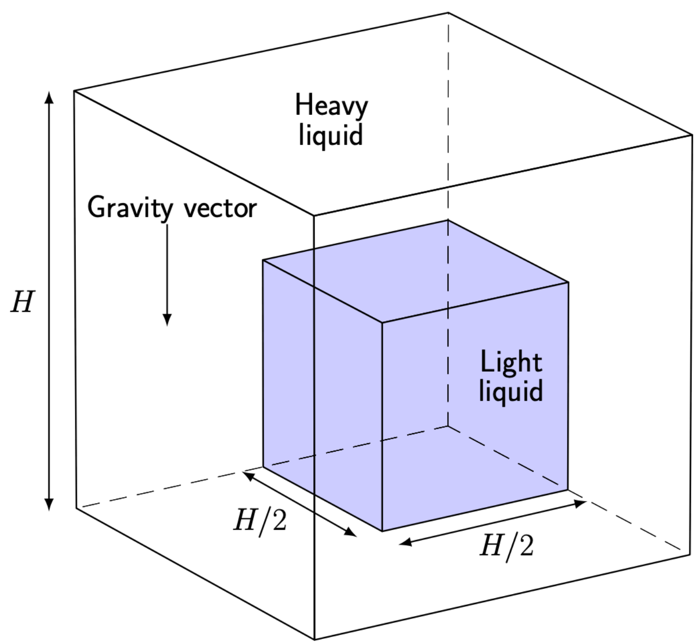

Figure 7: Configuration for the phase inversion test.

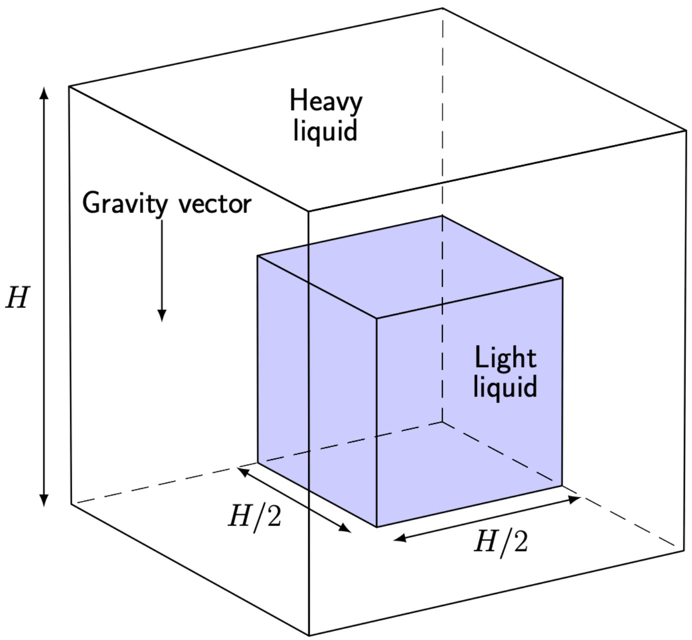

Figure 7: Configuration for the phase inversion test.

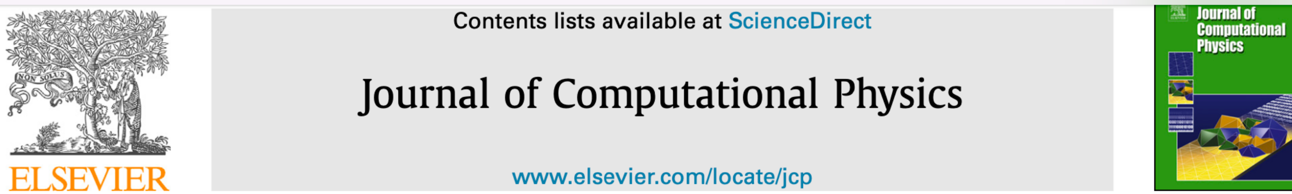
Contents lists available at ScienceDirect

Journal of Computational Physics

www.elsevier.com/locate/jcp

A phase inversion benchmark for multiscale multiphase flows

J.-L. Estivalezes [a,c], W. Aniszewski [b], F. Auguste [c], Y. Ling [d,e], L. Osmar [f], J.-P. Caltagirone [f], L. Chirco [d], A. Pedrono [c], S. Popinet [d], A. Berlemont [b], J. Magnaudet [c], T. Ménard [b], S. Vincent [g], S. Zaleski [d,h,*]

[a] ONERA, The French Aerospace Lab, F-31055 Toulouse, France
[b] Université de Rouen and CNRS, Complexe de Recherche Interprofessionnel en Aérothermochimie (CORIA) UMR 6614, F-76801 Saint-Etienne-du-Rouvray Cedex, France
[c] Institut de Mécanique des Fluides de Toulouse (IMFT), Université de Toulouse, CNRS, Toulouse, France
[d] Sorbonne Université and CNRS, Institut Jean Le Rond d'Alembert UMR 7190, F-75005 Paris, France
[e] Baylor University, Department of Mechanical Engineering, Waco, TX 76798, USA
[f] Bordeaux INP, University of Bordeaux, CNRS, Arts et Métiers Institute of Technology, INRAE, Institut de Mécanique et Ingénierie (I2M) UMR 5295, F-33400 Talence, France
[g] Université Paris-Est Marne-La-Vallée and CNRS, Laboratoire Modélisation et Simulation Multi Echelle (MSME), UMR 8208, F-77454, Marne-La-Vallée, France
[h] Institut Universitaire de France, Paris, France

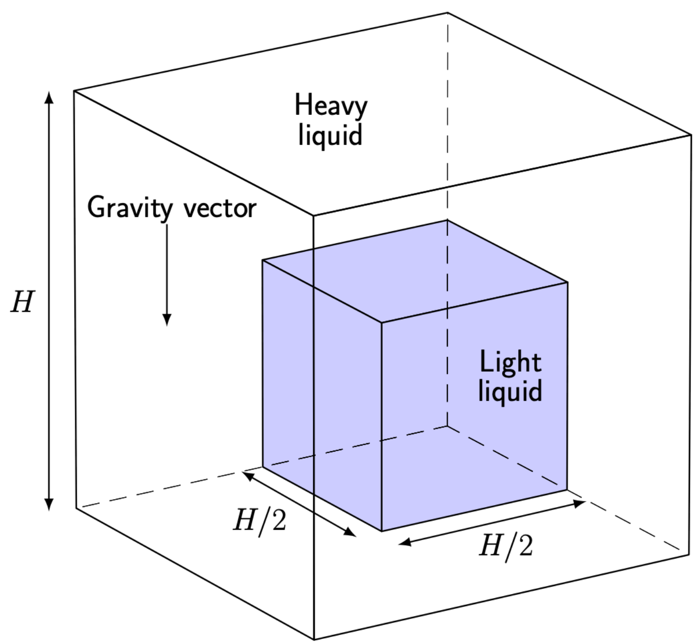

Figure 7: Configuration for the phase inversion test.

Contents lists available at ScienceDirect

Journal of Computational Physics

www.elsevier.com/locate/jcp

A phase inversion benchmark for multiscale multiphase flows

J.-L. Estivalezes [a,c], W. Aniszewski [b], F. Auguste [c], Y. Ling [d,e], L. Osmar [f], J.-P. Caltagirone [f], L. Chirco [d], A. Pedrono [c], S. Popinet [d], A. Berlemont [b], J. Magnaudet [c], T. Ménard [b], S. Vincent [g], S. Zaleski [d,h,*]

[a] ONERA, The French Aerospace Lab, F-31055 Toulouse, France
[b] Université de Rouen and CNRS, Complexe de Recherche Interprofessionnel en Aérothermochimie (CORIA) UMR 6614, F-76801 Saint-Etienne-du-Rouvray Cedex, France
[c] Institut de Mécanique des Fluides de Toulouse (IMFT), Université de Toulouse, CNRS, Toulouse, France
[d] Sorbonne Université and CNRS, Institut Jean Le Rond d'Alembert UMR 7190, F-75005 Paris, France
[e] Baylor University, Department of Mechanical Engineering, Waco, TX 76798, USA
[f] Bordeaux INP, University of Bordeaux, CNRS, Arts et Métiers Institute of Technology, INRAE, Institut de Mécanique et Ingénierie (I2M) UMR 5295, F-33400 Talence, France
[g] Université Paris-Est Marne-La-Vallée and CNRS, Laboratoire Modélisation et Simulation Multi Echelle (MSME), UMR 8208, F-77454, Marne-La-Vallée, France
[h] Institut Universitaire de France, Paris, France

New case with smaller Reynolds numbers

Results for case B

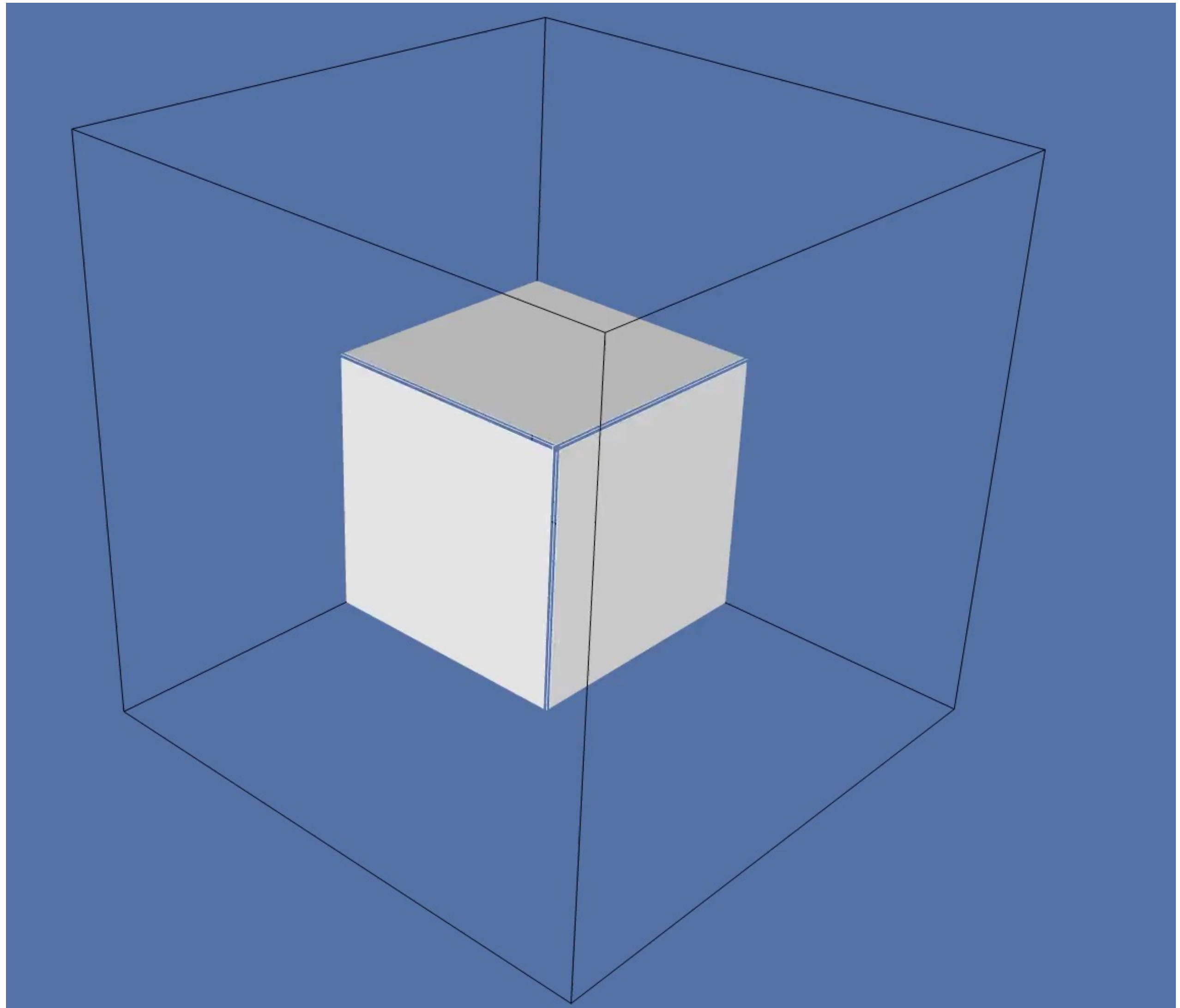

Sheet detection

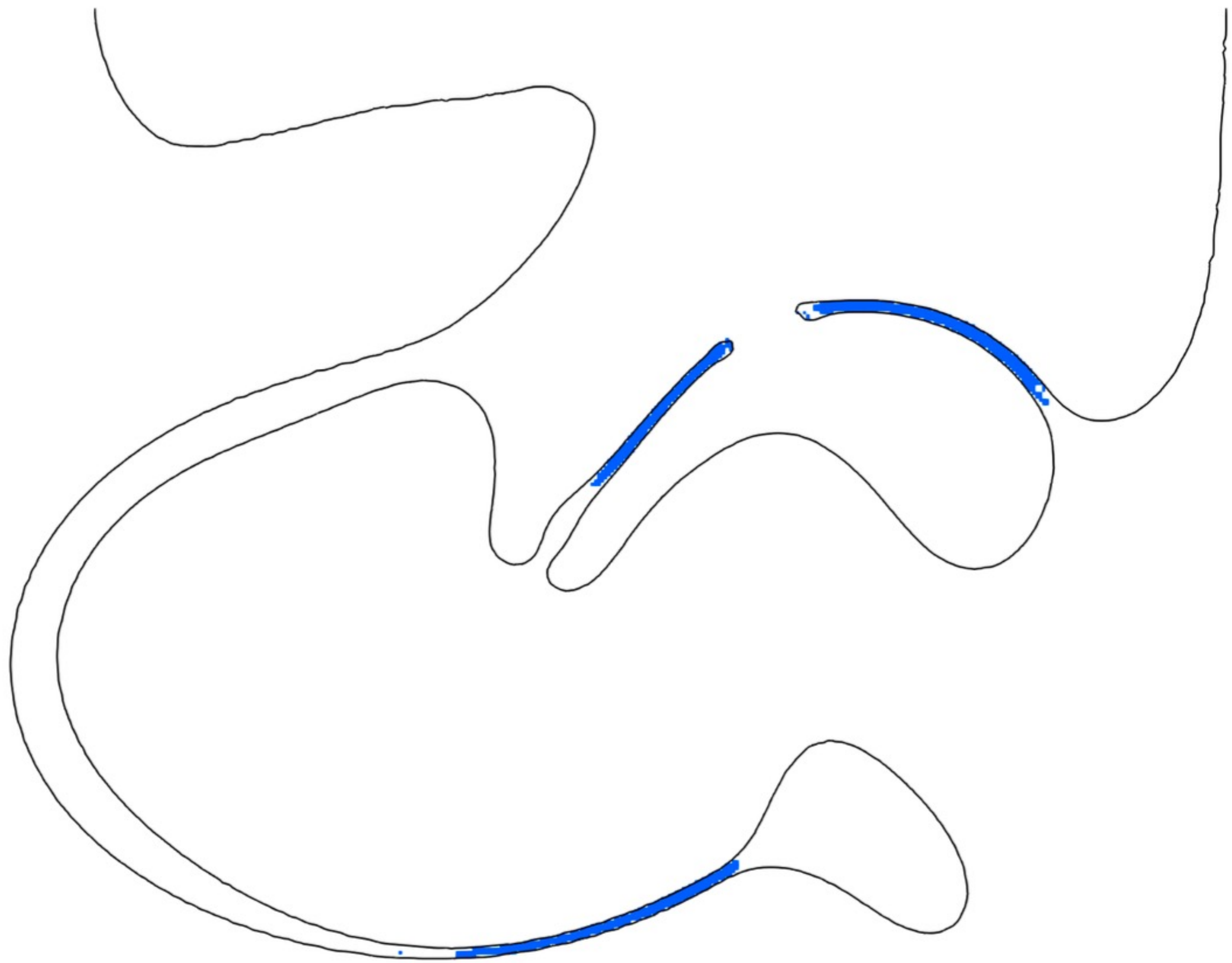

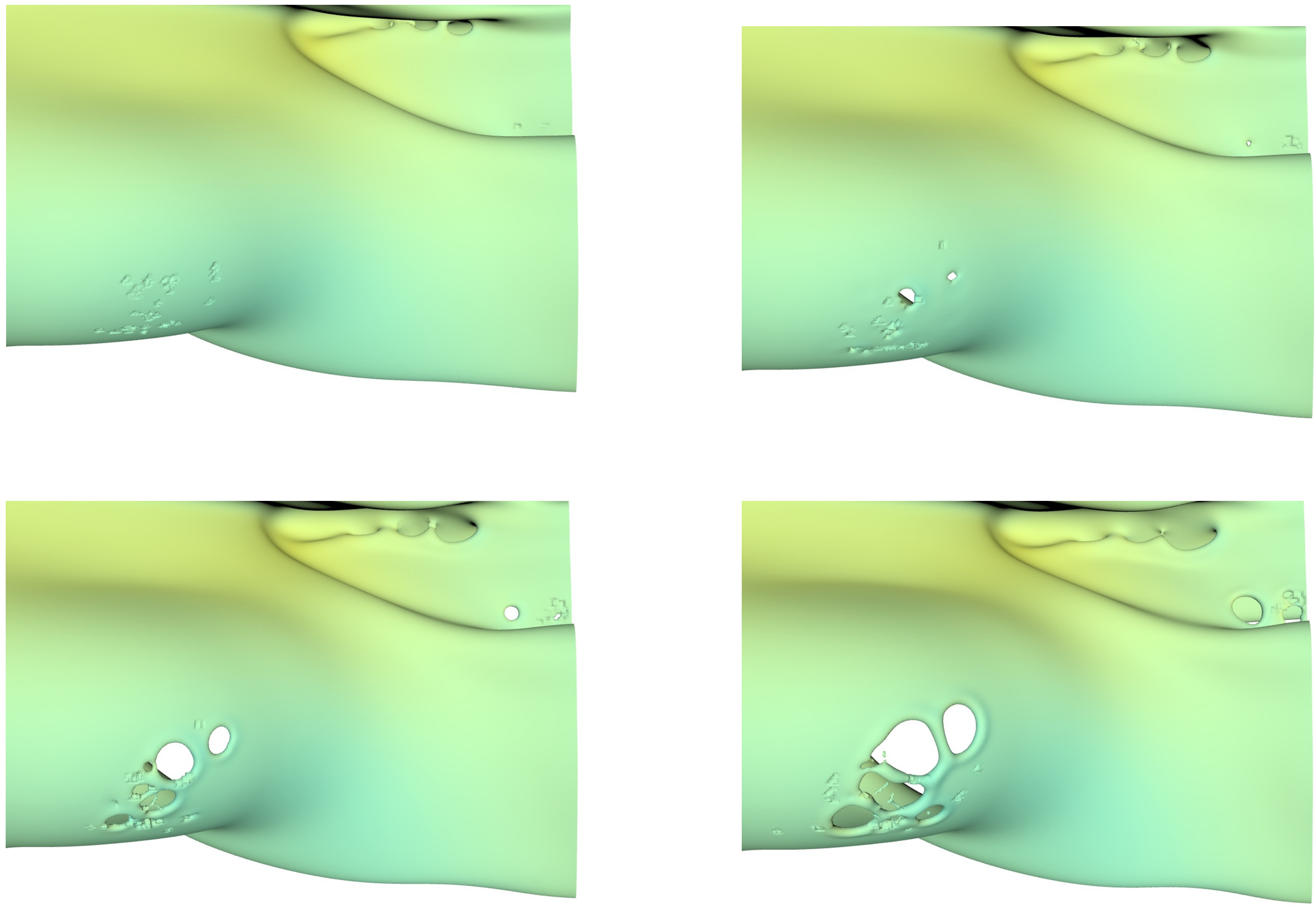

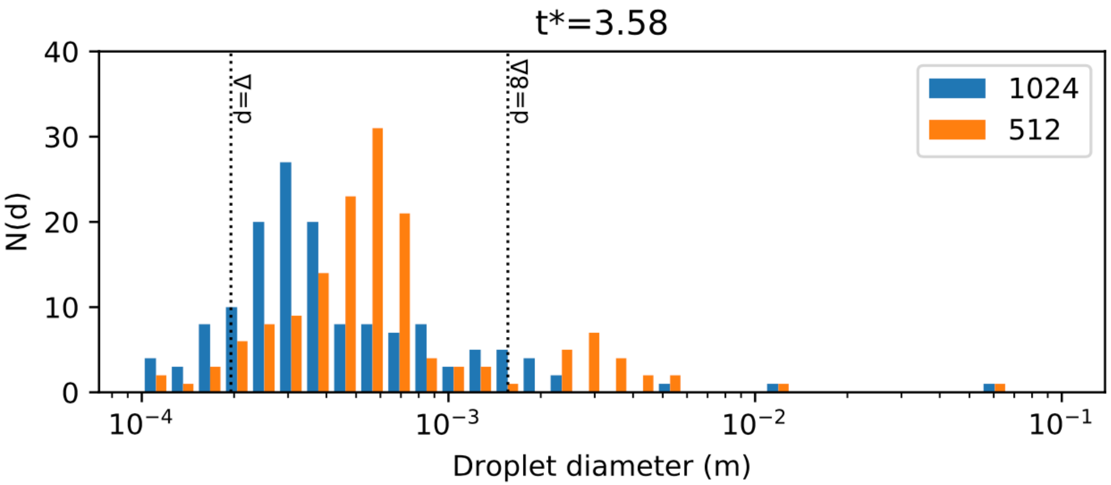

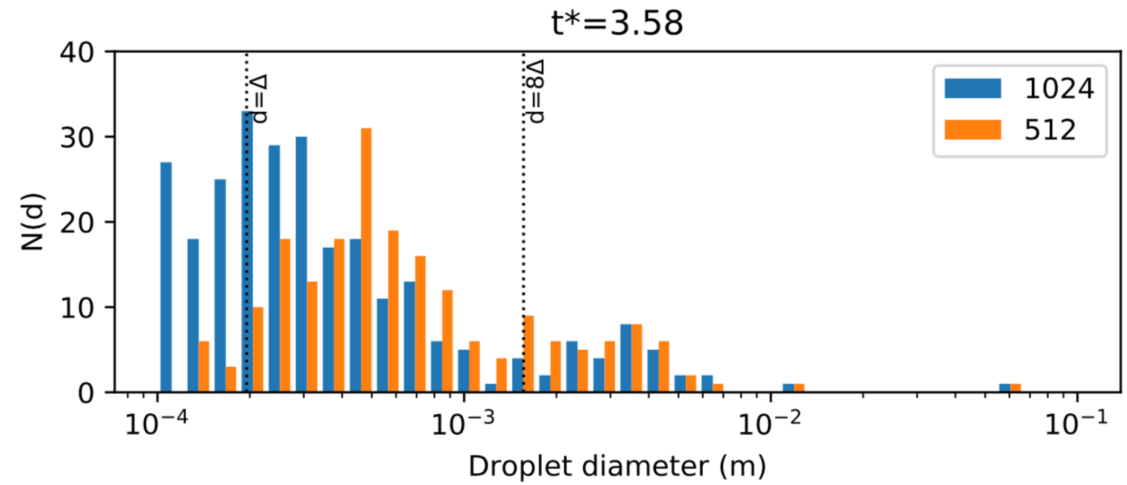

Droplet size distributions in the phase inversion test case

left: without manifold death   right: with manifold death

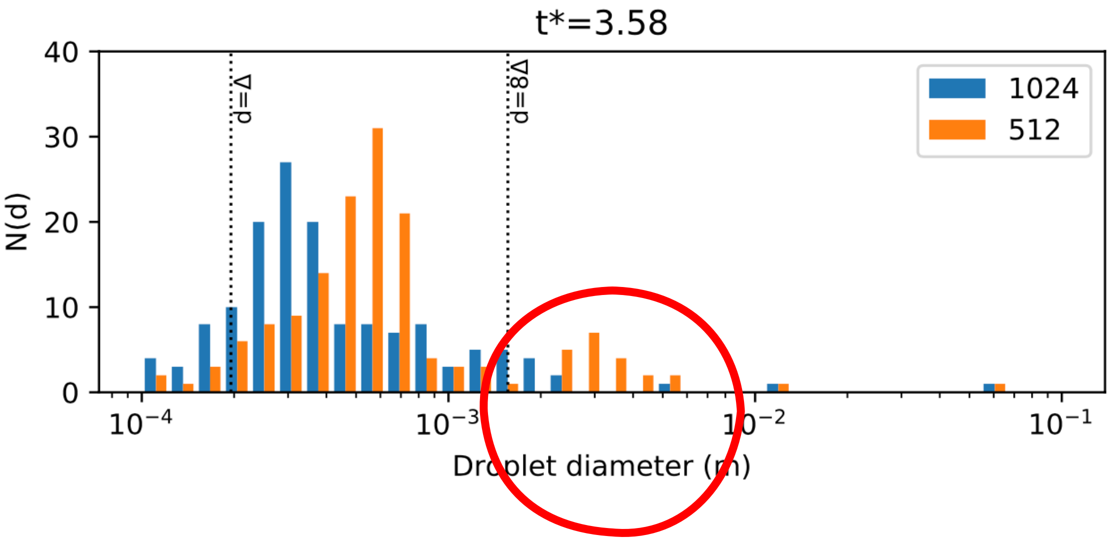

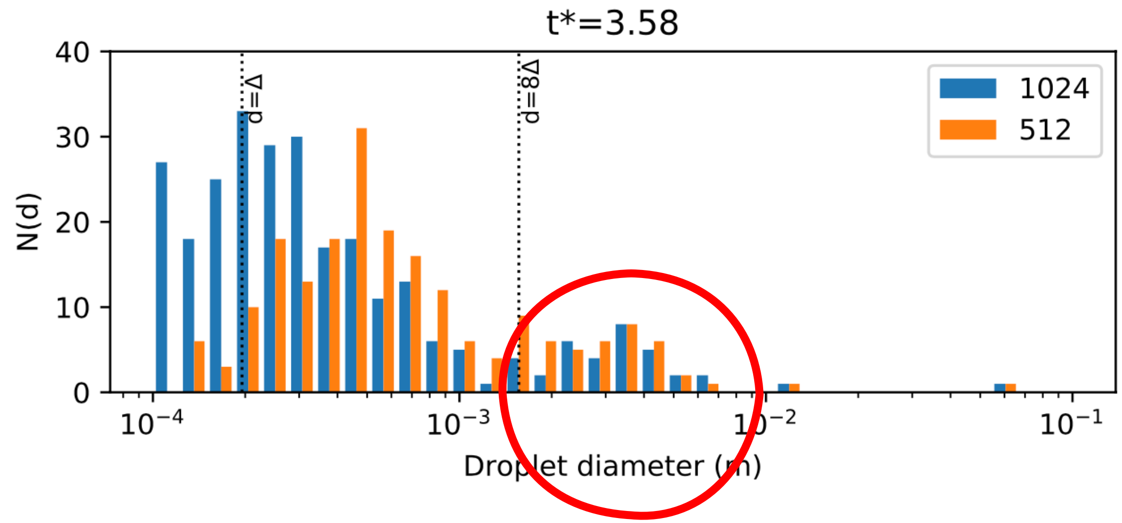

Not converging

Converging

Droplet size distributions in the phase inversion test case

left: without manifold death right: with manifold death

Conclusion

the story of massive simulations with a wide range of
spatial and temporal scales,such as thin sheets / boundary layers etc.
is only beginning.

The End

Question:

— What about remorse ?

Question:

— What about remorse ?

— Remorse, me ? None.

Question:

— What about remorse ?

— Remorse, me ? None.

— *Colleague:* Why am I not surprised ?

Question:

— What about remorse ?

— Remorse, me ? None.

— *Colleague:* Why am I not surprised ? *(Note: I treated him badly when I was department head)*

Things I would like to atone for

- working on deterministic chaos in 1979
- working on LGCA and LBM in 1986
- working on machine learning in 2018

Step 1: The signature method

- First, detect the thin sheets in the domain. To do that:
  1. Consider a point $\mathbf{x}_0 \in \mathbb{R}^3$ and translate the coordinate system so that the new origin is $\mathbf{x}_0 = \mathbf{0}$. Consider a radius R approximately the size of the sheet thickness h_c one wants to detect, and the bilinear form $f(x, x) = x_i x_j T_{ij}$.
  2. The quadratic moments T_{ij} on a spherical shell S of radius R can be find by integrating $T_{ij} = k \int_V x'_i x'_j \phi(x') d\mathbf{x}'$, where $\phi = 2C - 1$.
  3. After orthonormalisation of the quadratic form one finds a new set of coordinates in which $f(\mathbf{X}, \mathbf{X}) = \epsilon_i X_i^2$, where ϵ_i are the eigenvalues of the operator with matrix T_{ij}. The number of positive, negative and zero values of ϵ_i is the signature s of the quadratic form.
  4. The signature s is used to determine where we are in the phase (bulk - thin sheets - ligaments - interface).

Step 1: The signature method

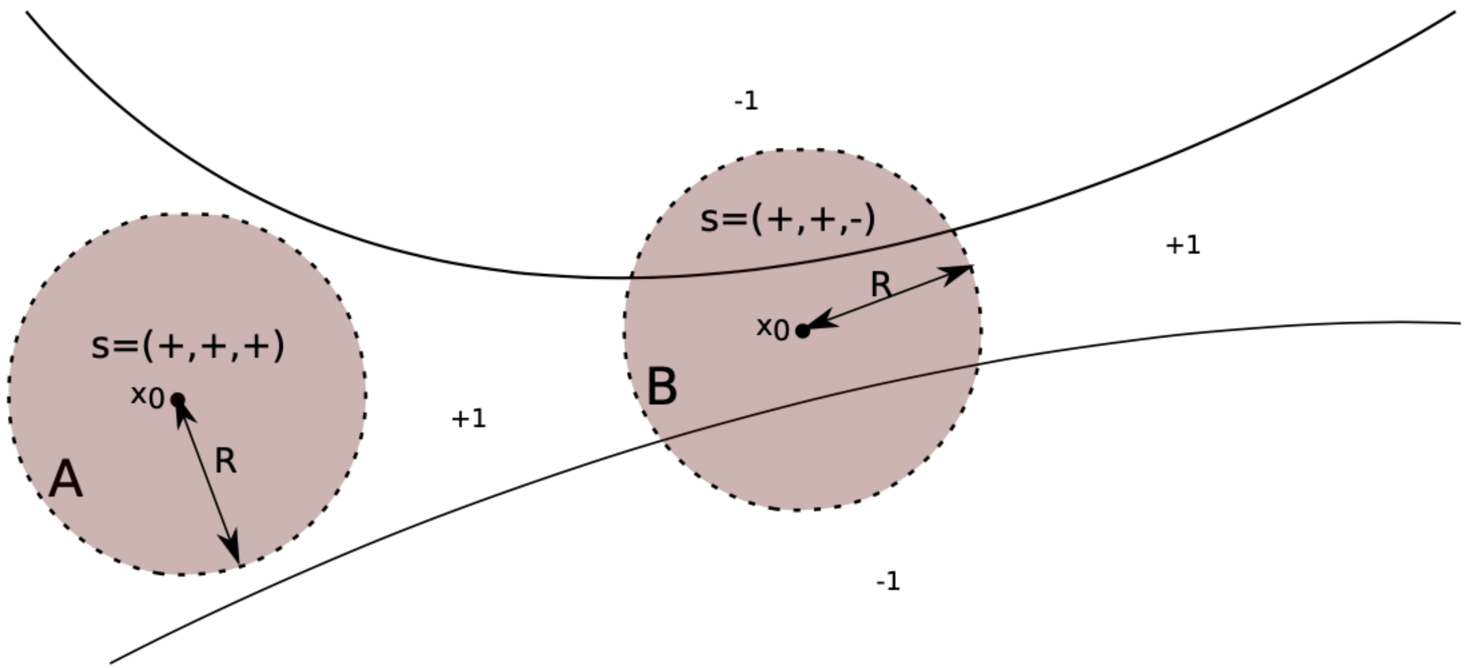

- $s = (+, +, +)$ bulk of phase
- $s = (+, +, -)$ sheet
- $s = (+, -, -)$ ligament
- $s = (+, +, 0)$ interface

Step 1: Implementation in the Basilisk code

- Replace spherical shell S (radius R) with a cubical one coinciding with the 5x5 stencil: $(5\Delta = L = 2R = 2h_c \longrightarrow h_c \approx 3\Delta)$.

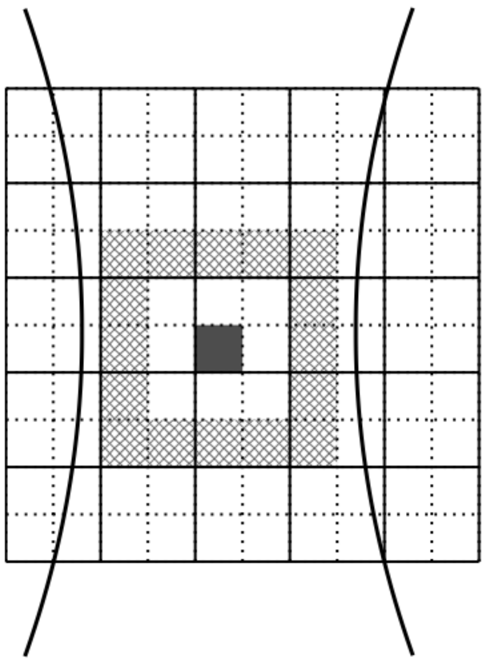

- If $h_c = 3\Delta$ sheet not detected

Step 1: Implementation in the Basilisk code

- Replace spherical shell S (radius R) with a cubical one coinciding with the 5x5 stencil: $(5\Delta = L = 2R = 2h_c \longrightarrow h_c \approx 3\Delta)$.
- Detect thicker sheets $\rightarrow$ compute the signature on a coarser level $h_c \approx 3\Delta_{L-1} = 6\Delta_L$.

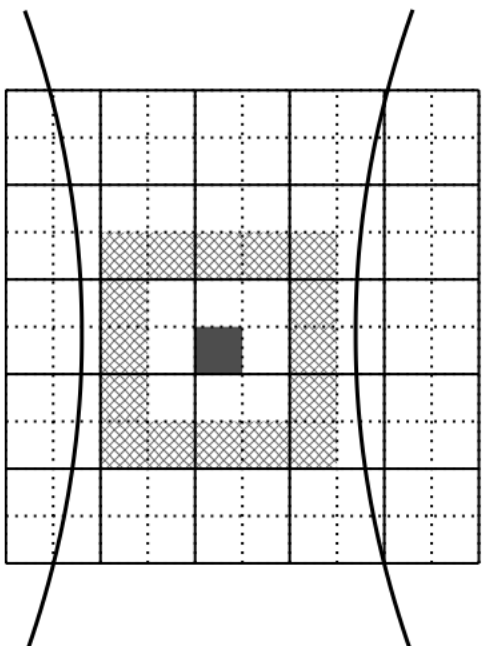

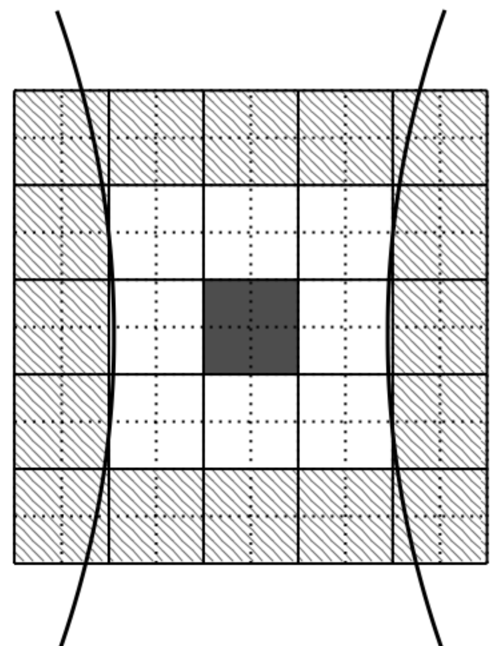

- One can detect sheets of h_c independently of the mesh resolution.
- Code available at: `http://basilisk.fr/sandbox/lchirco/signature.h`

- If $h_c = 3\Delta$ sheet not detected
- If $h_c = 3\Delta_{L-1} = 6\Delta_L$ sheet detected

Industrial example : ladle flow (metallurgy)

EU injects $157m into hydrogen iron and steelmaking project

Yusuf Latief - April 5, 2022

Facebook Twitter Linkedin

Image: 123rf

Hydrogen metallurgy will avoid the use of carbon.

It will require a redesign of ladle metal refinement processes. Carbon has to be added ! .

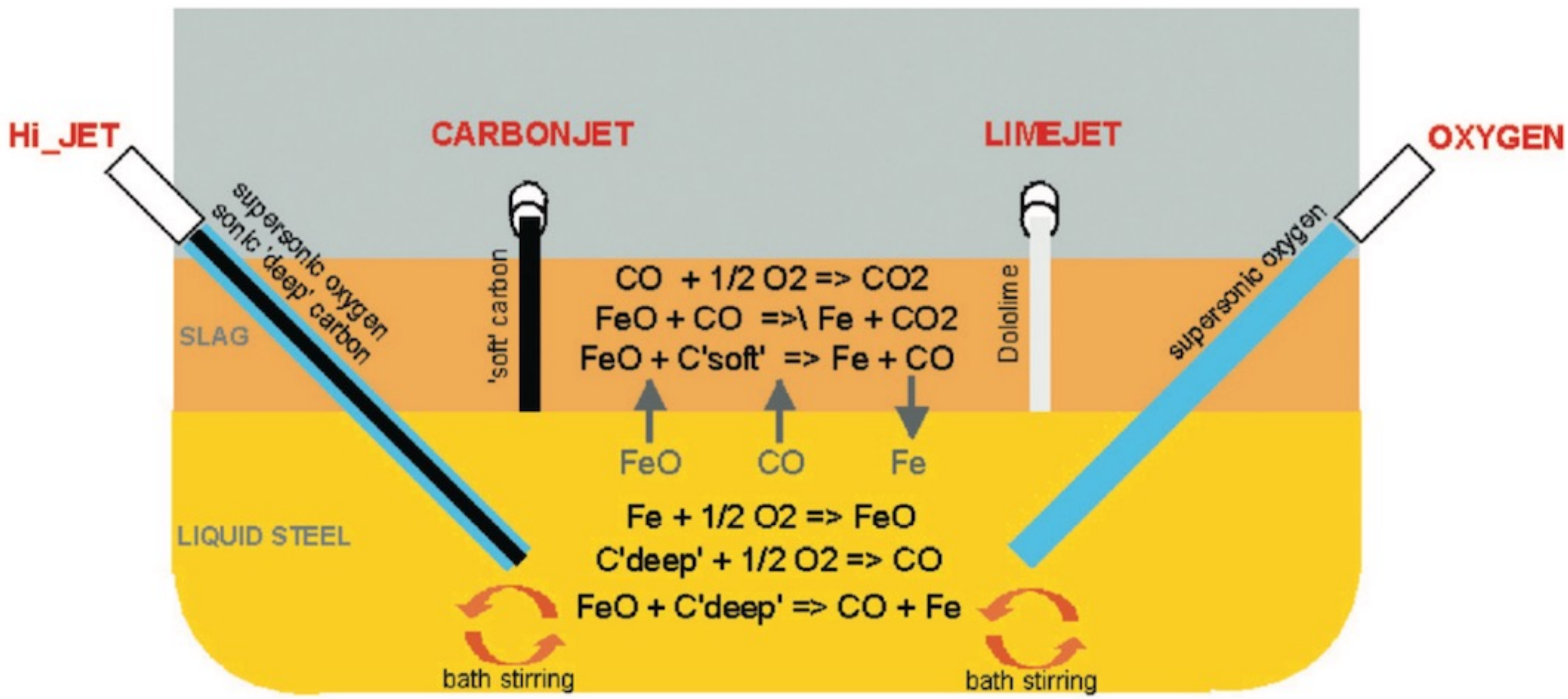

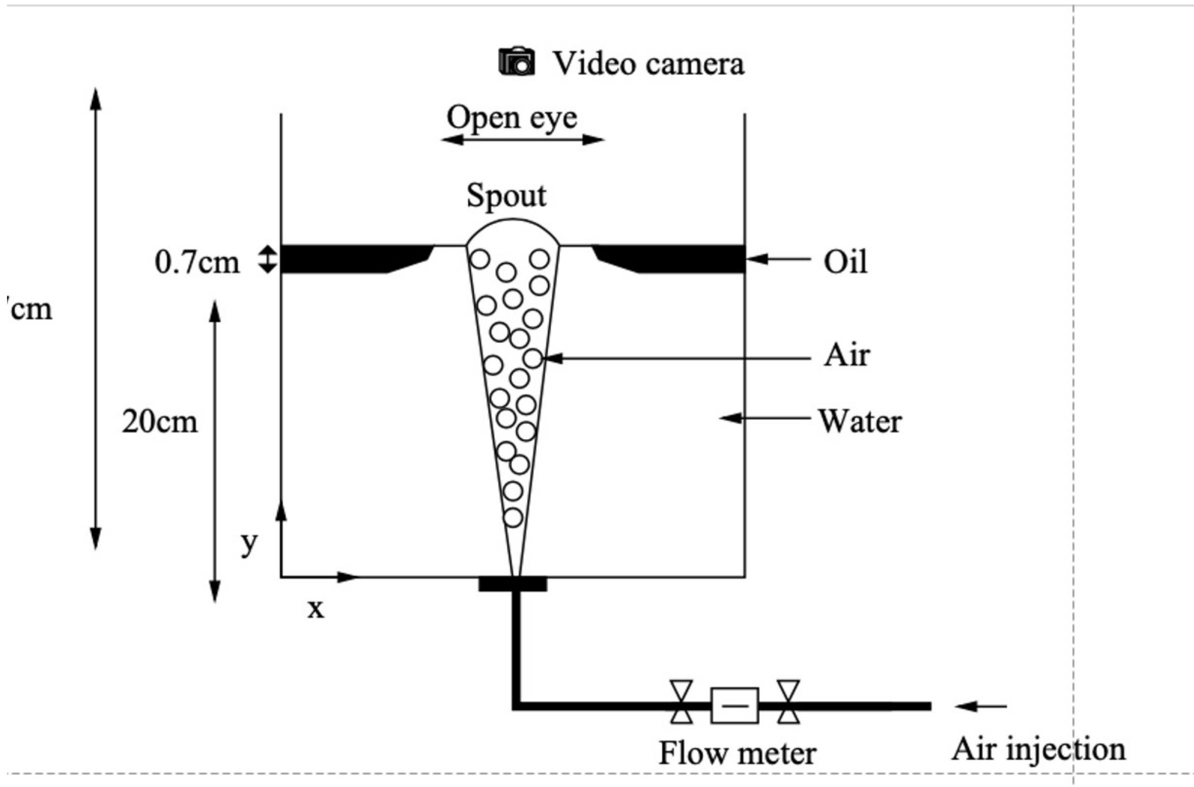

Schematics of the experiment

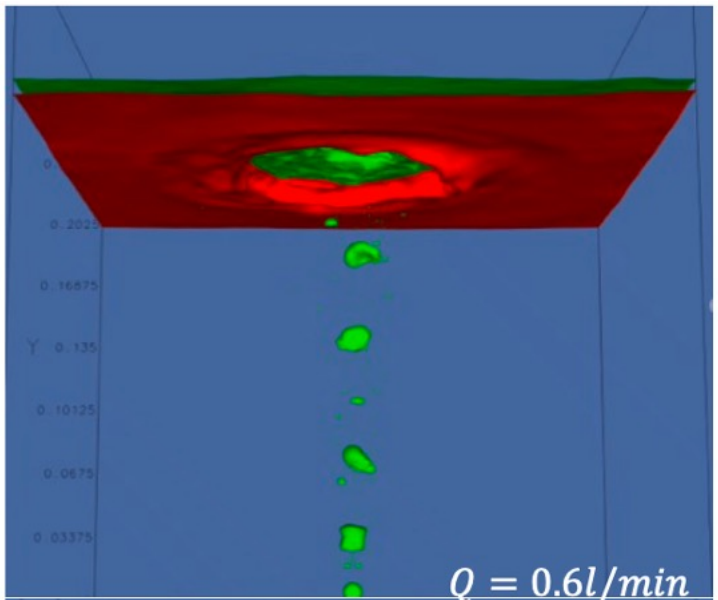

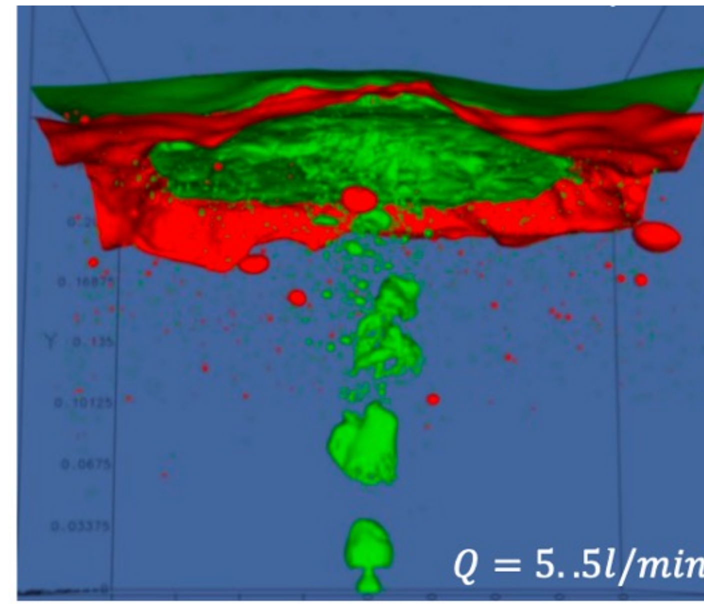

massive numerical simulation of the flow and mass transfer

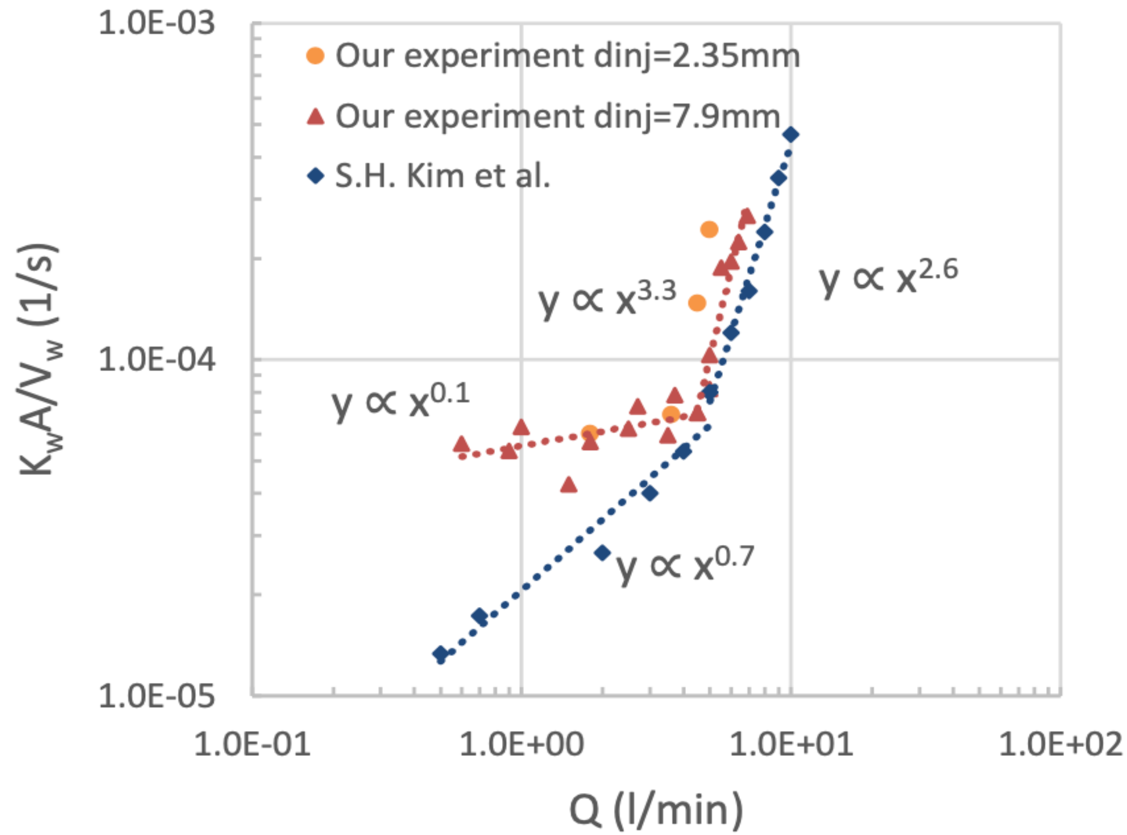

Experimental mass transfer measurements

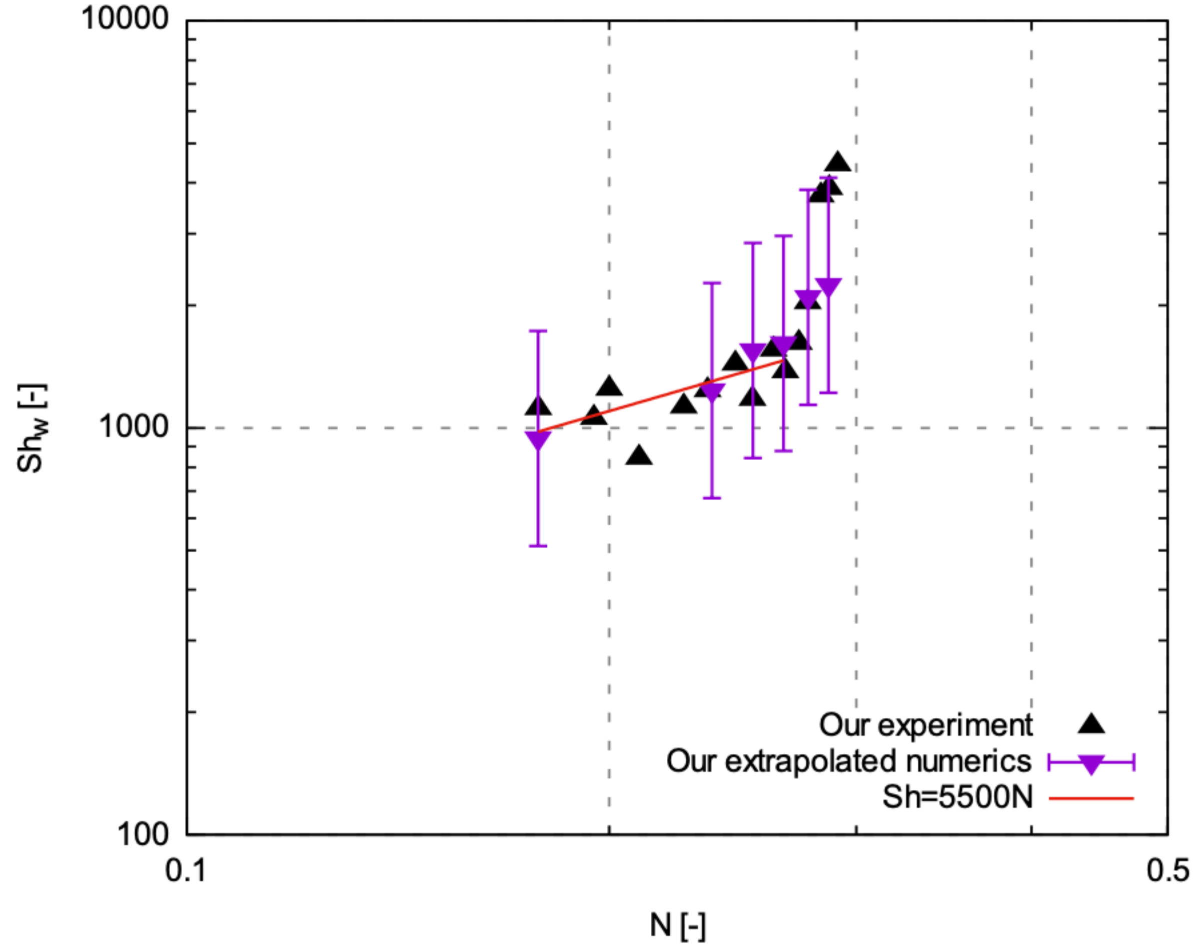

Numerical simulation, experiments and theory agree !

How do these types of simulations "scale" on very big computers ?

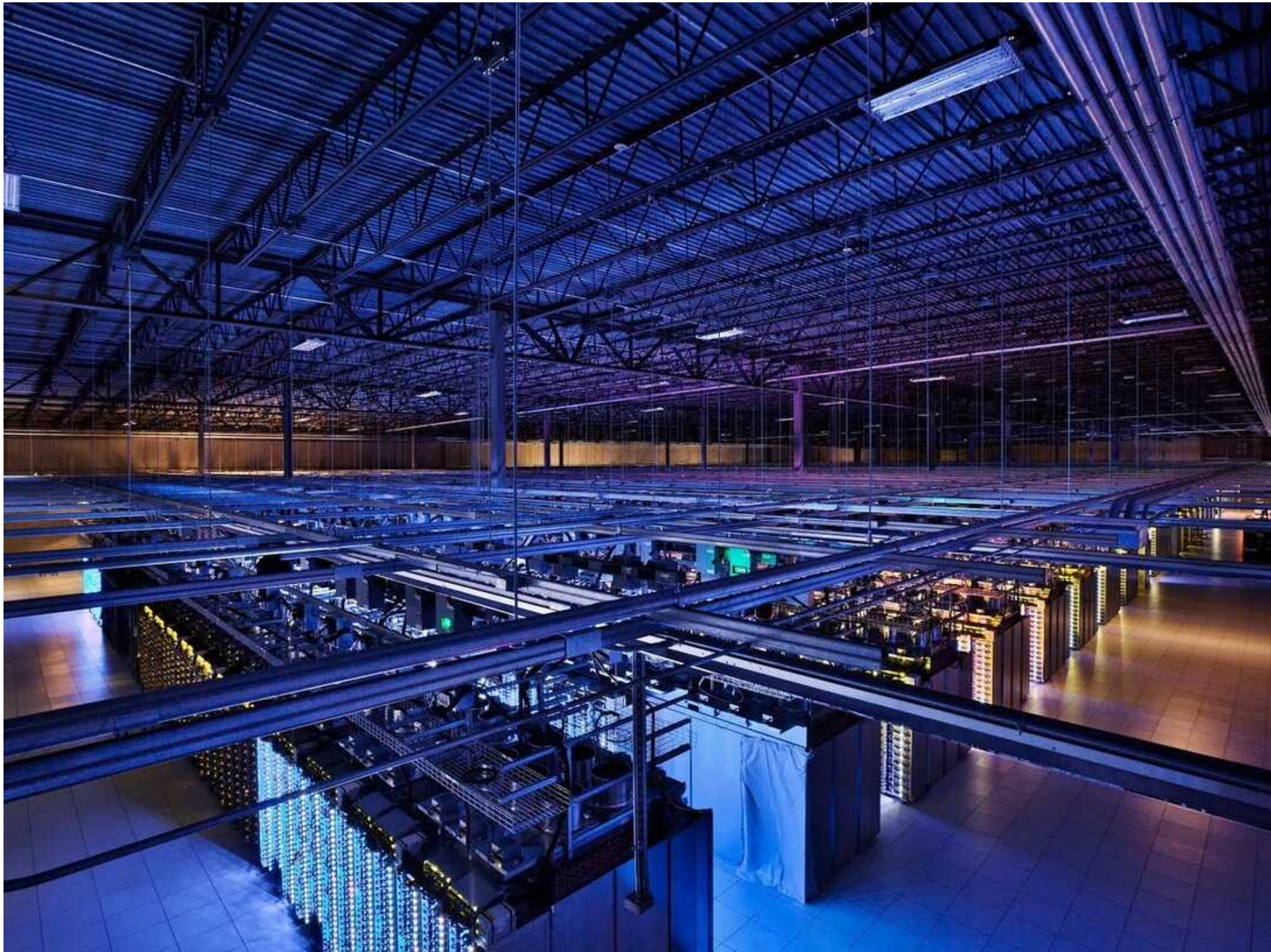

SORBONNE
UNIVERSITÉ
CRÉATEURS DE FUTURS
DEPUIS 1257


富岳
FUJITSU


IBM
summit

The performance of an octree code is controlled by two things:

- how the number of refined cells N_C evolves with the degree of refinement (the "level" l)
- how the speed Z (in cells/second/core) varies with the number of cores N_P and the level

The performance of an octree code is controlled by two things:

- how the number of refined cells N_C evolves with the degree of refinement (the "level" l)
- how the speed Z (in cells/second/core) varies with the number of cores N_P and the level

$$N_C \sim 2^{D_F l}$$

where D_F is a fractal dimension. For a full, regular grid D_F = 3 (the dimension of space)

Apply to ladle data

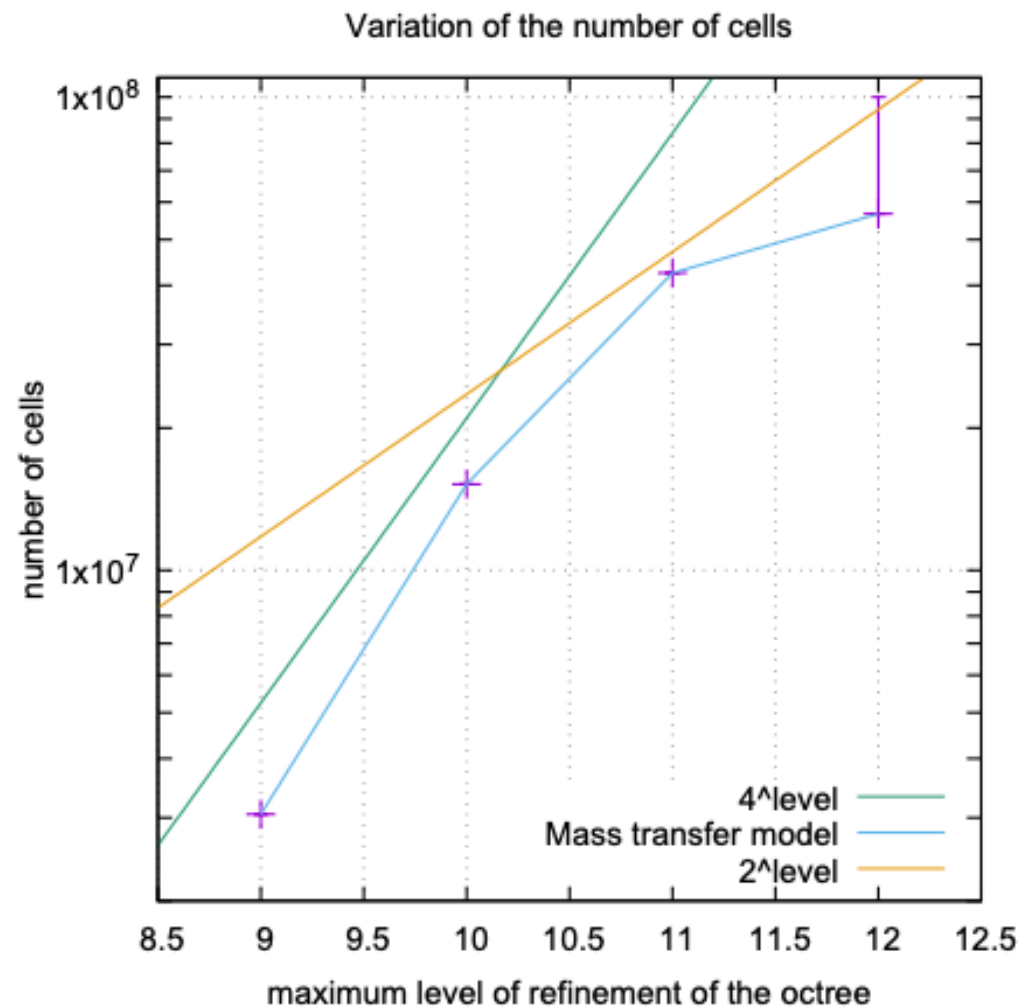

$4^\wedge\text{level} \rightarrow D_F = 2$

$2^\wedge\text{level} \rightarrow D_F = 1$

$L/\Delta x = 512$

$L/\Delta x = 4096$

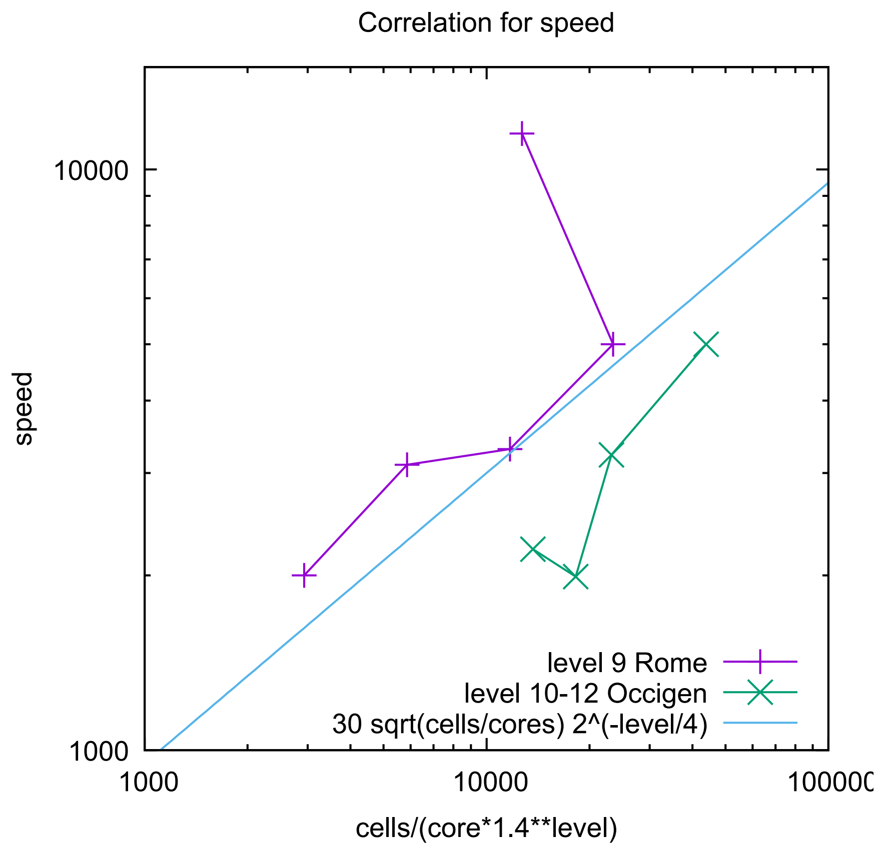

A rough trend can be obtained assuming

- the speed increases with processor density N_C / N_P .

- the speed Z decreases with the complexity of the memory structure, which can be measured by the tree depth, that is the "level"

$$Z \sim (N_c/N_p)^{\alpha} 2^{-\beta l}$$

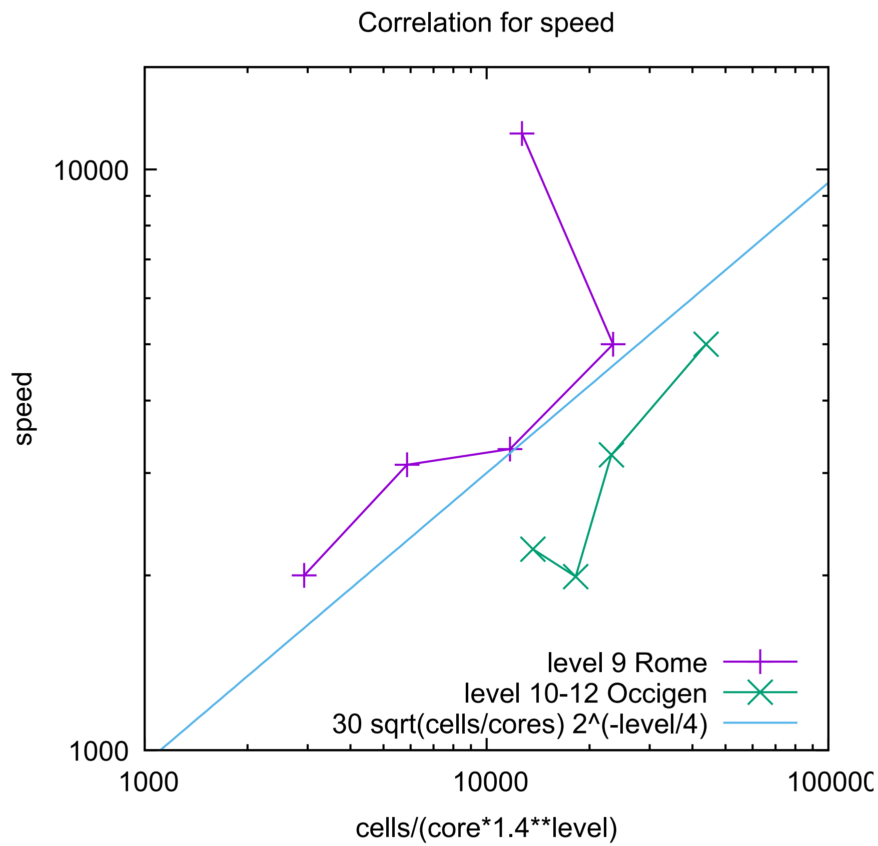

A rough trend can be obtained assuming

- the speed increases with processor density N_C / N_P .

- the speed Z decreases with the complexity of the memory structure, which can be measured by the tree depth, that is the "level"

$$Z \sim (N_c/N_p)^{\alpha} 2^{-\beta l}$$

From a log log plot on the left

$$Z \sim 30(N_c/N_p)^{1/2} 2^{-l/4}$$

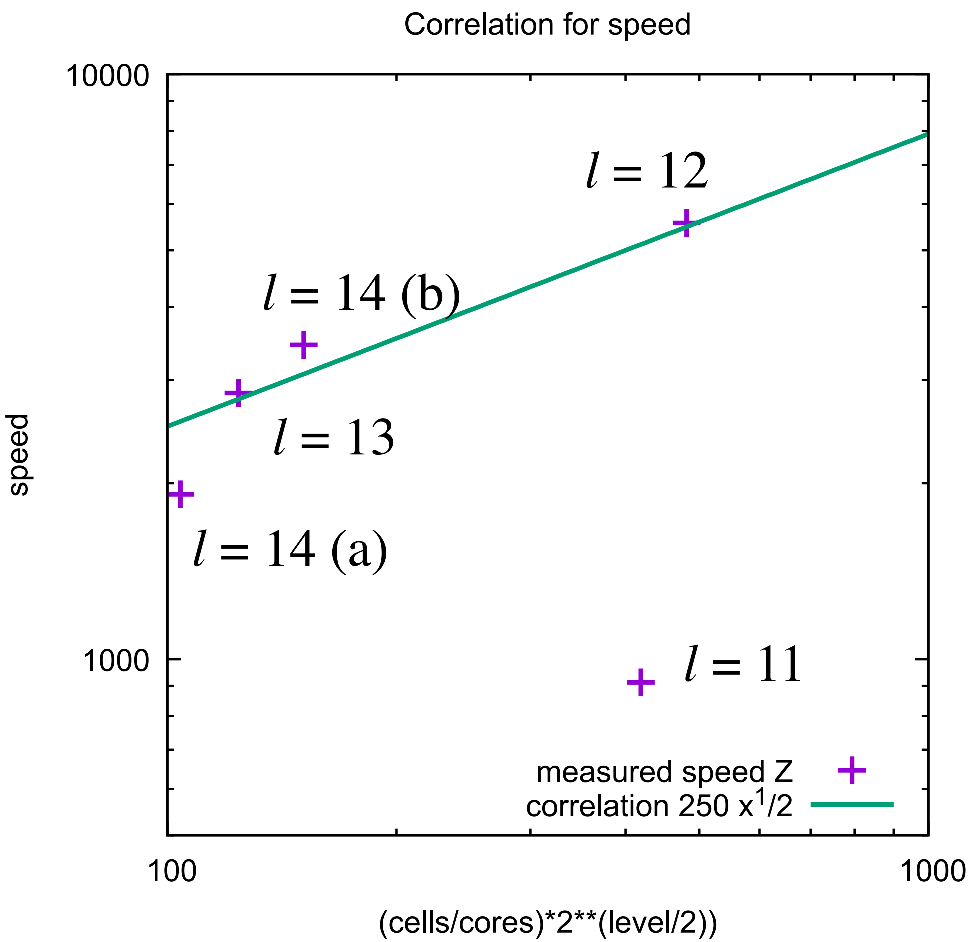

Compare to pulsed jet data

$$Z \sim 250(N_c/N_p)^{1/2}2^{-l/4}$$

largest speed: level 14, 14k cores.
smallest speed: the level 11 case.

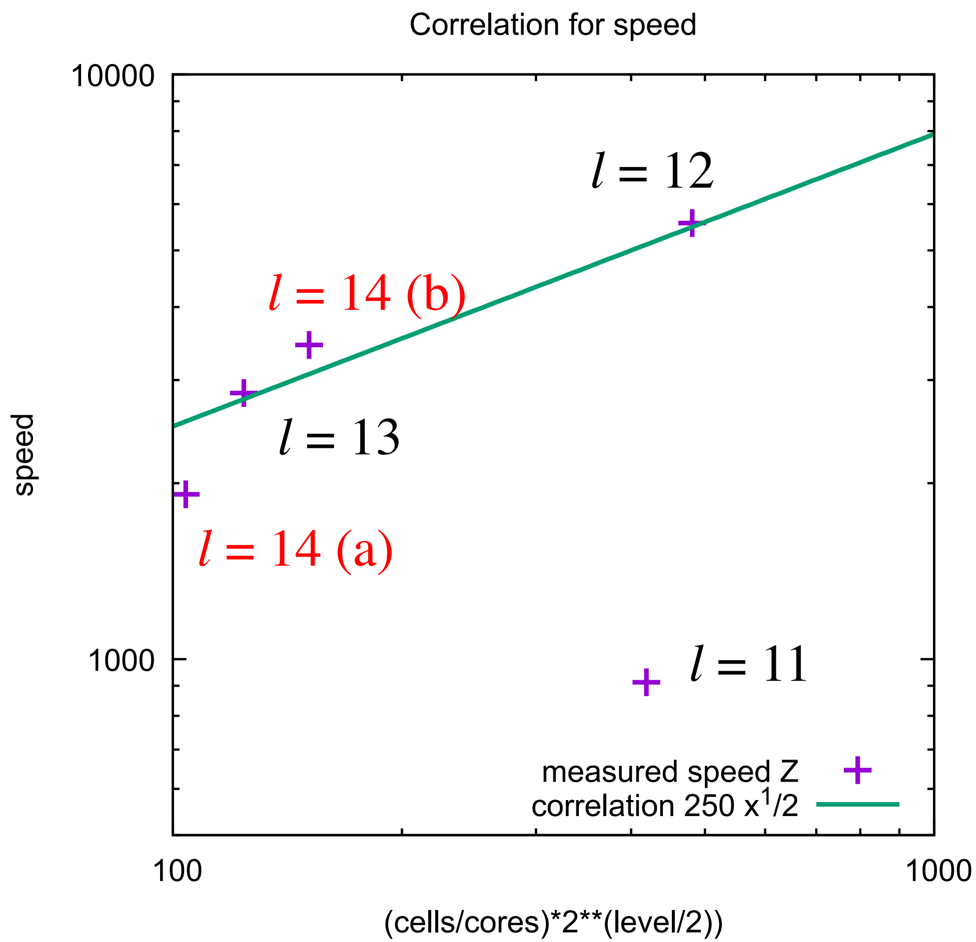

Compare to pulsed jet data

$$Z \sim 250(N_c/N_p)^{1/2} \exp\left(-0.17\, l\right)$$

largest speed: level 12, 1280 cores.
smallest speed: the level 11 case, 1600 cores

level 14 a: 12800 cores,
level 14 b: 14080 cores,

Conclusion

- simulations realized in practice go up to approx 15k cores irrespective of octree or regular

- speed (cells / second / core) on the octree goes up with the number of cells/core. This limits the optimal number of cores and eventually the speed.

- but since the octree has much less cells for the same accuracy it is eventually more efficient: level 14 is equivalent to 4 trillion cells.

Distribution of droplet sizes. Most refined simulation seems converged for d > 4 Δx_min. The slope fitting Pareto shows some real cough experiments (Xie et. al. 2009), *but small drops are over predicted.*